

## Geological Mapping of the 1985 Chinese--British Tibetan (Xizang--Qinghai) Plateau Geotraverse Route

W. S. F. Kidd, Pan Yusheng, Chang Chengfa, M. P. Coward, J. F. Dewey, A. Gansser, P. Molnar, R. M. Shackleton and Sun Yiyin

*Phil. Trans. R. Soc. Lond. A* 1988 **327**, 287-305

doi: 10.1098/rsta.1988.0130

### Email alerting service

Receive free email alerts when new articles cite this article - sign up in the box at the top right-hand corner of the article or click [here](#)

To subscribe to *Phil. Trans. R. Soc. Lond. A* go to: <http://rsta.royalsocietypublishing.org/subscriptions>

## Geological mapping of the 1985 Chinese–British Tibetan (Xizang–Qinghai) Plateau Geotraverse route

BY W. S. F. KIDD<sup>1</sup>, PAN YUSHENG<sup>2</sup>, CHANG CHENGFA<sup>2</sup>, M. P. COWARD<sup>3</sup>,  
J. F. DEWEY<sup>4</sup>, F.R.S., A. GANSSER<sup>5</sup>, P. MOLNAR<sup>6</sup>, R. M. SHACKLETON<sup>7</sup>, F.R.S.,  
AND SUN YIYIN<sup>2</sup>

<sup>1</sup> *Department of Geological Sciences, State University of New York, Albany, New York 12222, U.S.A.*

<sup>2</sup> *Institute of Geology, Academia Sinica, Box 634, Beijing, People's Republic of China*

<sup>3</sup> *Department of Geology, Imperial College, Prince Consort Road, London SW7 2BP, U.K.*

<sup>4</sup> *Department of Earth Sciences, University of Oxford, Parks Road, Oxford OX1 3PR, U.K.*

<sup>5</sup> *Geologisches Institut, Eidgenössische Technische Hochschule, CH-8092, Zürich, Switzerland*

<sup>6</sup> *Department of Earth, Atmospheric, and Planetary Sciences, Massachusetts Institute of Technology,  
Cambridge, Massachusetts 02139, U.S.A.*

<sup>7</sup> *Department of Earth Sciences, The Open University, Walton Hall, Milton Keynes, MK7 6AA,  
U.K.*

[Map and microfiche in pockets]

The 1:500,000 coloured geological map of the traverse route combines observations from the Geotraverse, previous mapping, and interpretation of orbital images. The position of all localities visited by Geotraverse participants and basic geological data collected by them along the traverse route are shown on a set of maps originally drawn at 1:100,000 scale, reproduced on microfiche for this publication. More detailed mapping, beyond a single line of section, was achieved in five separate areas. The relationships between major rock units in these areas, and their significance, are outlined in this paper. Near Gyanco, (Lhasa Terrane) an ophiolite nappe, apparently connected with outcrops of ophiolites in the Banggong Suture about 100 km to the north, was underthrust by a discontinuous slice of Carboniferous–Permian clastic rocks and limestone, contrary to a previous report of the opposite sequence. At Amdo, a compressional left-lateral strike-slip fault zone has modified relationships along the Banggong Suture. Near Wuli, (northern Qiangtang Terrane) limited truncation of Triassic strata at the angular unconformity below Eocene redbeds demonstrates that most of the folding here is of Tertiary age. The map of the nearby Erdaogou region displays strong fold and thrust-shortening of the Eocene redbeds, evidence of significant crustal shortening after the India–Asia collision began. In the Xidatan–Kunlun Pass area, blocks of contrasting Permo–Triassic rocks are separated by east-trending faults. Some of these faults are ductile and of late Triassic – early Jurassic age, others are brittle and part of the Neogene–Quaternary Kunlun left-lateral strike-slip fault system. Some more significant remaining problems that geological mapping might help to solve are discussed briefly, including evidence for a possible additional ophiolitic suture within the Qiangtang Terrane.

### 1. INTRODUCTION

The purposes of this chapter are to document the sources used to compile the 1:500,000 scale geological map of the Geotraverse route and its surroundings (map 1, in pocket) and to discuss briefly the detailed geological maps, originally drawn on the 1:100,000 scale topographic map

sheets provided by Academia Sinica, that record localities and basic data collected by all working groups during the traverse (microfiche 2).

Fifty-five days were spent on the traverse route, from June 4th to July 28th, 1985, covering a distance of about 1300 km along the main paved road from Lhasa to Golmud, with additional distances of several hundred kilometres on subsidiary traverses along less travelled dirt roads and tracks leading away from the main road. This required an average of about 30 km of section completed each day. Consequently, *detailed* geological mapping, in the strict sense of areally extensive and well-distributed observations, was not possible (nor was it originally intended) at most places along the traverse route. Where detailed observation of more than a narrow section line (i.e., mapping) was achieved, the results are discussed below. The immense scope for further investigations in many sections of the traverse route is well-illustrated by the current lack of detailed geological maps along most of its length, not to mention the vast remainder of the rest of the Qinghai–Xizang (Tibetan) Plateau. Some of the more critical geological problems remaining from the Geotraverse route whose solution would likely be provided or assisted by detailed mapping are also briefly discussed.

## 2. GEOLOGICAL MAP OF THE GEOTRAVERSE ROUTE

The coloured map (map 1, in pocket) is partly based on the field observations and subsequent laboratory results of the participants of the 1985 Academia Sinica – Royal Society Geotraverse, documented in the papers in this volume, on earlier work from various Chinese sources, and on the 1981–83 Franco-Chinese collaboration. Information from both the 1985 Geotraverse and the earlier sources has been extrapolated using interpretations of orbital imagery, which have also been used to modify previous map patterns in some places.

### (a) *Previous work*

The principal maps used for compilation of map 1 are:

- a) Geological map of the Southern Tethys of the Qinghai–Xizang Plateau [1:1 million scale]. (Yin Jixiang *et al.*, in press.)
- b) Geological map of Qinghai Province [1:1 million scale] (Qinghai Bureau of Geology and Mineral Resources 1981).
- c) Geological map of the Qinghai–Xizang (Tibet) Plateau [1:1.5 million scale]. (Ministry of Geology and Mineral Resources, Beijing, 1980).
- d) Geological map of Lhasa Sheet [1:1 million scale] (Xizang Bureau of Geology and Mineral Resources 1979).
- e) Geological map of Golmud Sheet, and Geological map of Najj Tal Sheet [1:200,000 scale] (Qinghai Bureau of Geology and Mineral Resources 1984).
- f) Carte géologique du sud du Tibet [1:500,000 scale] (J. P. Burg 1983).

Stratigraphic units, defined by previous work, to which reference is made in this chapter or in the map legend are discussed, with citations, by Yin *et al.* (this volume).

### (b) *Orbital imagery*

For most of the Qinghai–Xizang Plateau, the only orbital imagery at the time of the geotraverse consisted of multispectral scanner (MSS) images from the older series of LANDSAT platforms. Other imagery available to us consisted of a line of Metric Camera (colour film

original) images obtained from a Shuttle–Spacelab mission that closely follows much of the line of the Geotraverse. The large-format Camera (9 × 18 inch negative, black and white) flown on another Shuttle mission provides a few spectacularly high-resolution images from two paths crossing the northern end of the Geotraverse route.

The LANDSAT imagery was obtained in false colour composite prints at a scale of 1 : 250,000. Because these images are from the older 4-spectral-band mss instrument, they have a limited capability to discriminate bedrock lithologies (and lithologic units), especially when compared with the more recent Thematic Mapper (TM) 7-band instrument. Because of certain operating constraints on the LANDSAT 4 and 5 platforms, and a lack of a suitable data-relay satellite, TM images are not available for most of the Qinghai–Xizang (Tibetan) Plateau. Unlike the TM data, mss images do not generally yield significant additional geologic information over the standard false colour print when various computer-generated enhancements are applied to the original digital image data. It may be possible to make certain features more obvious but, in most cases, they are easily seen on the original “unenhanced” images.

The Metric Camera images (obtained as prints at a scale of about 1 : 240,000), being visible light products, have an even more limited capability to discriminate lithologies. Lithologic boundaries and units can be clearly seen *locally* on these two kinds of images, especially the LANDSAT images, but it is not possible in most places to distinguish bedrock units with any confidence, or to follow contacts precisely, over more than a few kilometres. For this reason alone, it would be inappropriate to use the imagery to extrapolate from the detailed traverse observations to fill each sheet of the 1 : 100,000 scale maps. There are two reasons why it is difficult to distinguish most lithologic units and/or their boundaries on the images; the rocks along the traverse route are with minor exceptions not structurally simple, and the rock exposures are quite extensively veneered with *felsenmeer* or solifluction materials in the less rugged areas, it being hard to trace structurally complex units in any area of rugged relief no matter how good the exposure. However, reliably distinguishable lithologic contrasts do occur in some local areas, usually where the contrast is very striking on the ground, and these can be used to check or modify previous maps for the compilation of the 1 : 500,000 traverse route map. For example, the contacts between granites and darker and/or more fractured rocks can be seen in several, but not all places, near Gyanco and Dongqiao, and in the southern Kunlun Shan. Contacts of limestones with darker sedimentary rocks also stand out in some places, for instance between Ordovician carbonates and Triassic arenites in the Golmud River valley, and between volcanics and carbonates near Yaxi Co. Where topography is modest, a fairly general lithologic distinction can be seen on the LANDSAT images between redbeds (of several ages) and other rocks, for example near Gyanco, Amdo, Yanshiping, and near Erdaogou. This can be done because the redbeds have, in many places, a distinctive yellow–orange tone on the false-colour images. However, where the topography becomes rugged, and where soil or solifluction cover is developed, this feature becomes less prominent, and it is clear that it does not show reliably all areas of redbed occurrence.

Although lithologies and their contacts are generally difficult to distinguish, stratification expressed by topographic features is more easily identified and followed on these images. It is not always possible to show the full amount of stratification detail available from the images on the 1 : 500,000 scale map, but the general trends and the major folds are included. Because of the poor expression of the stratification in most places, it is not possible to identify easily old, inactive faults subparallel with strike. The assumption must be that most of these fault structures are not detected reliably from the images.

The structures that are most prominent on the images are the active (Quaternary) faults, as has been known for some time (Molnar & Tapponnier 1978). These are distinguished from the older faults on the 1:500,000 map. The observations made during the geotraverse on these structures are discussed by Kidd & Molnar, this volume). Most concern the major east-trending left-lateral strike-slip fault system in the southern Kunlun Shan, of which two major fault strands, the Xidatan and Kunlun Pass Faults, are crossed by the traverse route. The north-trending normal faults, and related NE- and NW-trending strike-slip faults, seen in several places along the southern half of the route, have been recently described in detail by Armijo *et al.* (1986).

The orbital imagery, therefore, is extremely helpful in providing a general overview of the topography and geology, and for mapping some more detailed aspects of the geology, particularly neotectonic structures. It has limitations, however, in extrapolation of lithologic map units and older (inactive) structures. The speculative nature of most of these extrapolations means that the 1:500,000 map will probably need revision when ground investigation is done of areas not covered by our traverse or previous Chinese field work. Several of the Chinese maps, particularly the 1:1.5 million scale geological map of the Qinghai-Xizang plateau, have incorporated substantial input from interpretation of LANDSAT images. The areas in which this has been done are not readily separable from those in which there is ground-based map data. Therefore caution is needed in using particular map patterns or relations on the 1:500,000 scale traverse map for far-reaching conclusions, particularly for geology far from that known on the ground.

### 3. DETAILED TRAVERSE MAPS

#### (a) Introduction

Base maps used during the traverse were provided by the Academy of Sciences and consisted of a set of 69 topographic maps at 1:100,000 scale (figure 1) of excellent detail and quality. Most have a contour interval of 20 metres; some, in areas of rugged topography, have an interval of 40 metres. These maps proved ideal for the purposes of recording locations and basic geology throughout the traverse. In a few places, some Geotraverse groups locally went beyond the coverage of these maps; in these areas we used 1:100,000 scale black-and-white prints of the LANDSAT images as base maps, although it was clearly easier and preferable to use the topographic maps for location in the field rather than the images. A set of the topographic maps is lodged with the British Museum (Natural History).

Localities and basic geological information, such as observed lithologies, lithologic unit boundaries, faults, fold hinges, attitudes of bedding, foliation, lineation, etc., were recorded on a master set of maps during the traverse. These data were checked and supplemented from participants' field notes after the end of the traverse. The master set of geotraverse geologic maps is lodged in the collections of the British Museum (Natural History). The localities and all the geological information have been abstracted by redrafting from the 48 topographic map sheets that were used, for reproduction on microfiche (in pocket). The intention is that these maps show only data observed in the field, and modest extrapolations ("field glasses geology") made in the field at the time by those who visited the particular localities. Because all the localities visited by all participants are shown on these maps, each with its locality number, it will be clear which information is from outcrop observations and which consists of extrapolation

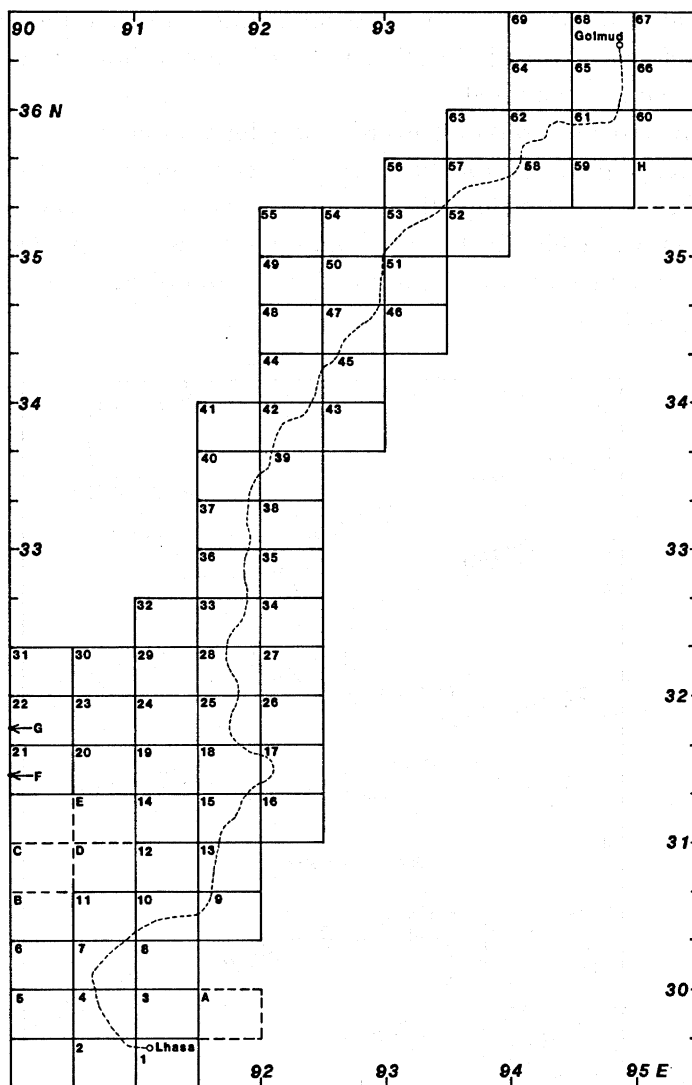


FIGURE 1. Index map to topographic map sheets (1:100,000 scale) provided for the Geotraverse. Lhasa-Golmud highway shown by dashed line. Numbers are keyed to map sheet names in the list below. Detailed geological maps drawn on this base (microfiche, in pocket) use these sheet numbers and names for identification. Not all map sheets were used and in cases where only a small proportion of a map sheet was used, it may be combined with an adjacent sheet in the microfiche geological maps. Areas labelled with letters A-H refer to geological observations made on LANDSAT image base maps; these areas are included with the other maps on microfiche.

- |               |                      |                      |
|---------------|----------------------|----------------------|
| 1. Lhasa City | 24. Jibuxiang        | 47. Erdaogou         |
| 2. Quxu       | 25. Erdaohe Station  | 48. Tangrijiapang    |
| 3. Lhunzhub   | 26. Nyimaqu          | 49. Gelushankecuo    |
| 4. Maqu       | 27. Nyainrong County | 50. Fenghuoshan      |
| 5. Jidaguo    | 28. Amdo             | 51. Lemacuo          |
| 6. Junmaching | 29. Zhashuqu         | 52. Duoqun           |
| 7. Yangbajian | 30. Cigetangcuo      | 53. Wudaoliang       |
| 8. Pangduo    | 31. Yatucuo          | 54. Gongmaorima      |
| 9. Baga       | 32. Chaqu            | 55. Cuorendeja       |
| 10. Damxung   | 33. 112th Station    | 56. Haidingluoer     |
| 11. Ningzhong | 34. Maisairi         | 57. Budongquan       |
| 12. Nam Lake  | 35. Dengka           | 58. 63rd Station     |
| 13. Gulu      | 36. Tanggula Pass    | 59. Zheseke          |
| 14. Bengcuo   | 37. Wenquan          | 60. Reshui           |
| 15. Sangxiong | 38. Longyala         | 61. Naij Tal         |
| 16. Dareng    | 39. Yanshiping       | 62. Qingbanshan      |
| 17. Nagqu     | 40. Wenquan Station  | 63. Diayingshan      |
| 18. Gajia     | 41. Jiri             | 64. Tuotuoalalin     |
| 19. Baerda    | 42. Tongtian Bank    | 65. Dishantou        |
| 20. Jiangcuo  | 43. Cuojiangqin      | 66. Duoyahé          |
| 21. Baingoin  | 44. Tuotuo River     | 67. Golmud East Farm |
| 22. Dongkacuo | 45. Yaxicuo          | 68. Comm. of Golmud  |
| 23. Dongqiao  | 46. Bayingzangtuoma  | 69. Dazachuo         |

from them. The locality numbers can be used to relocate precisely the sampling and fossil localities to which reference is made in other papers in this volume and in any subsequent publications on the material collected.

The locations of the cross-sections of Coward *et al.* (this volume) are given on each map; in most cases, one section crosses several sheets and the continuation is indicated by subscript letters in sequence. In a few places along the Geotraverse route, some detailed mapping beyond a single line of section was achieved. Results from those areas are now discussed briefly. The location of each of the detailed maps (figures 3, 4, 6, 7, and 8) are given with respect to the traverse route on figure 2.

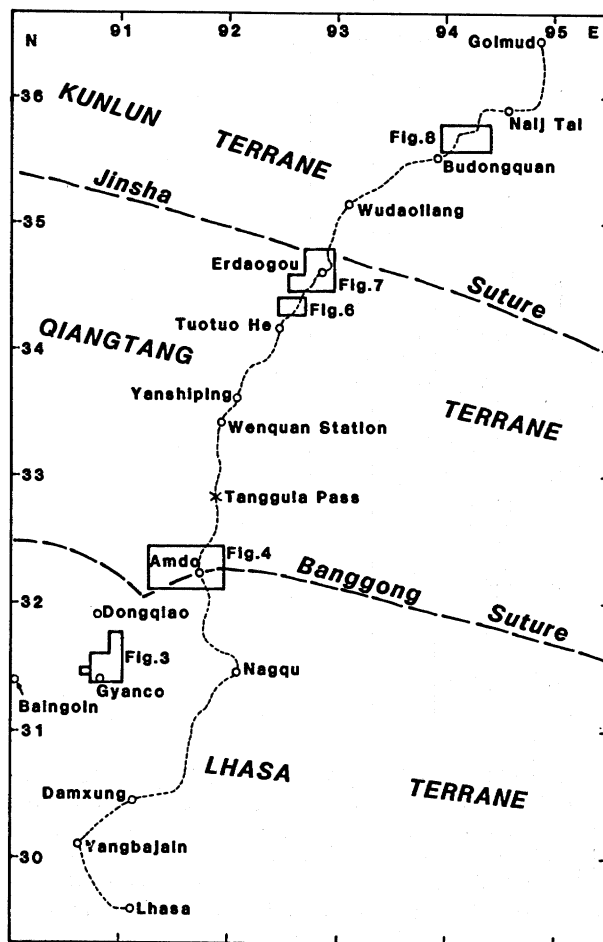


FIGURE 2. Sketch map showing location along the traverse route of detailed geological maps (figures 3, 4, 6, 7, and 8).

(b) *Gyanco–Pung Co*

In this area (figure 3), stratigraphic and structural relationships are exposed between the Banggong Suture-derived ophiolite nappe, Carboniferous–Permian clastics, limestones of uncertain age (?Permian or ?Jurassic), and Jurassic flysch. Mid-Cretaceous red clastics and andesite–rhyolite volcanics are also present, and mid-Cretaceous granitoid rocks and NNW-trending andesite dykes were observed to intrude all lithologies except the Cretaceous clastics

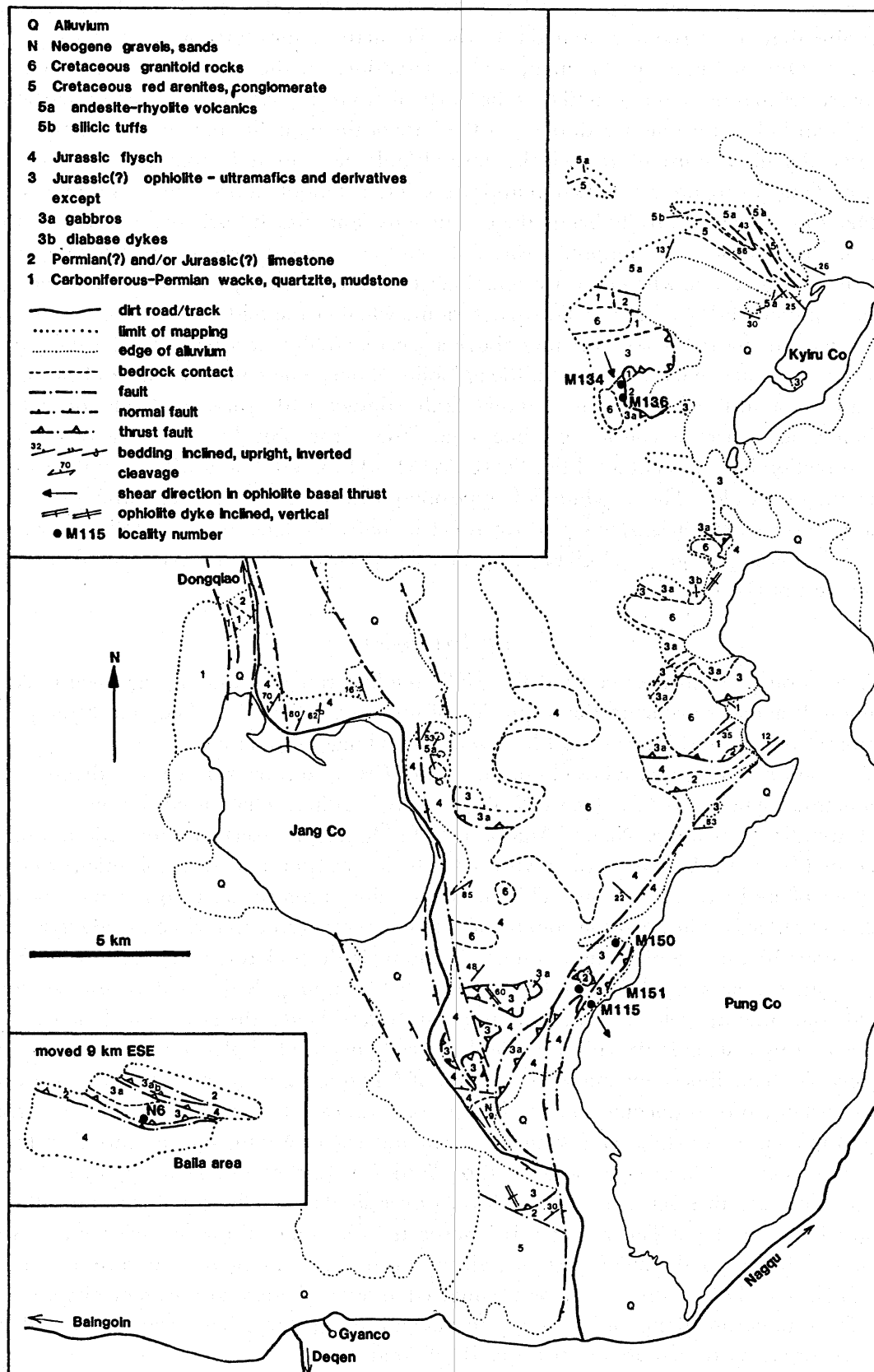


FIGURE 3. Geology in the vicinity of Gyanco and Pung Co. For location, see figure 2. This figure, and the other detailed maps, may be found easier to interpret if some or all of the units are coloured. The inset of the Baila area has been moved 9 km ESE from the true position with respect to the main area of the map.



and volcanics. A previous report on a larger area that encloses this one (Girardeau *et al.* 1984) maintains that the carbonates and the Carbo-Permian clastics form a nappe on top of the ophiolite. Our mapping in this area, and observations to the west near Baila (figure 3), demonstrates that this is not so, and that the Carboniferous-Permian clastics and the carbonates all lie in an imbricate zone (or duplex) at the base of the ophiolite nappe. The mapping also suggests why the confusion arose: if the normal faults near to and subparallel with the west shore of Pung Co are not recognised, it appears as if the ophiolite ultramafic rocks exposed near the lake shore are structurally below these sediments (and also Jurassic flysch) exposed to the west in the hillside. Our mapping was not extensive enough, given the less-than-perfect exposure, to determine whether any original large-scale relationships are preserved among the various ophiolite lithologies, nor did we determine whether the mid-Cretaceous volcanics and clastics were deposited unconformably above a severely folded or a basically flat-lying nappe pile. Structures at the basal contact of the ophiolite nappe, where serpentinite and carbonated derivatives of ultramafics are in original fault contact with Jurassic flysch, or with the Carboniferous-Permian clastics, or limestone, show clear SSE-directed sense-of-shear and shear direction indicators at localities M115, M134, M136, M150 and M151, on the west side of the Pung Co valley. These include S-C-type oblique foliations, oblique vein and fracture sets, steps in fibrous vein slickensides, and asymmetric folds. Oblique S-C-type foliation was also seen in the same position, and giving the same shear sense, at locality N6, near Baila, about 20 km west of Gyanco.

(c) *Amdo region*

The mapping in this area covered the ENE-trending range straddling the town of Amdo. Ophiolite lithologies occur on the south side of this range (figure 4). They mark the present location of the suture between the Lhasa and Qiangtang Terranes.

In the southwest, red clastic rocks of uncertain, Cretaceous or Tertiary age define a large asymmetrical syncline with a steeply N-dipping axial surface, which is cut by two prominent NNW-trending tear faults. Nearer Amdo, ophiolite lithologies (serpentinite and gabbro) are imbricated in south-directed thrusts with redbeds that contain andesitic volcanics, which are probably of mid-Cretaceous age. This imbricate zone projects westward above the large syncline of redbeds. The northern contact of ophiolite serpentinite in the section along the river valley about 10 km west of Amdo is a steep S-dipping fault, probably with a N-directed thrust component. Other steep faults and a moderately S-dipping, N-directed thrust cut folded redbeds and andesitic volcanics north of this point. East of Amdo, the extension of these redbeds is truncated by a steep fault with a S-side down component of displacement against mid and late Jurassic shale, limestone and arenites; west of Amdo it is not clear whether the equivalent contact is faulted or is unconformable. The Jurassic strata belong to the Qiangtang Terrane. They form a large, west-plunging anticline north and east of Amdo, and they are thrust north over redbeds of uncertain age (Cretaceous or Tertiary). In the same area (figure 4), some of these redbeds are themselves thrust northward over similar but finer-grained and softer red strata, which may be of Tertiary age. It is suspected that some of the redbeds west of Amdo unconformably cover the overthrust Jurassic strata, but a lack of good exposure prevented a firm conclusion. The northern redbeds are inferred to rest with angular unconformity on folded Jurassic strata of the Qiangtang Terrane, because a prominent erosion surface with reddening below it (figure 4) is seen about 20 km NNE of Amdo.

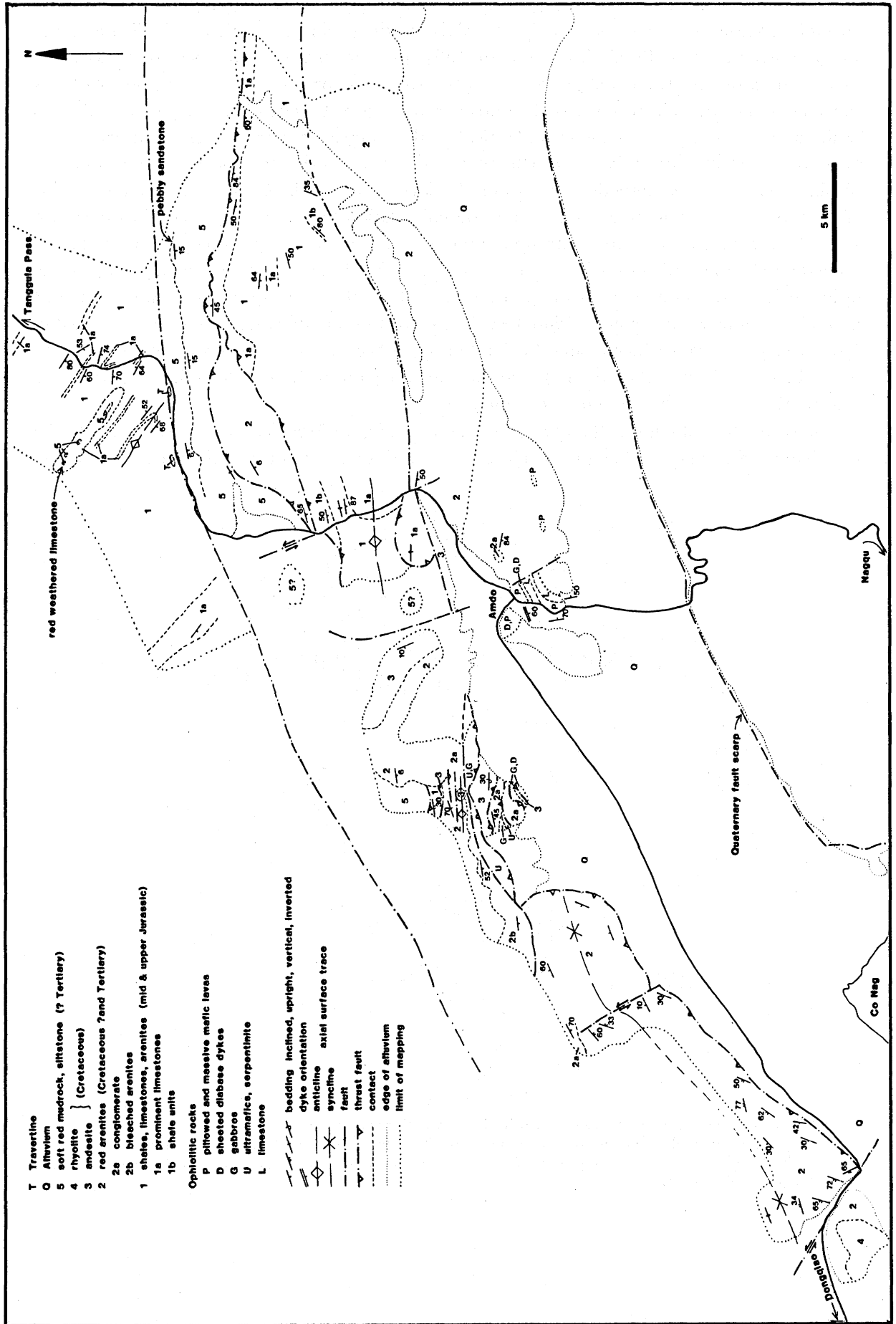


Figure 4. Geological map of the Amdo area. For location, see figure 2.

The fold trends (ESE) in these Jurassic rocks of this part of the Qiangtang Terrane are strongly oblique to and truncated by the ENE-trending fold and fault trends of the Amdo range. Furthermore, oblique slickensides and offset markers in outcrop imply that at least some of the faults in the Amdo range have a significant left-lateral strike-slip component of displacement. The overall structure of the narrow range, with outward-directed thrusts and steep faults with strike-slip components is identical to the "flower-structure" described from well-documented strike-slip fault zones with oblique compressional motion. This compressional displacement explains both the truncation of folded strata of the Qiangtang Terrane in this area, and the strong modification of the original relationships of the ophiolite in the suture zone. The structures seen in the Amdo region are thus largely the product of tectonic events younger than the initial suturing of the Qiangtang and Lhasa Terranes, even though these ophiolite occurrences now mark the position of the (modified) suture in this transect. At least a small amount of the compressional strike-slip tectonism affecting this area is probably Quaternary; several rivers crossing the Amdo range have a sharply antecedent relationship to it (see Kidd & Molnar, this volume), and the fault scarp on the south side of the Co Nag valley (figure 4) is also clearly an active tectonic feature.

The truncation of folds in the Qiangtang Terrane (figure 5) is more or less restricted to the length of the area mapped in figure 4. The trend of the Banggong Suture, inferred from ophiolite

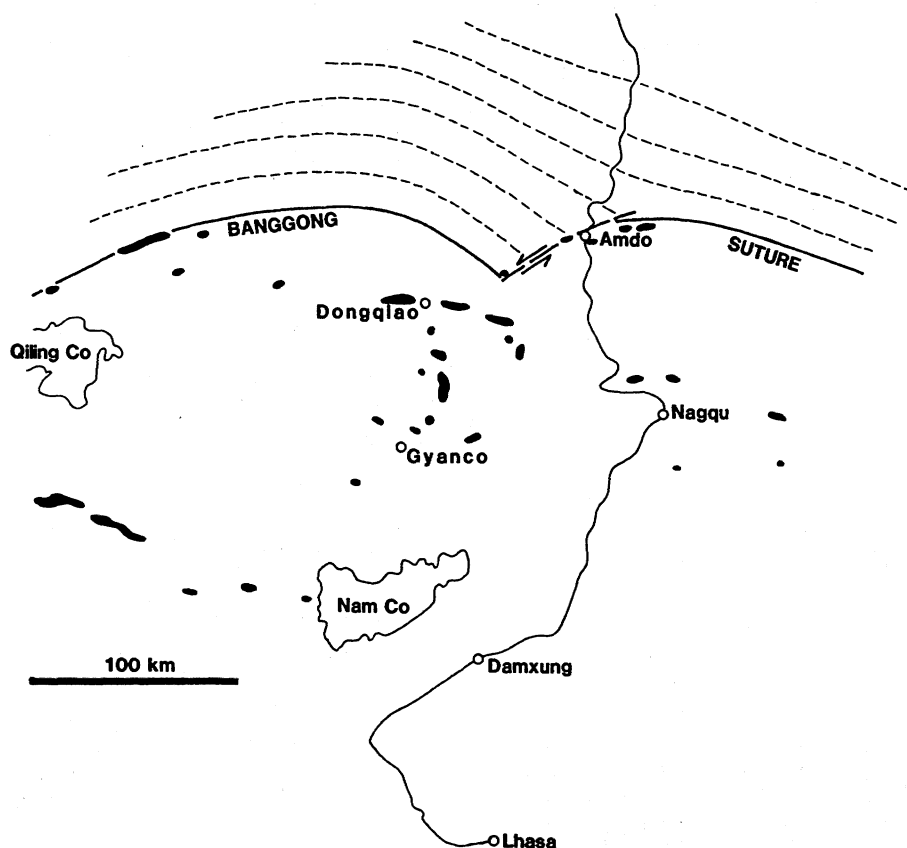


FIGURE 5. Sketch map of ophiolite occurrences in the Lhasa Terrane near the line of the geotraverse. Position of Banggong Suture and its concordance with the trend of folds in the southern Qiangtang Terrane (dashed lines) is indicated. Left-lateral strike-slip offset of the suture occurs near Amdo, coincident with truncation of the Qiangtang fold trends.

occurrences shown on the Geologic map of the Qinghai–Xizang Plateau, become parallel with these folds farther east and west (figure 5). The Amdo strike-slip zone, however, does not appear (from LANDSAT image interpretation) to extend obliquely into either the Qiangtang or Lhasa Terranes and its strike-slip displacement is therefore likely to have been accommodated by additional thrusting in the general vicinity of the suture beyond the ends of the Amdo range.

(d) *Tuotuo River–Wuli area*

Mapping in this area (figure 6) was aimed at understanding the relationship between the Eocene red clastics of the Fenghuoshan Group and the underlying Triassic Batang Group carbonates, andesitic volcanics, and clastics, and Jurassic Yanshiping Group clastics. The map shows that an angular unconformity occurs at the base of the Fenghuoshan redbeds but, from measured dips, and from the limited truncation of the underlying Batang Group (figure 6) it is concluded that the latter was only gently folded, at least in this area, prior to redbed deposition. The relations of the Yanshiping Group to this unconformity were not determined conclusively. However, if the extremely pure pale quartzite seen along part of the northern outcrop of the Batang Group is at the base of the Jurassic sequence, its occurrence at two places below redbeds to the north near Erdaogou (figure 7) suggests little discordance between the redbeds and the Jurassic sequence, as long as the latter is of modest thickness in this area. Previous maps show the volcanics and carbonates below the redbeds near the main road as of Permian age, correlative with the Wuli Group, (see Yin *et al.*, this volume). The lithologic types and sequence, and the fossils of Norian age in the limestones at locality M225 (Smith & Xu, this volume) show that these strata belong to the Triassic Batang Group.

Structures observed (vein and fracture sets, slickensides) in the well-lithified redbeds of the Fenghuoshan Group on the southern edge of this range indicate southward overthrusting over adjacent poorly-lithified marls and sands (presumed Neogene in age). Unlike the Erdaogou area (see below), no strong evidence for Quaternary thrusting was seen here, but most of the folding of the strata in this area is of Tertiary age. The implications of this observation for the age of folding in the Qiangtang Terrane as a whole are discussed below.

(e) *Erdaogou area*

Upright folds and mostly northward-dipping thrust faults in the Eocene Fenghuoshan Group redbeds must be related to crustal shortening during the India–Asia collision. The map of this area (figure 7) and the cross-section derived from it (see Coward *et al.*, this volume) yield substantial shortening values, a minimum of about 40% by folding alone. The LANDSAT image and the topographic maps give a fairly clear idea, from well-developed stratification trends, where the major folds and thrusts are located. With the distributed ground observations, including abundant younging indicators in the redbed arenites, most of the structures shown are identified with confidence.

A prominent thrust outcrops in the southernmost range of hills placing the well-lithified Eocene red arenites over soft red marls and pale sands that are presumed from their state of lithification to be younger than the Eocene strata. A well-exposed small thrust duplex of the lithified red arenites occurs in the flank of the hill on the east bank of the river Qu Ma Liu (Moron Us; Leeder *et al.*, this volume) adjacent to the main road (locality M191), and a similar imbrication, in this case involving the young marls, is seen about 7 km west of this point. Evidence for very young (Quaternary) thrust tectonics is suggested by the presence of an

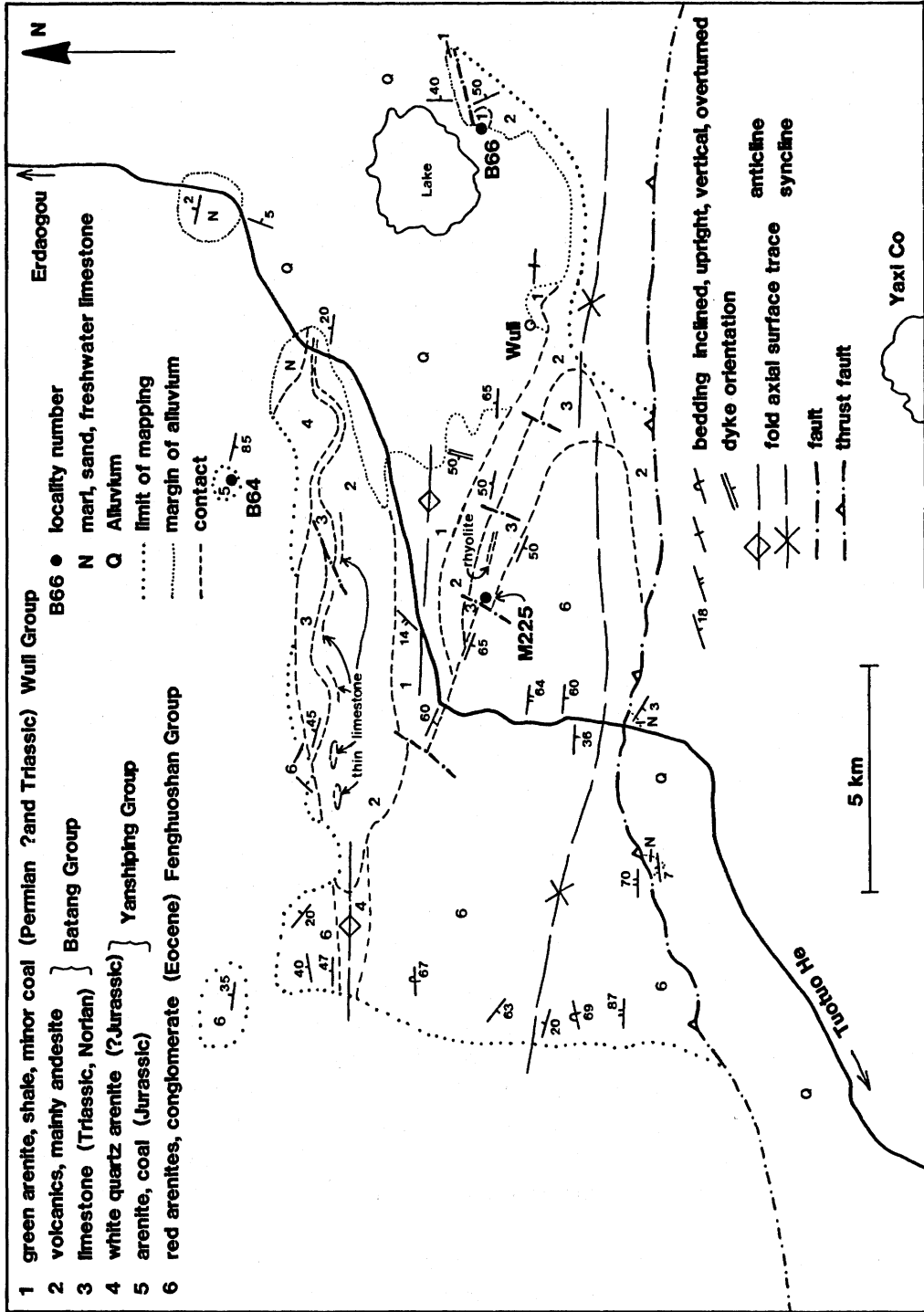


FIGURE 6. Geological map of an area near Wuli. For location, see figure 2.

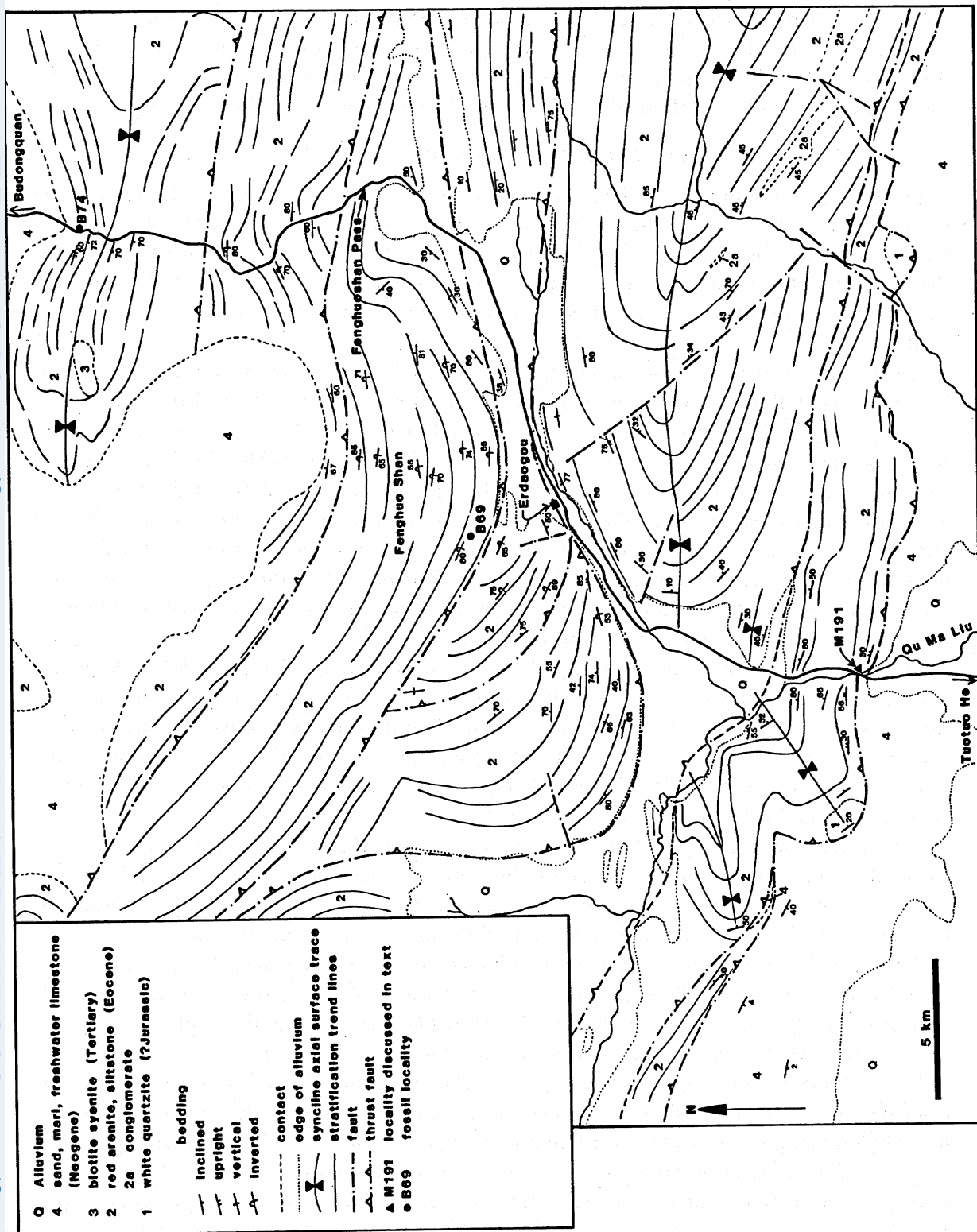


FIGURE 7. Geological map of the Erdaogou area. For location, see figure 2.

incised meander in a small side valley joining the east side of the valley of the Qu Ma Liu (Moron Us), where the thrust outcrops by the main road (locality M191). The local antecedent relationship that this river, and others like it farther east, has with this southernmost range of the Fenghuoshan also suggests late Neogene-Quaternary uplift, most likely by movement on this thrust (see Kidd & Molnar, this volume and Leeder *et al.*, this volume).

(f) *Xidatan Valley–Burhan Budai Mountains*

The Burhan Budai mountains form the southern side of the Xidatan valley, which marks the location of the main strand of the Kunlun Fault system, a major left-lateral strike-slip zone (see Kidd & Molnar, this volume). The bedrock on the southern side of this valley was mapped (figure 8) to try to determine the nature and age of the contacts between the several contrasting rock units that occur there, and to see whether any of the faults related to the Kunlun Fault.

A prominent ductile high strain zone in the form of a grey-black phyllonite unit several hundred metres thick occurs at lower elevations on the southern margin of the valley. The thickness suggests that it must be a zone of major displacement. The phyllonite contains a single strong phyllitic foliation dipping on average moderately to steeply north. Boudinaged quartz veins are common in this foliation. It is affected by a pervasive set of outcrop-scale open to tight folds with gently-dipping axial surfaces and gently east- or west-plunging hinge lines. Both these later folds, and a less intense to phyllitic cleavage are seen in the two major structural blocks to the south of the phyllonite; that is, all the bedrock south of the Xidatan in this map area shares the same outcrop-scale structural sequence, which is thought from regional evidence to have been formed in late Triassic – early Jurassic times.

In one locality (M306), north of the phyllonite, dark grey highly-strained limestone and pale-coloured pure limestone in variably disrupted thick beds occur in a melange-like disrupted grey slaty matrix. Evidence in outcrop of south-directed thrusting (offset layers, asymmetric folds) suggests that this material perhaps formed part of the hanging wall to the phyllonite, in which evidence of south-directed thrust-sense shear (asymmetric boudins of veins, shear-band cleavage) was also seen locally.

However, at the eastern end of the mapped area, green phyllitic rocks, partly arenaceous and feldspathic, resembling those seen structurally below the carbonates farther east in the Dongdatan area, occur to the north of the phyllonite. Either a large lateral ramp structure, or (perhaps more likely) the original occurrence of the carbonates in an imbricate slice adjacent to the phyllonite, are needed to explain this change, unless the carbonates form part of a slice bounded by a younger strike-slip fault and have been displaced many kilometres from the nearest source to the east. As the contact between the carbonates and the phyllonite is not exposed, this problem cannot be resolved without further mapping.

The southern boundary of the phyllonite is, in most places, a brittle subvertical fault that truncates the phyllonite foliation. In one locality (M244), by contrast, a short section of strongly-foliated green phyllites with thin arenite layers occur under a contact with very dark phyllonites, the contact dipping north concordant with the cleavage. Because this occurrence is so restricted, it is unclear whether this represents the footwall of the phyllonite zone or just a lens of somewhat less-strained rock within it. The brittle fault that truncates the phyllonite elsewhere was found exposed in only one locality (M284), where layering and foliation is locally folded on both sides within about 5 metres of the fault. The fault itself consists of gouge about

GEOLOGICAL MAPPING

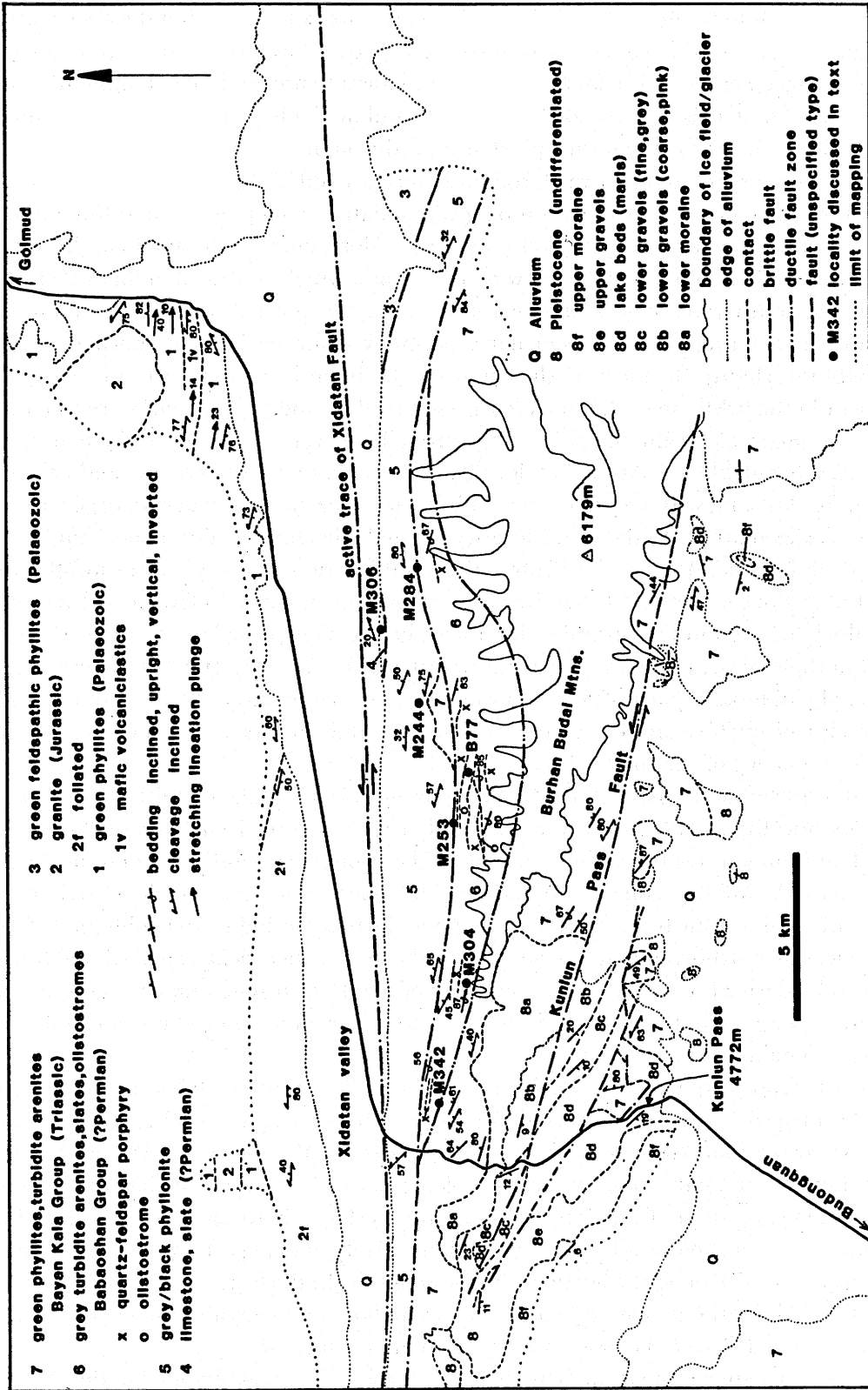


FIGURE 8. Geological map of the Xidatan-Kunlun Pass - Burhan Budai Mountains area. For location, see figure 2.



1 metre wide largely derived from the phyllonite. Vertically-plunging asymmetric minor folds of foliation adjacent to the gouge and in larger intact wall-rock lenses within the gouge, oblique S-C foliation in some of these lenses, and horizontal groove slickensides all suggest left-lateral strike-slip displacement on this fault. The displacement sense and the dominantly brittle character imply that it is related to the present Kunlun Fault system but there is no geomorphological evidence for Quaternary activity on this fault.

West of the main road, and eastward from near the east end of the Xidatan valley, this fault places phyllonite against steeply north-dipping well-foliated green phyllites and thin quartzose turbidite arenites of the Bayan Kala Group (figure 8). Along much of the length of the Xidatan valley, however, a lens up to about 2 km wide intervenes, which consists dominantly of steeply north-dipping, south-younging (and upward-facing) grey quartzose turbidite arenites and slates (Babaoshan Group). These seem not as strongly deformed or metamorphosed as the green phyllitic turbidites to their south, based on the intensity and appearance of foliation development in the pelites in each unit. Well-preserved flute and groove marks are seen on bed bases in a number of localities. Thick olistostromal deposits are exposed in two sections (localities M253 and M304). At the first locality, limestone, quartzose arenite, and calcareous quartz arenite clasts, most 10 cm or less across, but with a few up to 5 m across, occur in a dark grey shaly (slaty) matrix. At the other locality, a single fossiliferous limestone boulder 10 m long is exposed in shale. Because these submarine mudflow deposits only appear locally within the turbidite sections it is inferred that they are confined to channels. A few silicic tuff beds up to 10 cm thick are seen in the turbidites in at least one section (near M284). In every section examined in these rocks, there are somewhat irregular sills, typically 100–300 metres thick, of badly-altered, epidotised quartz-feldspar porphyry that occupy about 20–30% of the section. These are clearly intrusive into both the olistostrome and the turbidites and were intruded prior to development of the single cleavage.

The southern contact of the tectonic lens containing this assemblage of lithologies was seen in one valley (locality M342); elsewhere it is mostly covered by the icefield on the higher parts of the Burhan Budai, or (at the main road) cut by the younger strike-slip fault on the northern side of the lens. At M342 a zone about 150 m wide appeared to be a syn-cleavage fault with mixing of lithologies from both sides. Rather poor shear sense indicators (oblique S-C type cleavage) suggest north-over-south thrusting on the now subvertical zone. Abundant float presumed to be derived from this zone, consisting of highly transposed quartz veins in a dark pelitic matrix, was seen in the valley of locality M284; the source, somewhere above the snout of the glacier, could not be reached.

One other narrow section of rocks has been reported to be within the Babaoshan Group. This occurs at locality B77 where a small section (about 25 m) of arenites, shales, tuff, and a coal bed with Mesozoic plant fragments is exposed (Yin *et al.*, this volume). The coal and the associated fluvial sediments seem unlikely lithological associates of the turbidites and olistostromes that make up most of the Babaoshan Group. Perhaps this occurrence is a block in the olistostrome that occurs in the adjacent valley. Alternatively, it may perhaps occur in a separate tectonic lens (“horse”) along the northern boundary fault. In the latter case it could be related to the clastics with local red beds and coaly beds seen about 50 km east in the Dongdatan, and which overlie folded Permo-Triassic rocks with angular unconformity.

The Pleistocene sequence near the Kunlun Pass (figure 8) is regionally tilted to the SSW, and locally dips as much as 23°. This deformation is connected, but not in a precisely understood

way, with the interaction of the Kunlun Pass Fault and the Xidatan Fault, because the area of maximum tilting is in the zone where the faults approach one another. The apparently irregular distribution of outcrop of the Triassic Bayan Kala Group south of the Kunlun Pass Fault (figure 8) is largely due to palaeotopography. South- to southwest-trending valleys filled by the Pleistocene sequence alternate with ridges of the Triassic arenites and phyllites; the ridges terminate to the south because of the southerly tilting.

#### 4. PROBLEMS NEEDING FURTHER MAPPING

Some geological problems can be solved by examining a single good exposure or section, but others require well-distributed information (in other words, mapping) for their solution. It is, in many cases, only by looking systematically and in detail through an area that some of the key localities and sections are found, and the variability assessed in stratigraphic and structural sequences and other features. We contest vigorously the idea that all, or everything of significance, is solved by one geotraverse. This is particularly true where outcrop is discontinuous and the structure complex, as along most of the traverse route. In the interest of brevity, only a few questions are raised here; in other words, the discussion below is not comprehensive.

The timing of the beginning of the collision between the Lhasa and Qiangtang Terranes is poorly known, and it is not known whether the late Jurassic uplift of the Dongqiao ophiolite is indicative of thrusting of ophiolite onto continental lithosphere of the Lhasa block (“obduction”) or reflects some other intra-oceanic event. This is so because the relations between the Triassic platform carbonates of the Lhasa Terrane and the Jurassic flysch are ill-defined. Was the flysch deposited over carbonates and continental basement and, if so, when did it start? Conversely, was it tectonically transported from an oceanic environment significantly later than its depositional age? The significance of the isolated occurrences of Triassic carbonate turbidites could be related; do they represent a response to platform rifting or are they an early response to thrust loading of the Lhasa Terrane? The basic relationships and ages of these strata will have to be established by mapping to answer these questions.

Also in the Lhasa Terrane, only extensive accurate mapping of the mid Cretaceous and younger rocks will yield useful estimates of the crustal shortening that there has been prior to and subsequent to mid-Cretaceous times, essential information for testing crustal thickening models for the India–Asia collision. Similar comments are applicable to Tertiary rocks elsewhere on the plateau, although our mapping near Erdaogou (see above) illustrates that modest efforts can quickly improve understanding.

There is still a large question to be answered about the age of folding in the Qiangtang Terrane. In the north, around Wuli, most of the shortening is younger than Eocene (see paragraph 3*d* above). In the southernmost part, just north of Amdo, the folding of the mid and late Jurassic strata predates some of the redbeds (paragraph 3*c* above). The problem rests on the age of those redbeds; are they Cretaceous, or are they Tertiary, and could the folding be Tertiary as it is in the north? If the folding in the south is Cretaceous, where in the Qiangtang Terrane does the change occur to the younger deformation seen in the north?

Besides the obvious need to define what lies below the Jurassic covering the southern two-thirds of the Qiangtang Terrane along the traverse line, the relationship of the Triassic Batang Group arc volcanics to Permian rocks is ill-defined. Could the arc volcanics be allochthonous, overthrust from the Jinsha Suture?

For the Kunlun Terrane, systematic mapping will reveal the large-scale structural relations of the Permo-Triassic sections north of the Xidatan Fault to older rocks (cf. Coward *et al.*, this volume) – essential information in understanding the tectonic significance of these Permo-Triassic rocks (were they deposited in extensional basins?). Although isotopic ages may help to solve the problem of whether there are one or two sequences of volcanics in the northern Kunlun, and whether they are Devonian, Carboniferous, or Permo-Triassic, mapping would contribute greatly to the confidence placed in the ages, if it revealed the original relationship(s) of the volcanics to the Carboniferous strata, for example.

As a final and more general problem, the location of sutures and the occurrence of ophiolites are critical to the interpretation of the assembly of the crust of the Qinghai-Xizang Plateau.

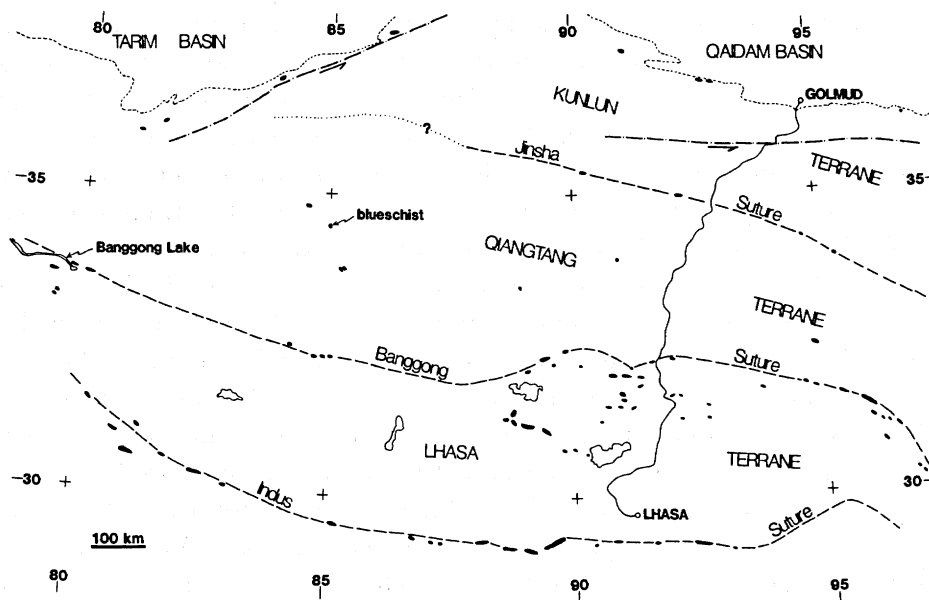


FIGURE 9. Sketch map of ophiolite occurrences in the central and western parts of the Qinghai-Xizang Plateau, with the known sutures indicated. Ophiolite and blueschist occurrences within the Qiangtang Terrane may indicate the presence of one (or perhaps more) additional sutures.)

Figure 9 shows the occurrence of ophiolites from the 1 : 1.5 million scale Geological Map of the Plateau, with the addition of two localities from the samples and detailed topographic maps of Hedin (Hennig 1915). The ophiolites scattered across the Lhasa Terrane south of the Banggong Suture are thought, from mapping, to be remnants of a large nappe (Girardeau *et al.* 1984, 1985, Chang Chengfa *et al.* 1986). However, the nature of the ophiolite and blueschist occurrences within what is currently identified as the Qiangtang Terrane are unknown. This possible suture within the Qiangtang Terrane is as well if not better defined, at least by ophiolites, than much of the length of the Jinsha Suture. Whether this is an additional suture, and whether it might help explain the odd distribution of Gondwana-type Carboniferous-Permian at the western end versus Cathaysian-type at the eastern end of the Qiangtang Terrane, are questions that could be answered by detailed mapping of these purported ophiolites and their surroundings. Similar comments apply to the possible occurrence of small arc-type terranes and an additional suture within the southern Kunlun and Songpan-Ganzi area east and southeast of the northern part of the geotraverse route.

We thank David Rothery for his work in selecting and producing the LANDSAT imagery used for the geotraverse. Kevin Burke and the Lunar and Planetary Institute are thanked for access to image processing facilities and for loan of enlargements of Large Format Camera images.

We also thank Susan L. Anderson for design and much of the drafting of the 82 detailed geological data maps reproduced here on microfiche, the Department of Geological Sciences, State University of New York at Albany, for providing essential equipment and material supplies for the drafting of these maps, and Diane Paton for typing the microfiche-reproduced tables. Pan Yun and Wang Ping are thanked for translating Chinese geographic names from the topographic maps.

## REFERENCES

- Armijo, R., Tapponnier, P., Mercier, J. L. & Han Tonglin 1986 Quaternary extension in southern Tibet: field observations and tectonic implications. *J. geophys. Res.* **91**, 13803–13872.
- Burg, J. P. (compiler) 1983 *Carte géologique du sud du Tibet (1:500,000 scale)*. C.N.R.S., Paris, and Ministry of Geology, Beijing.
- Chang Chengfa & 26 others 1986 Preliminary conclusions of the Royal Society and Academia Sinica 1985 geotraverse of Tibet. *Nature, Lond.* **323**, 501–507.
- Girardeau, J., Marcoux, J., Allègre, C. J., Bassoullet, J. P., Tang Youking, Xiao Xuchang, Zao Yougong & Wang Xibin. 1984 Tectonic environment and geodynamic significance of the Neo-Cimmerian Donqiao ophiolite, Bangong-Nujiang suture zone, Tibet. *Nature, Lond.* **307**, 27–31.
- Girardeau, J., Marcoux, J., Fourcade, E., Bassoullet, J. P. & Tang Youking 1985 Xainxa ultramafic rocks, central Tibet, China: tectonic environment and geodynamic significance. *Geology* **13**, 330–333.
- Hennig, A. 1915 Zur petrographie und geologie von sudwest-Tibet. Vol. 5 in *Southern Tibet* (ed. S. Hedin), 220 pp., Norstedt, Stockholm.
- Ministry of Geology and Natural Resources 1980 *Geological map of the Qinghai-Xizang (Tibet) Plateau (1:1.5 million scale)*. Ministry of Geology and Natural Resources, Beijing.
- Molnar, P. & Tapponnier, P. 1978 Active tectonics of Tibet. *J. geophys. Res.* **83**, 5361–5375.
- Qinghai Bureau of Geology and Mineral Resources 1981 *Geological map of Qinghai Province (1:1 million scale)*. Qinghai Bureau of Geology and Mineral Resources, Xining.
- Qinghai Bureau of Geology and Mineral Resources 1984 *Geological maps of Golmud and Naij Tal sheets (1:200,000 scale)*. Qinghai Bureau of Geology and Mineral Resources, Xining.
- Xizang Bureau of Geology and Mineral Resources 1979 *Geological map of Lhasa sheet (1:1 million scale)*. Xizang Bureau of Geology and Mineral Resources, Lhasa.
- Yin Jixiang, *et al.* (in press) *Geological map of the southern Tethys of the Qinghai-Xizang Plateau (1:1 million scale)*. Institute of Geology, Academy of Sciences, Beijing.

**K**

**KIDD *et al.***

**Appendix. Detailed maps of geological  
observations**

Detailed Maps of geological observations to accompany Chapter 11 -  
Geological mapping of the 1985 Chinese-British Tibetan  
(Xizang-Qinghai) Plateau geotraverse route

W.S.F. Kidd, Pan Yusheng, Chang Chengfa, M.P. Coward, J.F. Dewey,  
A. Gansser, P. Molnar, R.H. Shackleton, Sun Yiyin.

Maps compiled by J.F. Dewey and W.S.F. Kidd; revised and drawn  
by W.S.F. Kidd

Originals plotted and drawn on topographic map base at 1:100,000 scale. A full set of original topographic map sheets, and another full set with (unrevised) geological data and localities plotted during the traverse are deposited in the British Museum (Natural History). Data shown on the maps reproduced here on microfiche have been checked against, and supplemented or revised from the map sheets and notes of the Royal Society participants of the geotraverse. A copy of the notes of most of the Royal Society participants is also deposited in the British Museum (Natural History).

Most of the topographic map sheets used are divided into east and west halves for these microfiche reproductions, identified by the index number or letter and as the east (E) or west (W) part. Map sheets are identified by number or letter as given in the index map (Frame 2). A few sheets have only one portion taken from the centre; these are identified as centre (C) with the index number. Some sheets have been combined with adjacent sheets where the distribution of data permitted. In two cases, observations fall outside the area covered by available topographic base maps. These have been shown on bases taken from orbital-derived images (specifically LANDSAT and metric camera images).

The boundaries of the original topographic maps are nominally at 30 minute longitude intervals and 20 minute latitude intervals (Frame 2 index map) but do not necessarily coincide exactly with such geographic coordinates. Exact placement cannot be made from data available to the authors.

Where map boundaries are not exactly juxtaposed between two adjacent map sheets, an indication of the position of a map corner is given along the border of one of the two maps reproduced here

Locality and/or outcrop numbers on these maps are given with a letter and sequential number (e.g. B244). Any locality can be connected with the working group(s) that visited it by the letter used, according to the list below. Further details on any locality may be found in the notebook(s) of the member(s) of the particular group, deposited in the British Museum (Natural History).

Working group letters used for localities on the maps

- B - Leader, Smith (Stratigraphy, Sedimentology, and Palaeontology)
- G - Harris, Pearce (Geochemistry, Petrology and Isotopic studies)
- H - Molnar (Neotectonics)
- M - Kidd, Dewey (Structure, Mapping)
- N - Kidd, Molnar (Mapping, Neotectonics, Structure)
- P - Watts, Lin (Palaeomagnetism)
- S - Coward, Shackleton (Structure, Mapping)
- T - Gansser (Mapping)
- X - samples renumbered by G; from localities visited by B,H,S and T (see Frame 92).

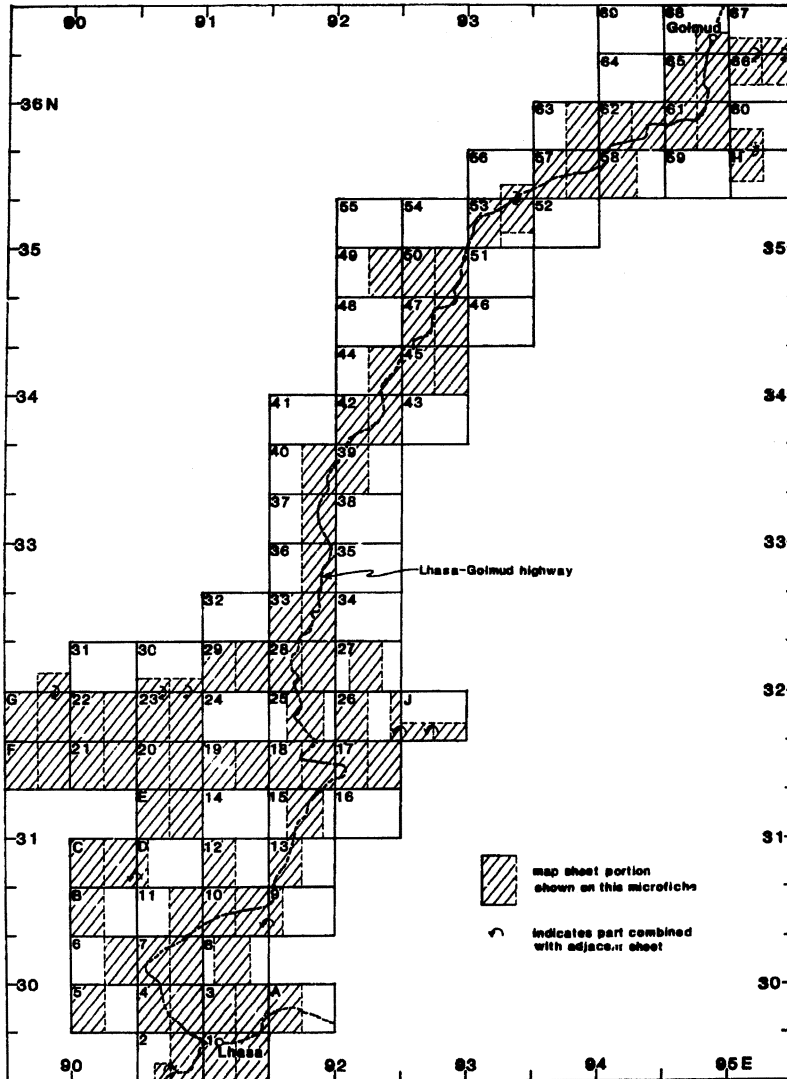
Lists of all localities by group, keyed to the map sheet on which each occurs, are found on this microfiche (Frames 86-92).

Acknowledgments

We thank Susan L. Anderson for design and much of the drafting of these maps. Thanks also to Diane Paton for typing the tables, and the Department of Geological Sciences, State University of New York at Albany for providing essential equipment and material supplies.

Pan Yun and Wang Ping are thanked for their help in translating Chinese geographic names from the topographic maps.

INDEX MAP



**EXPLANATION for symbols used on microfiche maps**

**Lithology indicators**

Indicators have no age implications. Ages of litho-units are designated on each separate map sheet.

Ages of plutonic rocks based on isotopic dates or intrusive/province relations

Where lithology indicators are used in combination, the order used does not necessarily imply relative abundance.

A number (e.g. Ra2) distinguishes one similar unit from another on the same map sheet.

**Sedimentary rocks and sediments**

- A -- granite, allstone
- Ra -- red granite, allstone
- Q -- quartzite
- Al -- flysch
- W -- wacke
- Sl -- siltstone
- Sh -- shale
- Sm -- mudstone, argillite
- Rm -- red mudstone, siltstone, marlstone
- S -- slate
- So -- siltstone
- Cg -- conglomerate
- Cb -- breccia
- L -- limestone, carbonate
- Lop -- limestone conglomerate/breccia
- H -- chert
- F -- coal
- E -- gypsum
- Ml -- lake beds, soft marl, sand
- Mg -- gravel
- Mo -- moraine
- T -- travertine

**Volcanic rocks**

- Ym -- mafic
- Vmp -- pahoehoe lava
- Va -- andesite/dacite
- Vr -- rhyolite/rhyolite
- Vc -- volcanoclastic, tuff, agglomerate

**Metamorphic rocks**

- Kn -- granitic gneiss
- Ks -- schist
- Ka -- amphibolite
- Sp -- phyllite
- Ph -- phyllonite
- Sv -- phyllite/cleaved mafic volcanoclastic
- S -- slate

**Plutonic rocks**

- Q -- granite/adamellite, or undifferentiated granitoid rocks
- Qd -- granodiorite
- Ql -- diorite/gtz diorite
- Qy -- syenite
- Vp -- porphyry dikes and sills
- Bd -- dolerite
- Bg -- gabbro
- Bgp -- gabbro & pyroxenite
- U -- ultramafic rocks, serpentinite

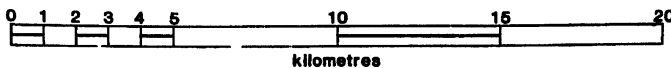
**Other symbols**

- edge of bedrock outcrop
- dirt road/track
- main road
- limit of mapping
- geological contact
- fault
- fault, with Quaternary movement
- fault displacement; normal reverse strike-slip teeth/ticks in direction of dip

- OM244 locality/outcrop with number -- see Frame 1 for explanation of prefix letters
- C B67\* fossil-bearing locality or section of prefix letters
- Amdo town, village, or highway depot
- hot spring
- 6179 spot height (metres) (highest and/or lowest specified elevations on map)
- lake

- bedding, flat, inclined, upright, vertical, overturned: dips in degrees
- younging (in absence of bedding measurement)
- cleavage/phyllitic cleavage, inclined, vertical
- gneissic foliation/schistosity, inclined, vertical
- minor fault orientation
- plunge of minor fold hinge (degrees)
- plunge of fabric lineation (mineral stretching)
- dike orientation

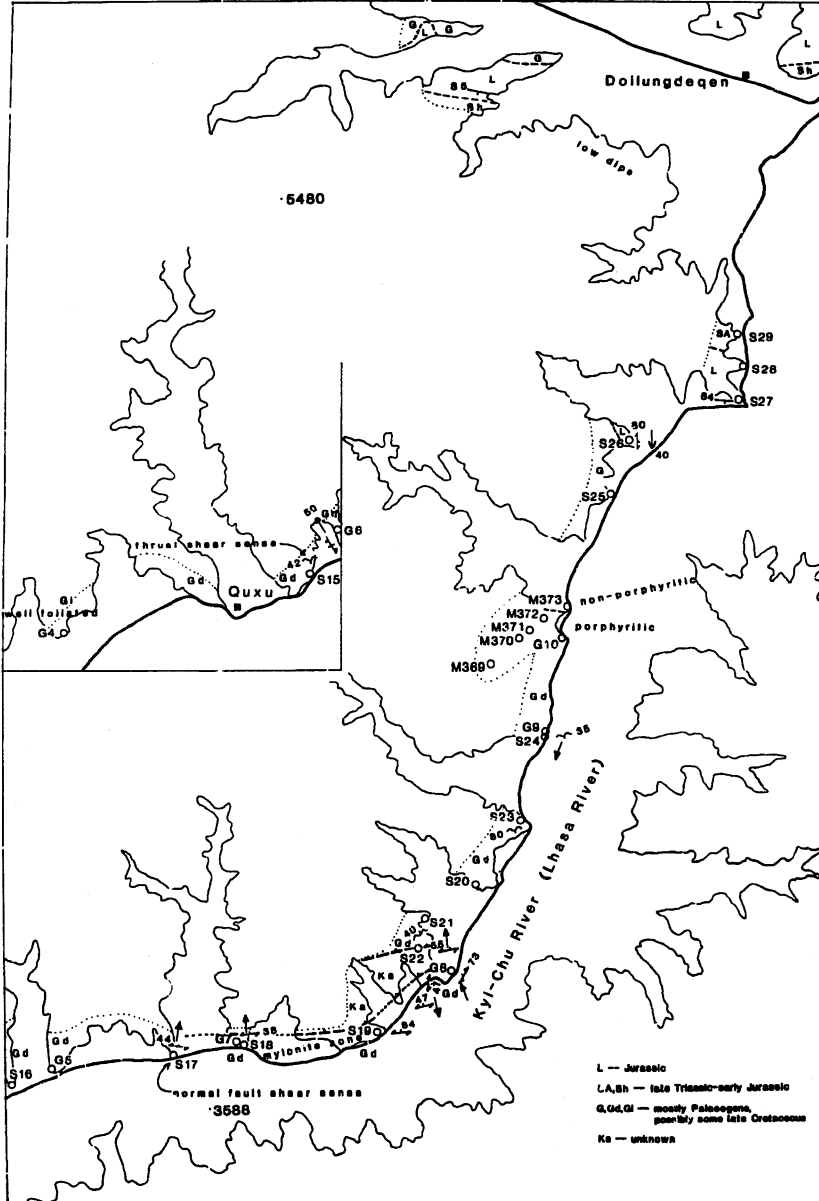
**Scale**



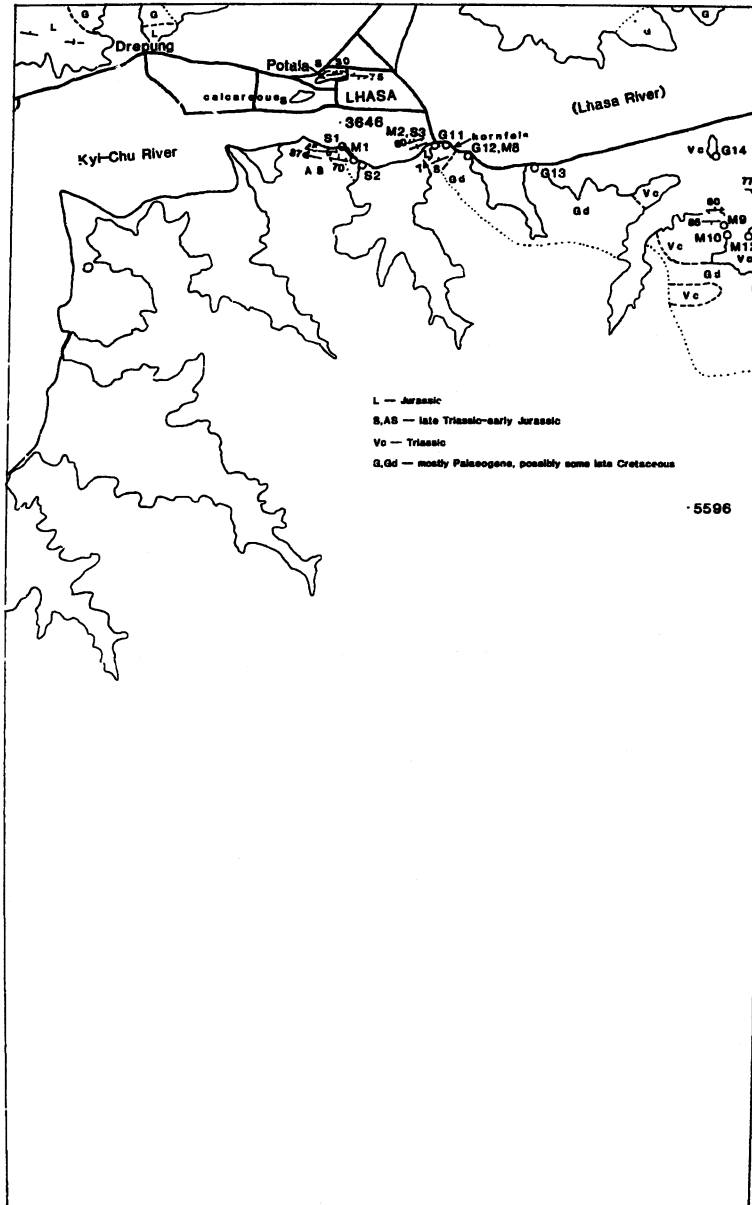
Maps drawn at 1:100,000. Base: PRC 1:100,000 topographic maps, most dated 1973-75 (see Frame 1).

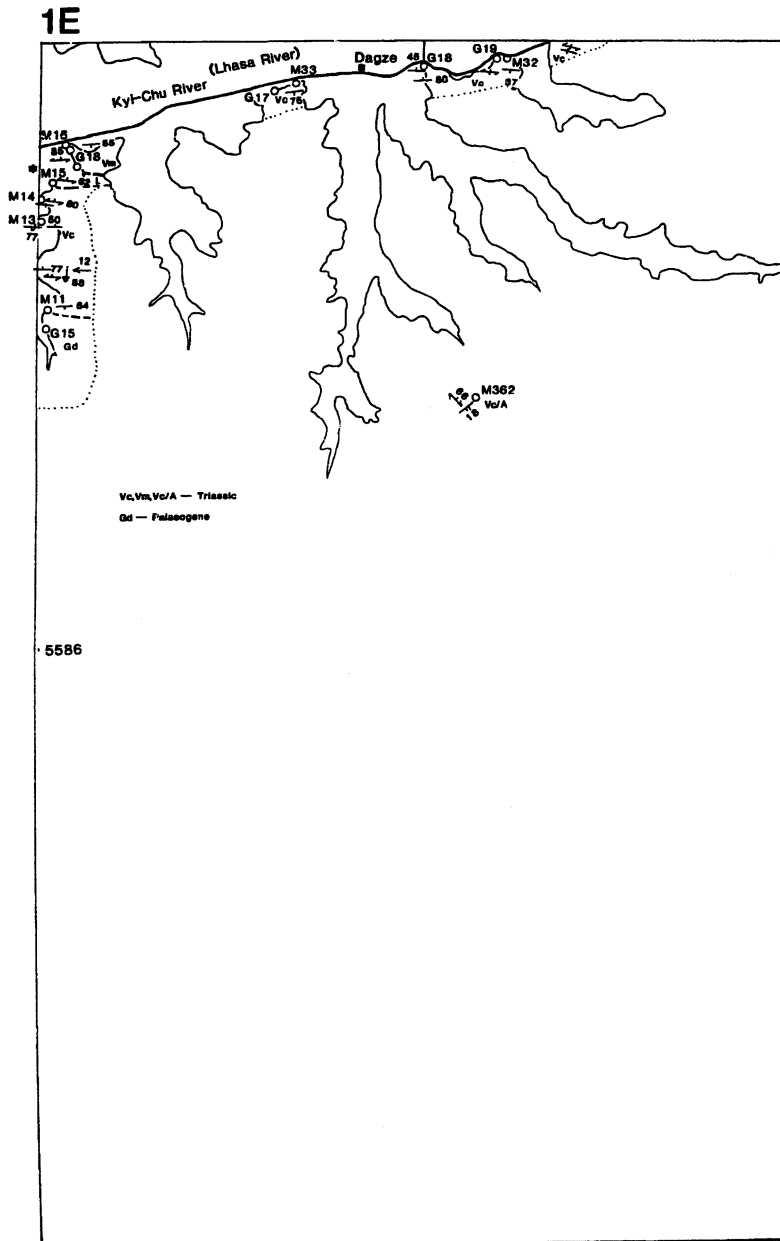


2E+2W

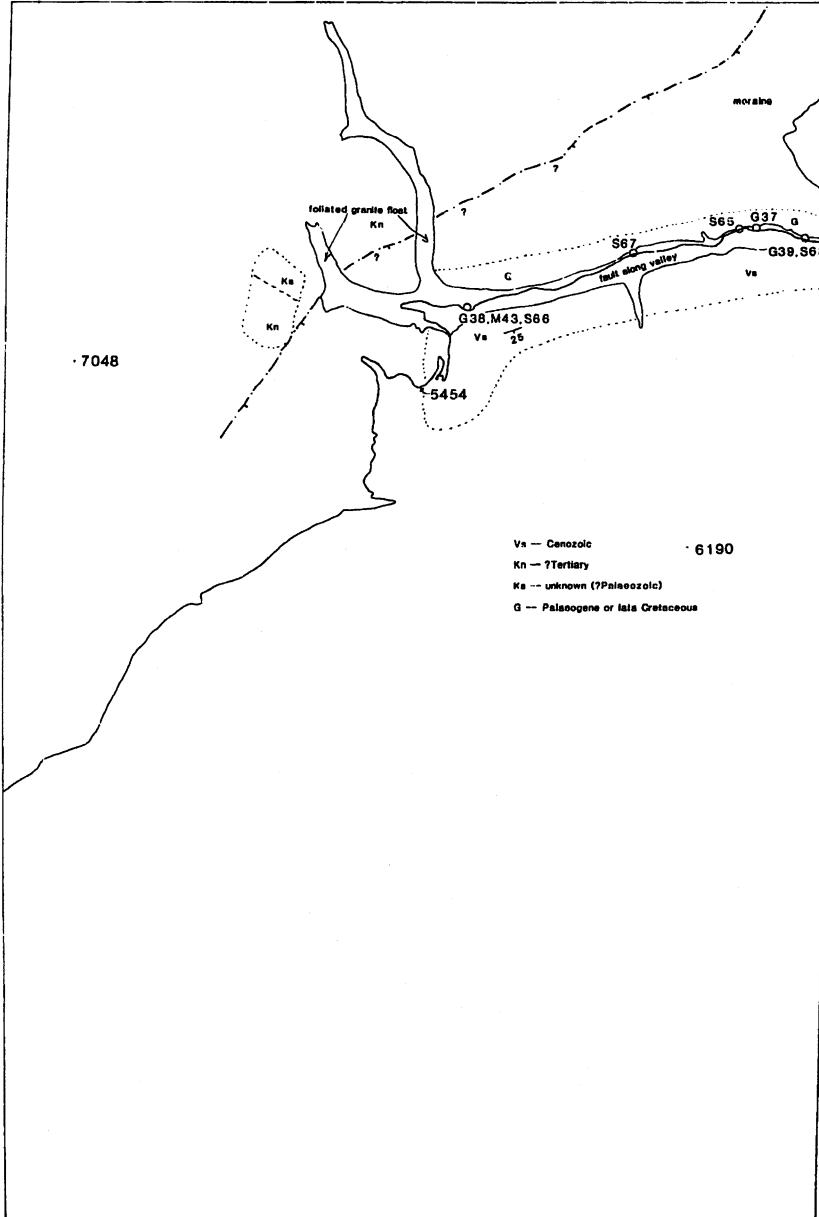


1W

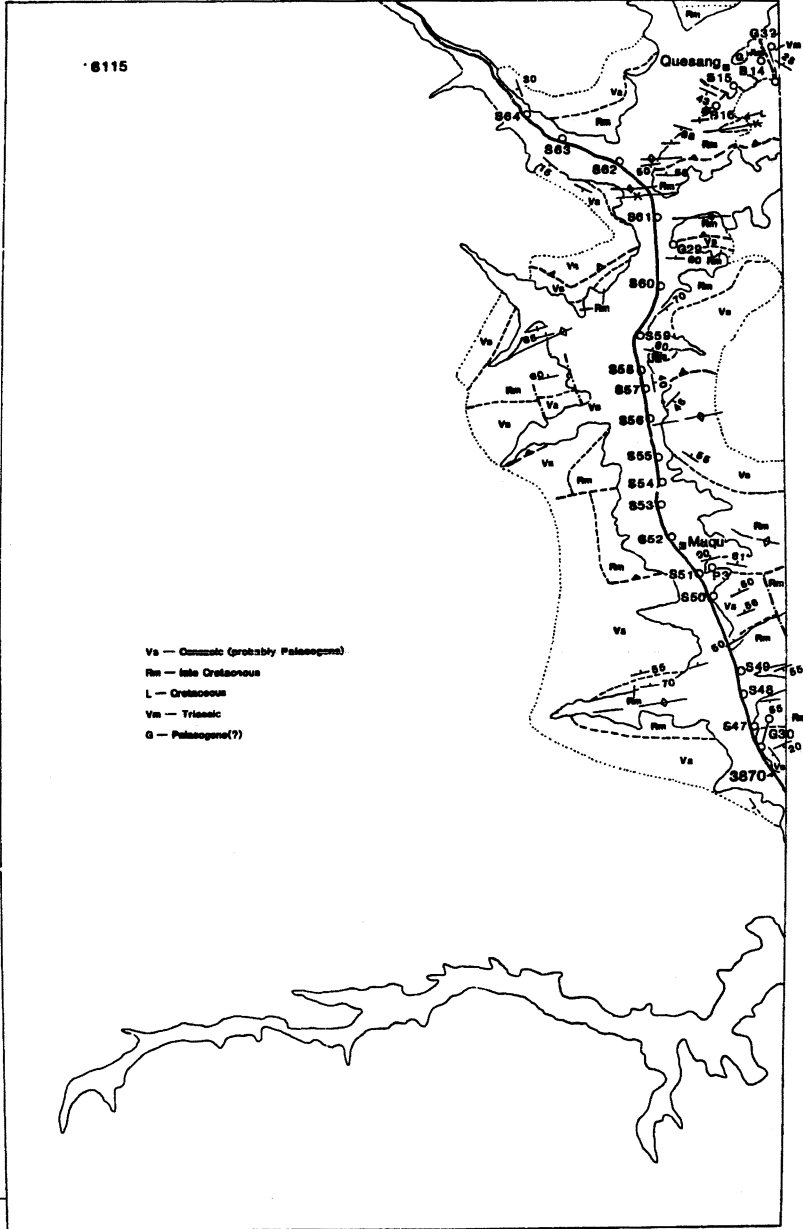




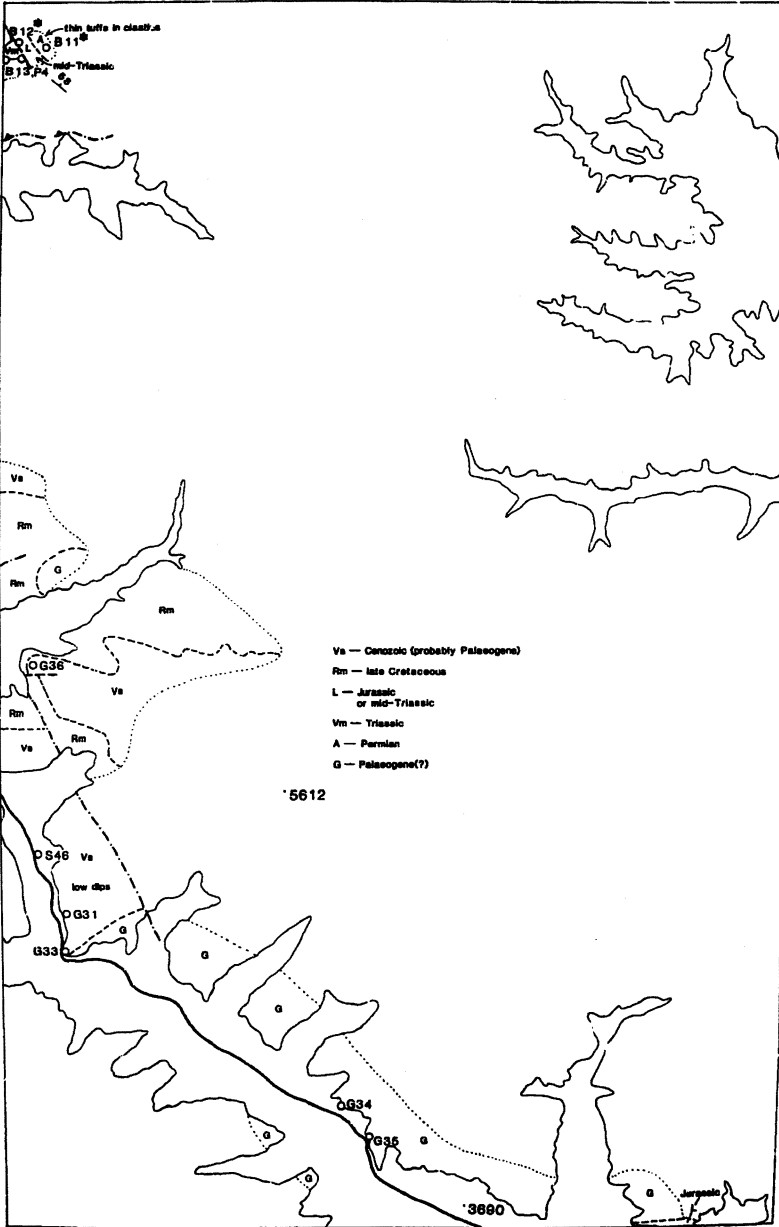
5W



4W

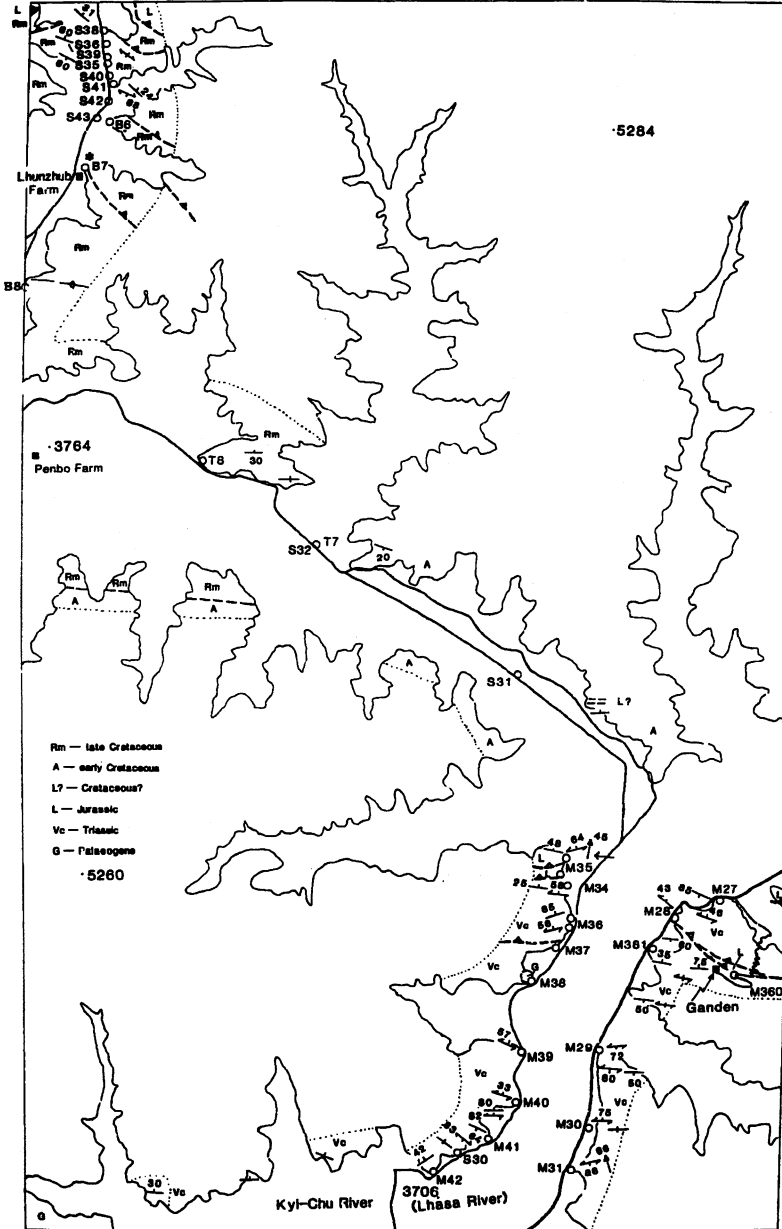


4E



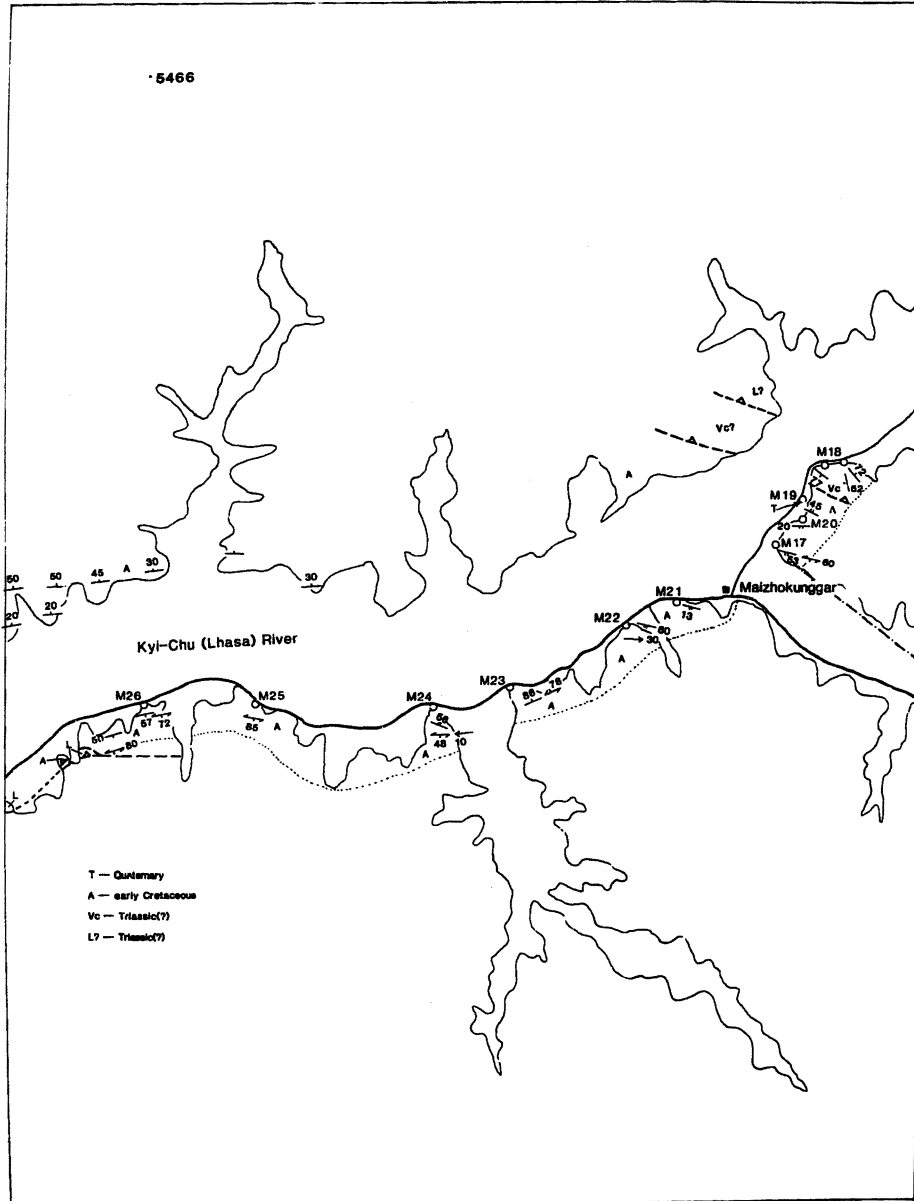


3E

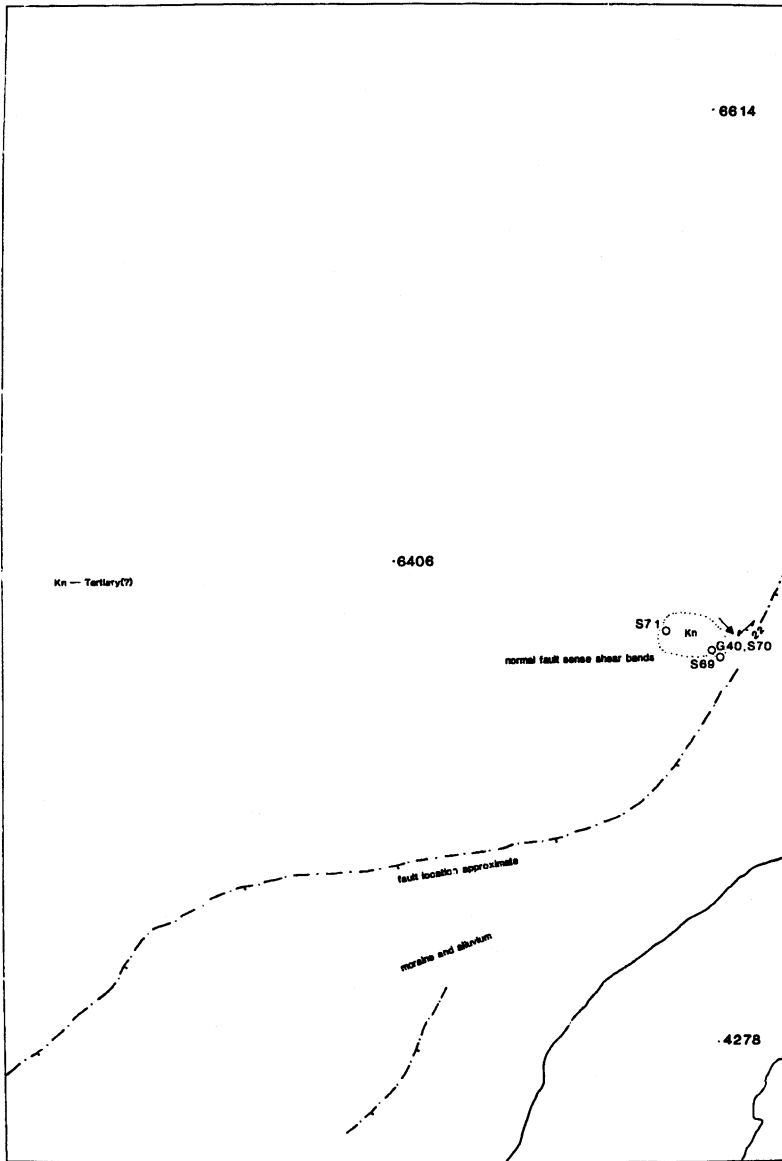




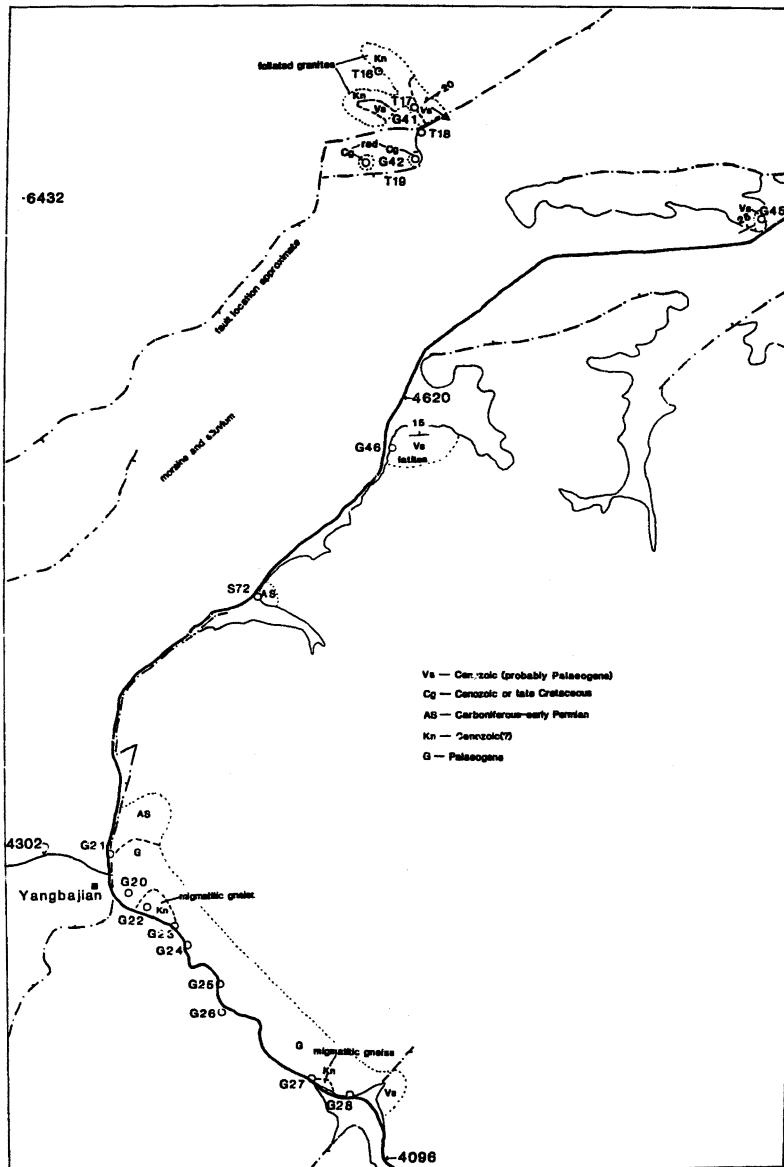
AW



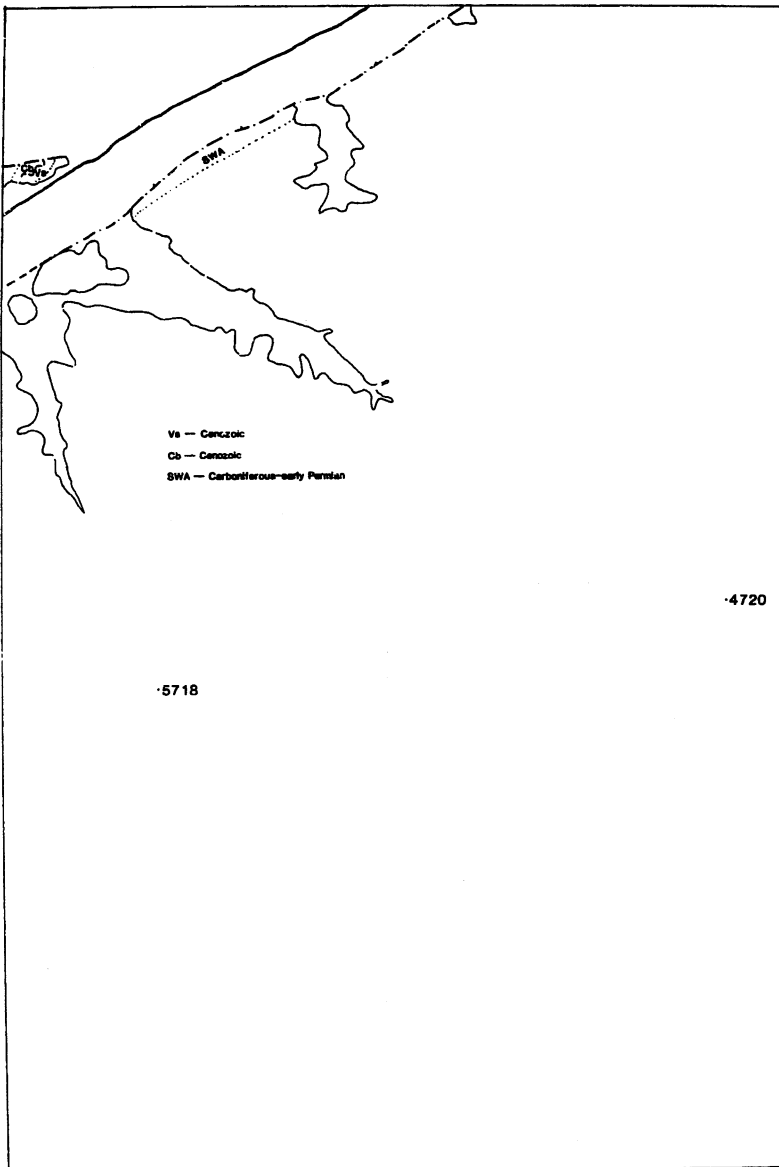
6E



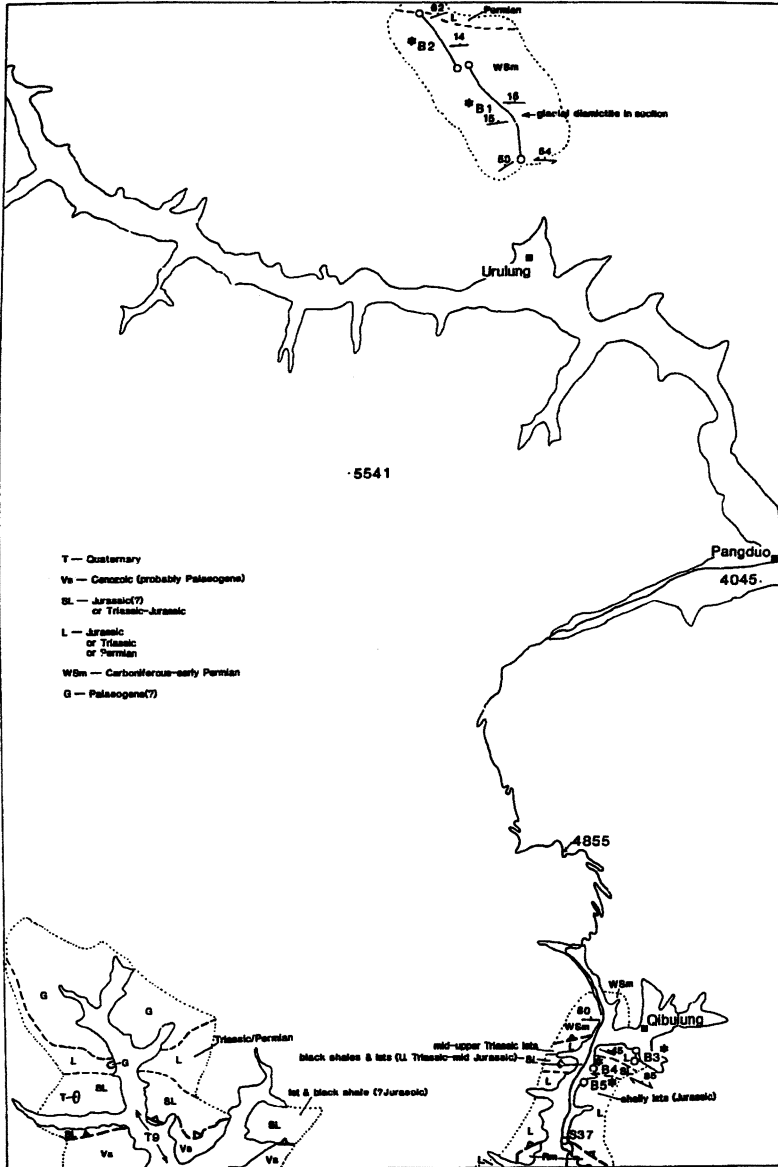
7W



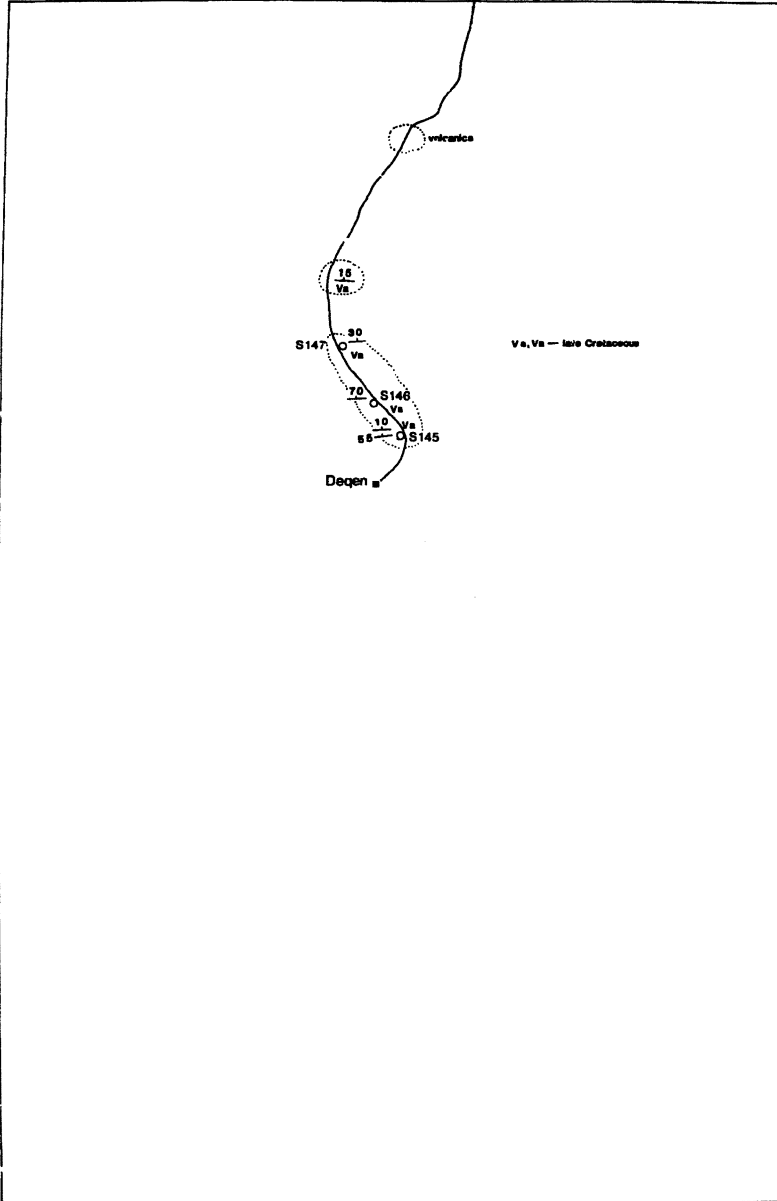
7E



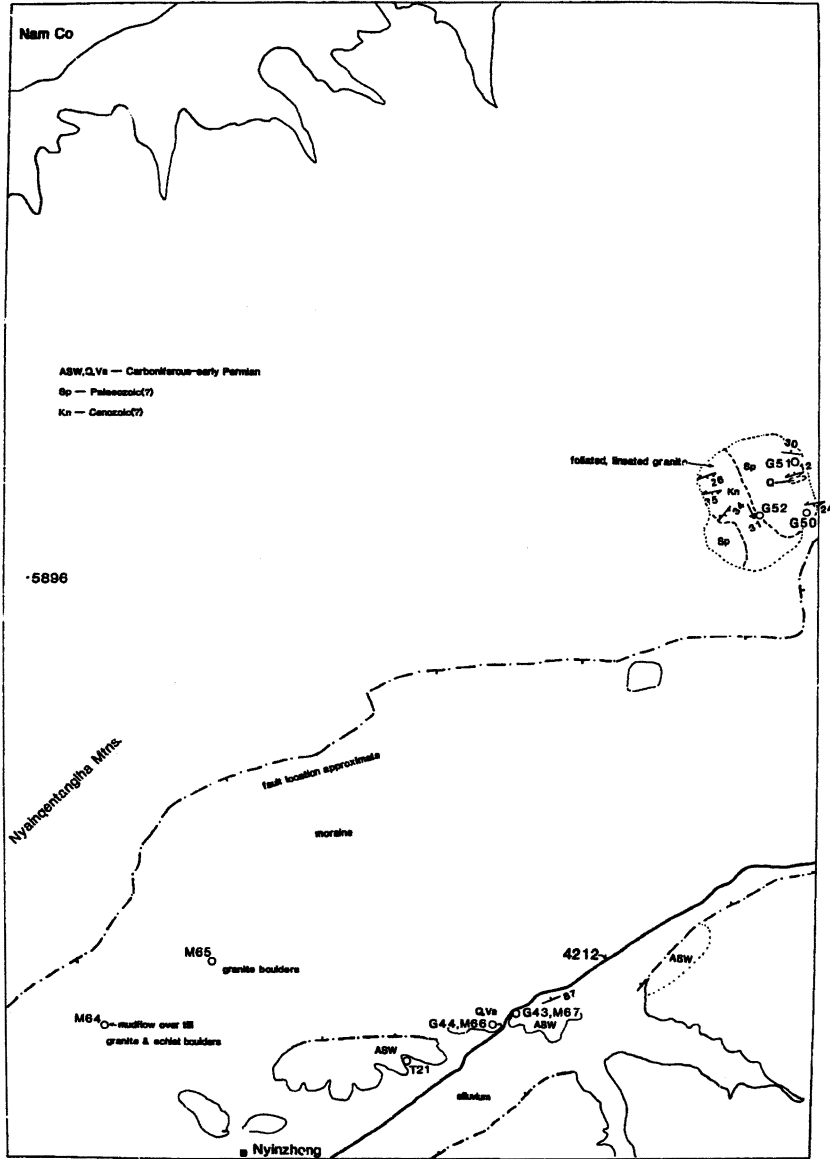
8C



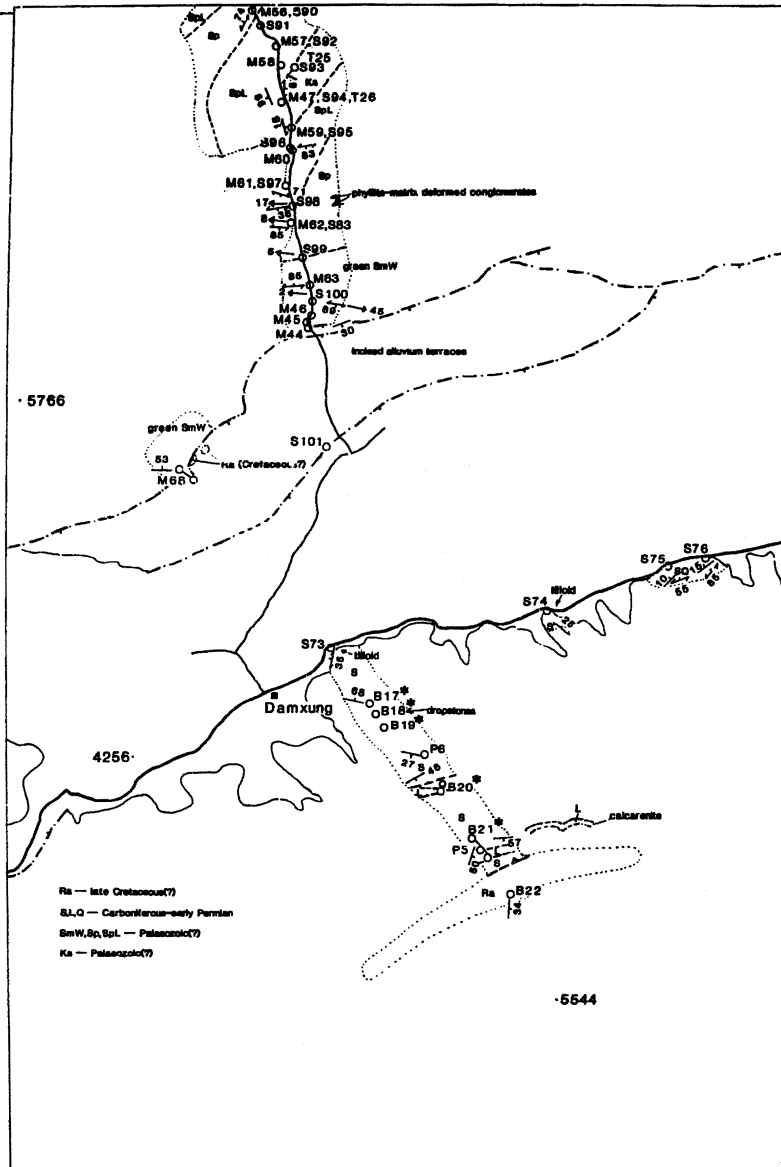
**BW** From enlargement of Spacelab metric camera image. NOT from topographic base



# 11E

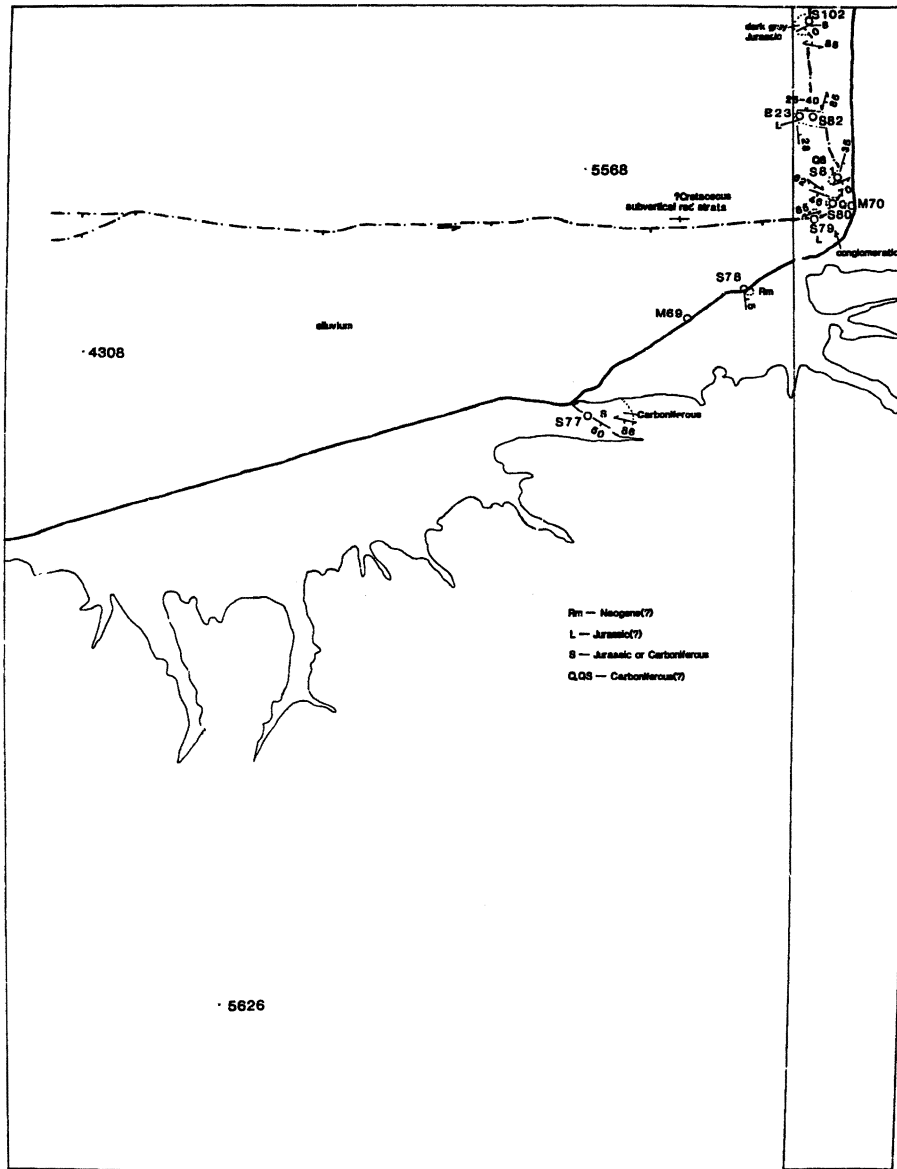


10W

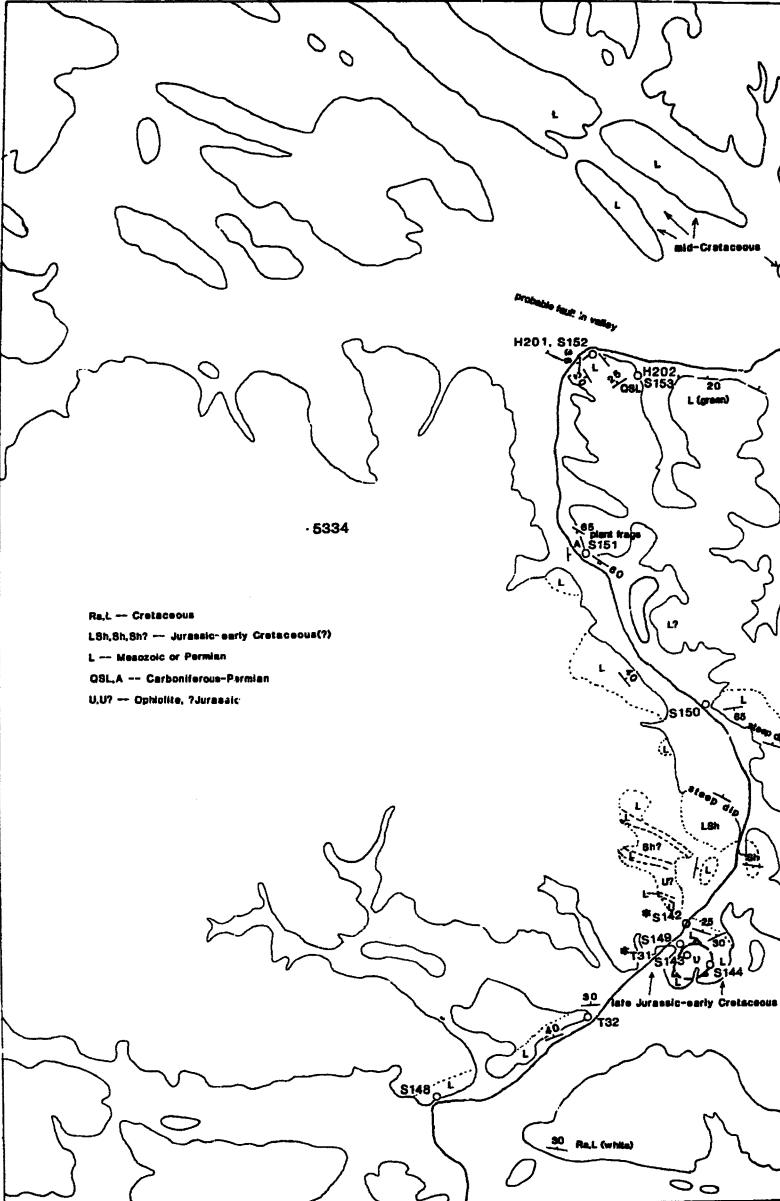




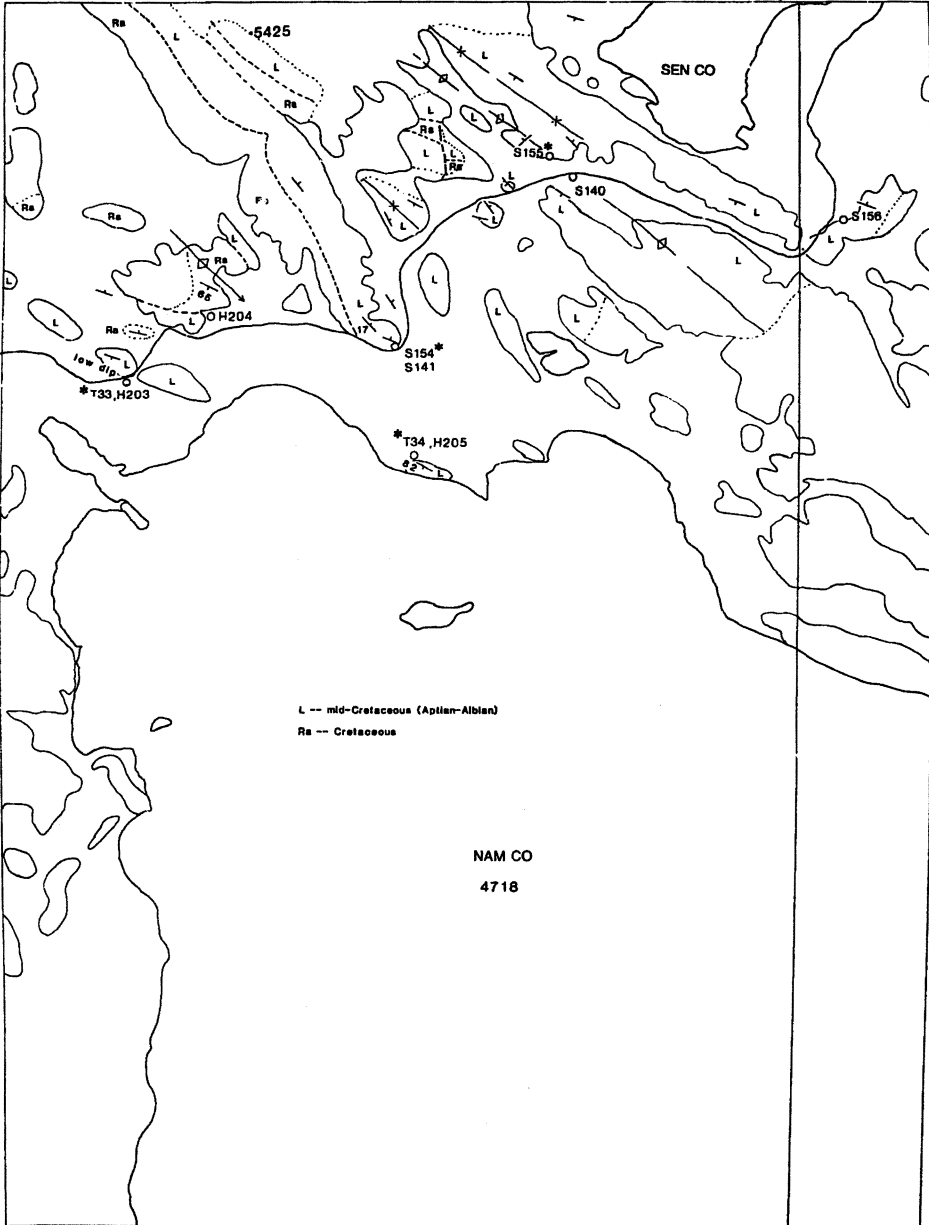
10E+9W



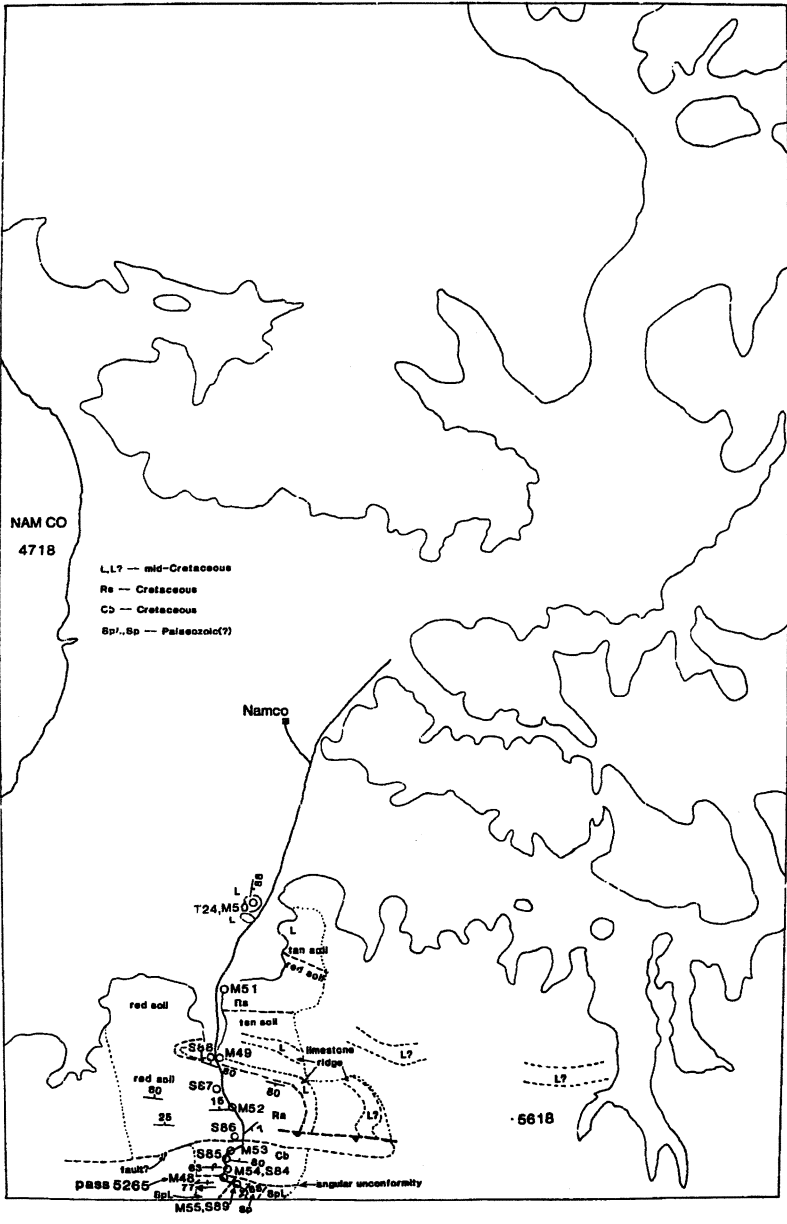
CW



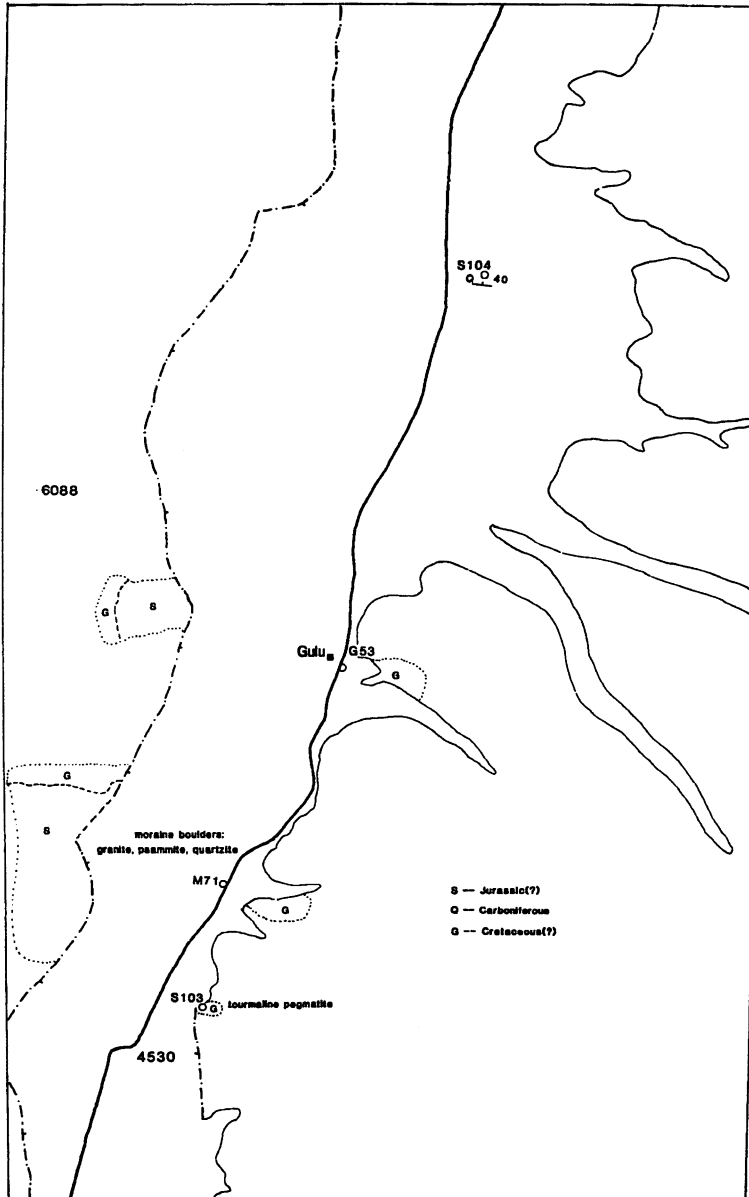
CE+DW



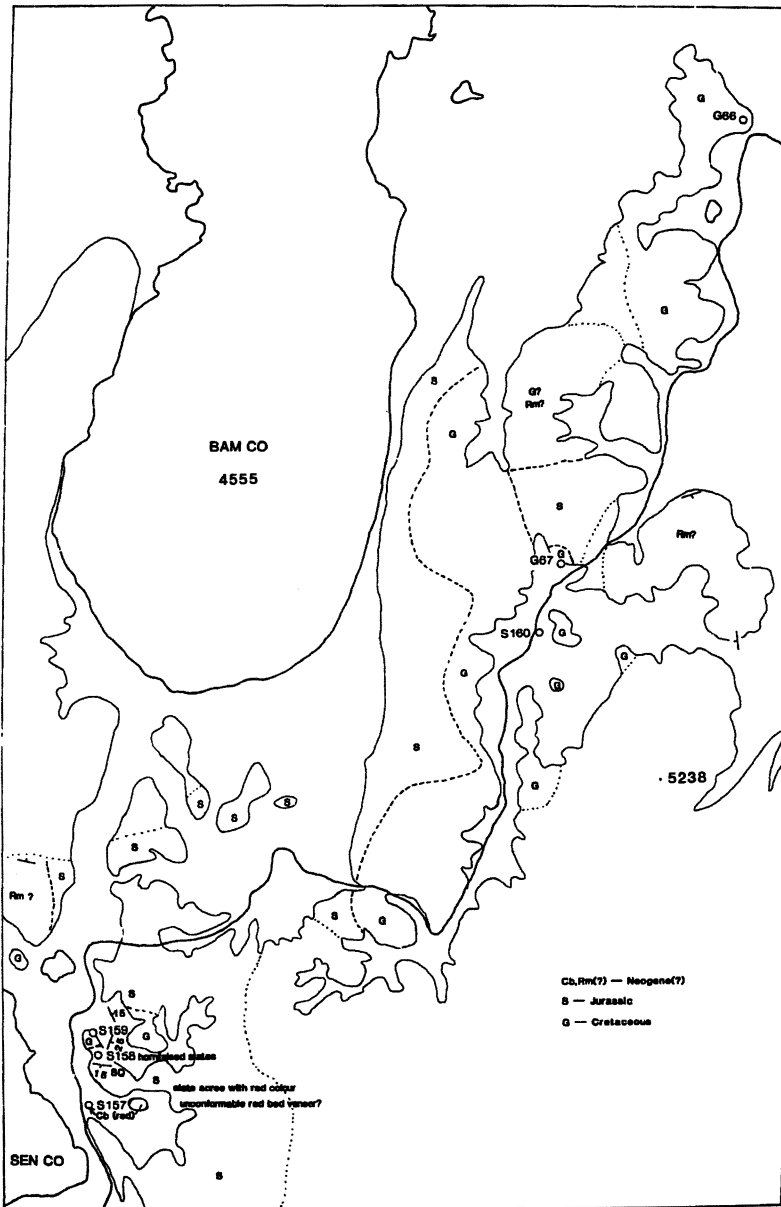
12W

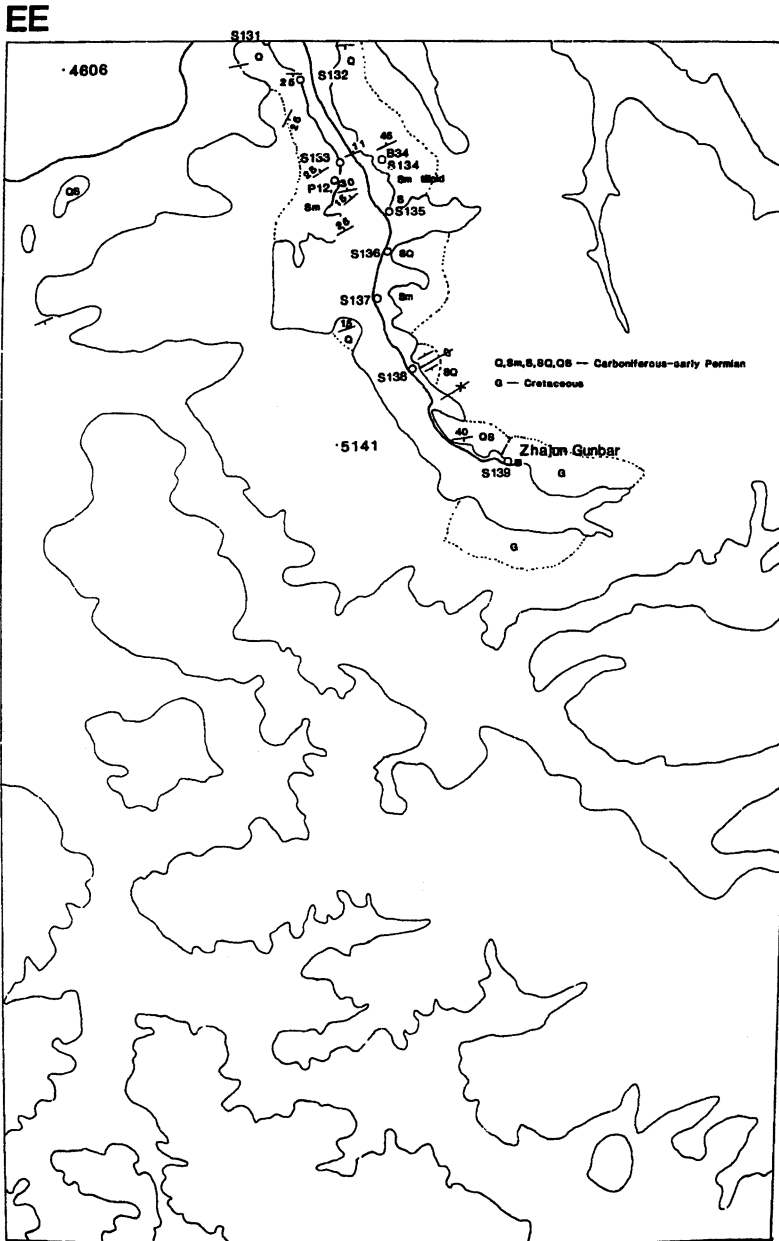


13W

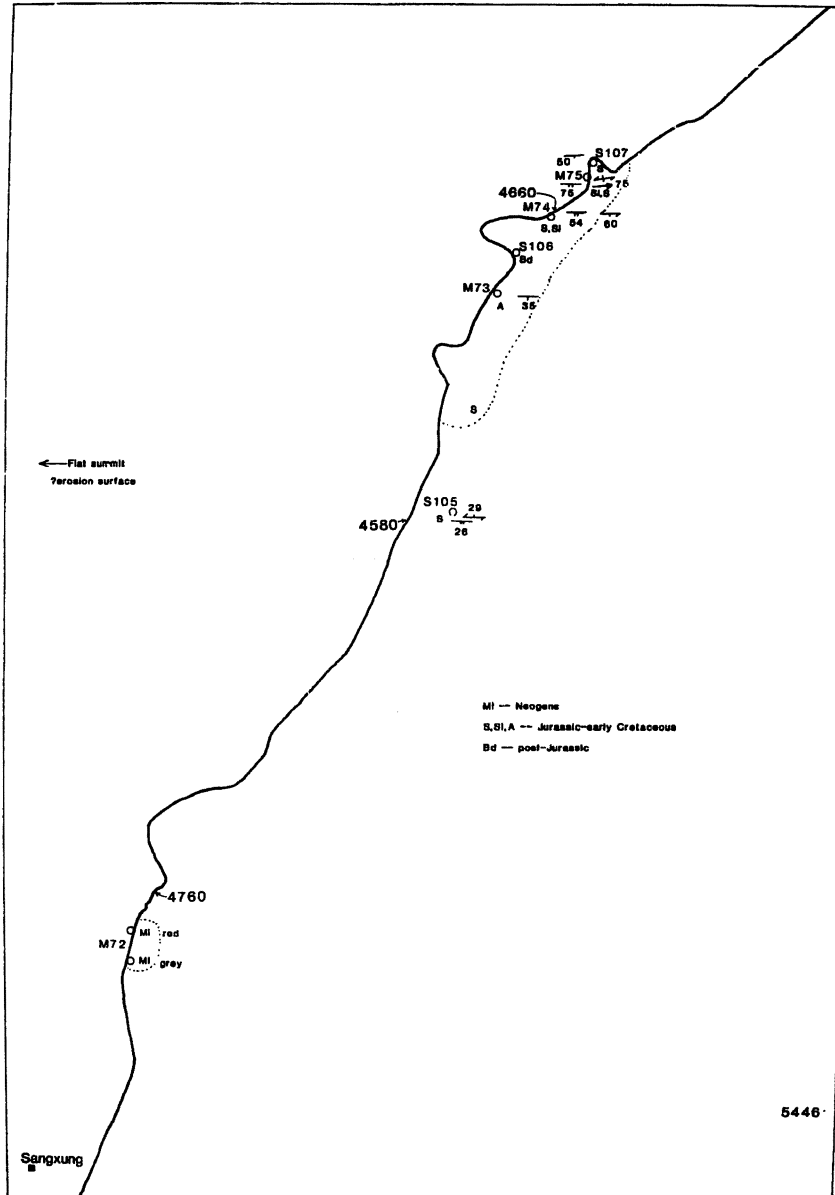


EW



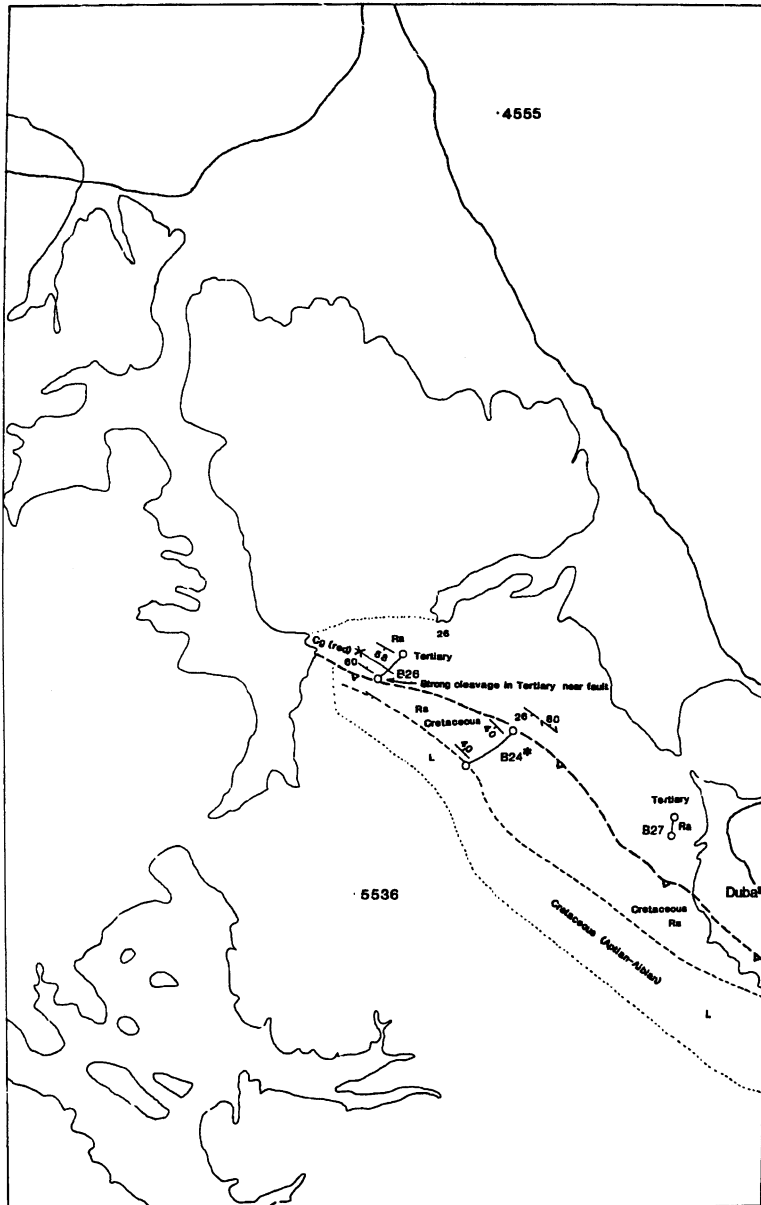


15C

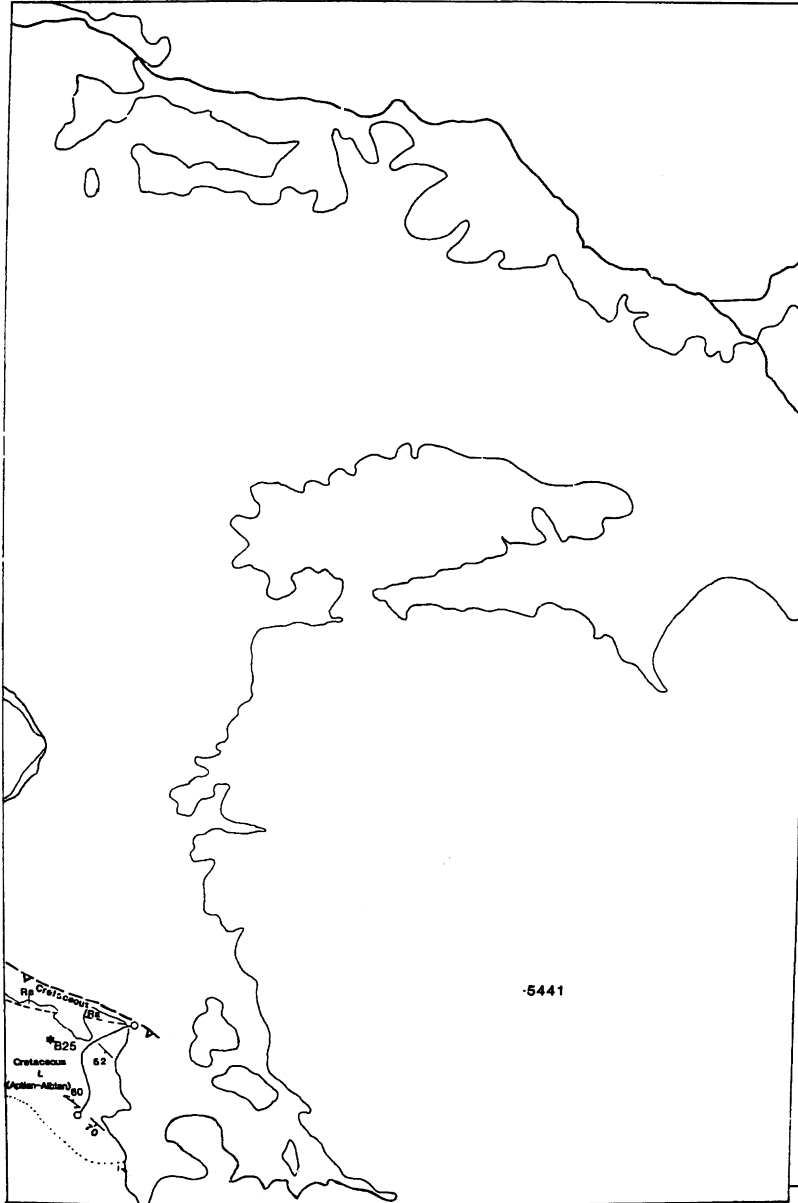




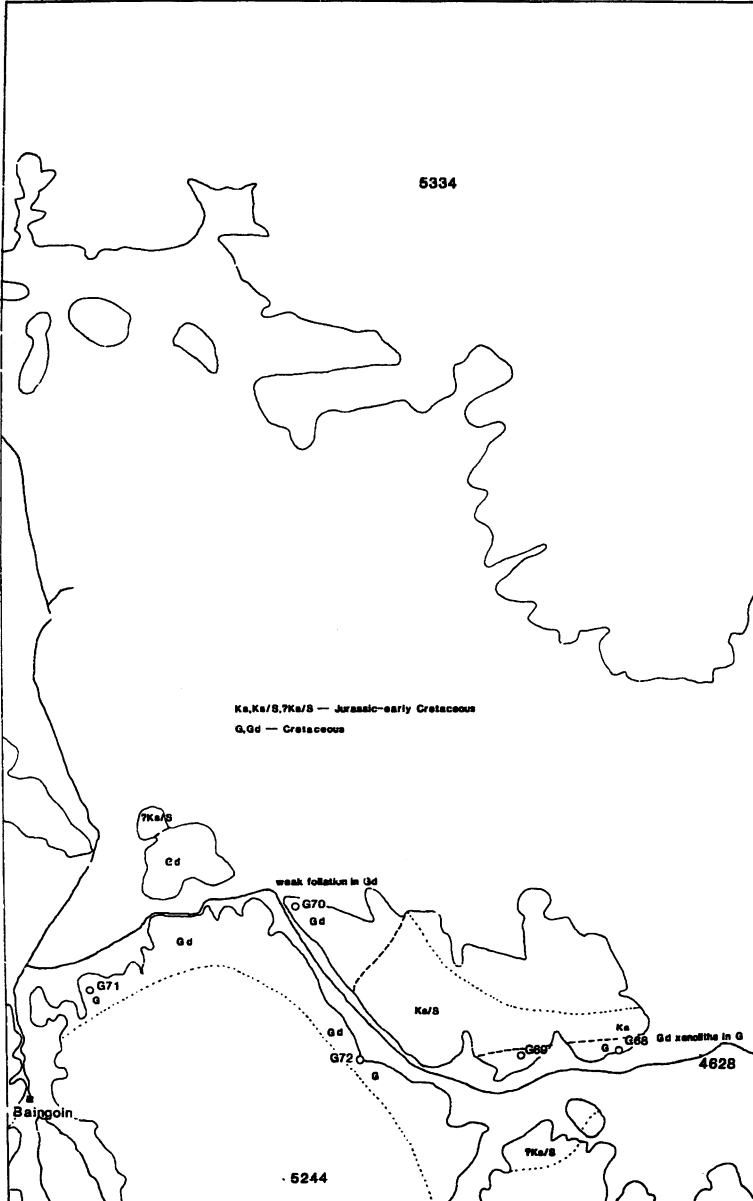
FW



FE



21W

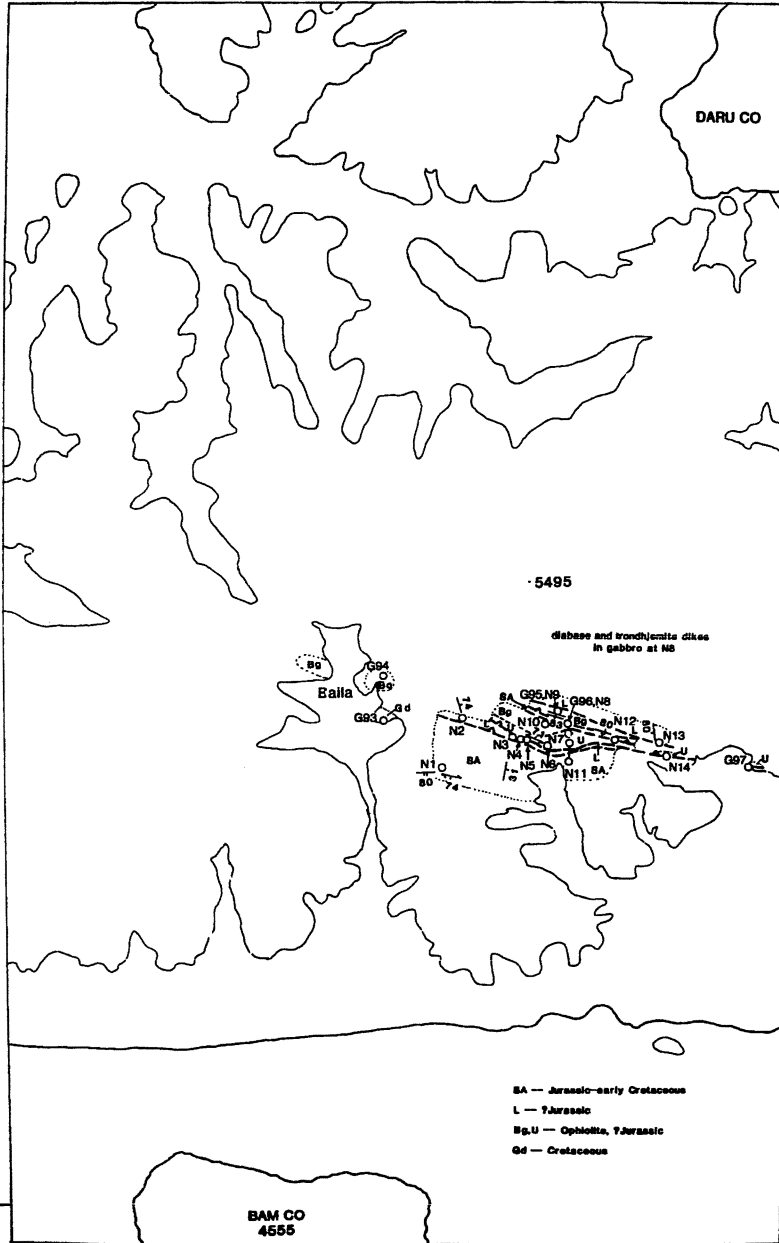


21E

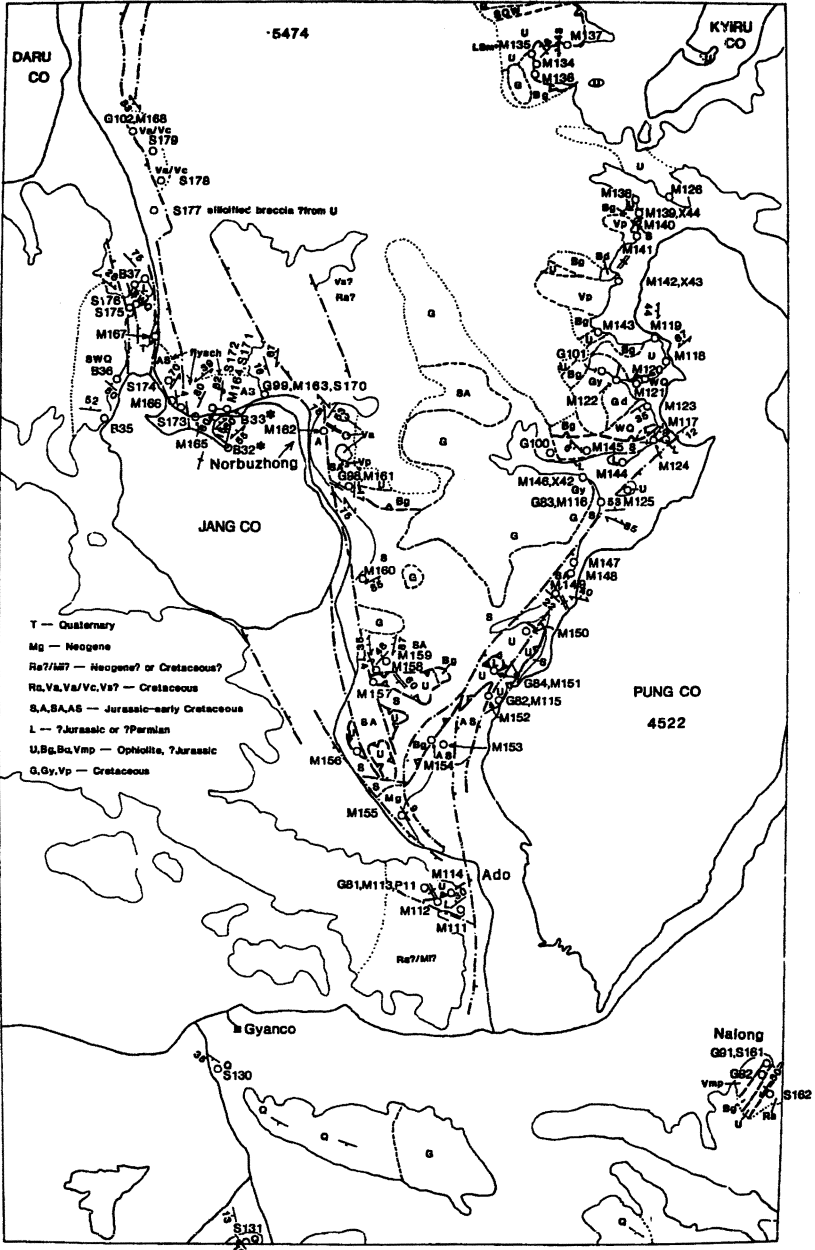


No localities on sheet 21E

20W

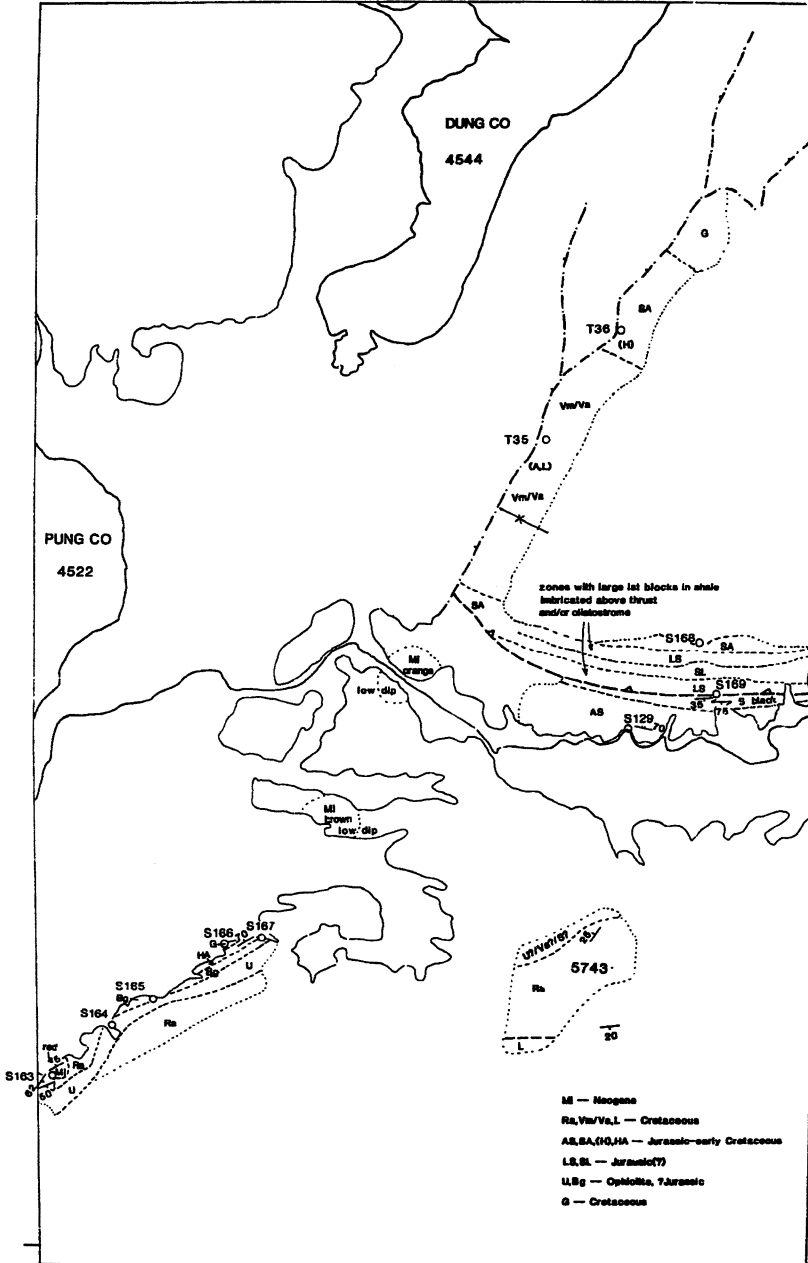


20E

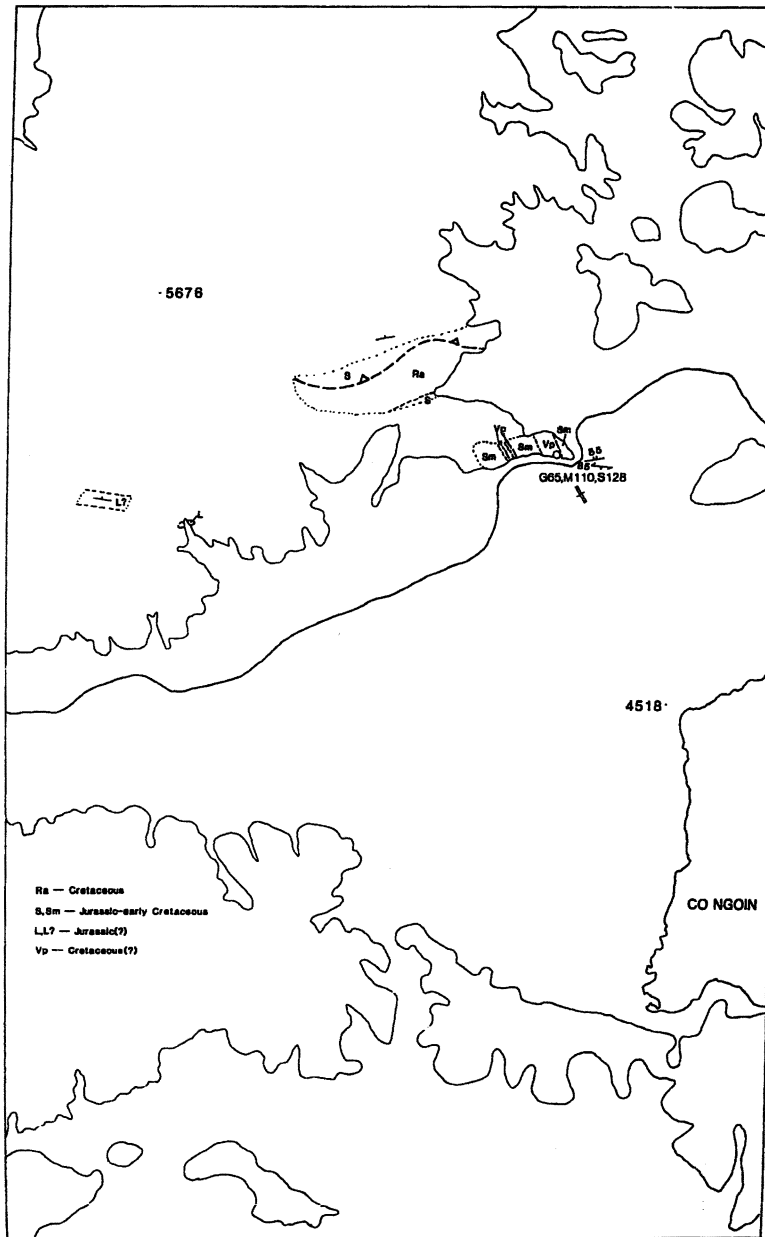


19W

34

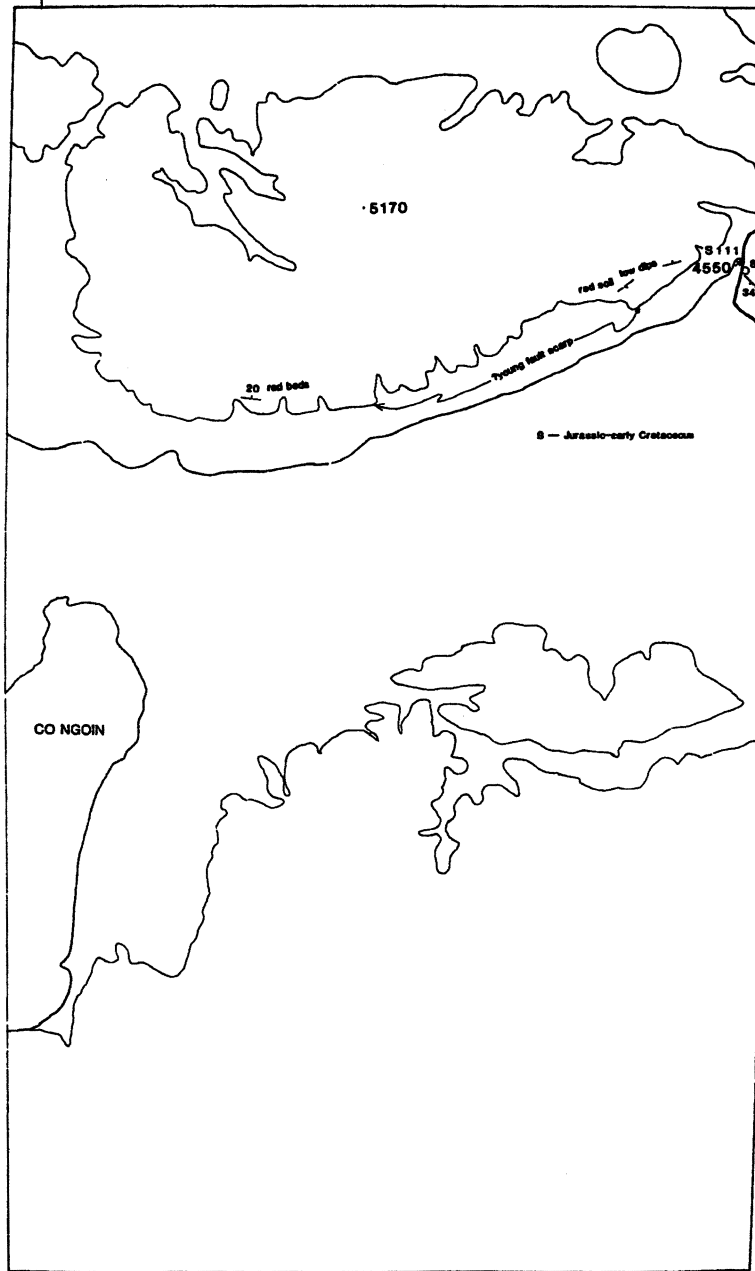


19E

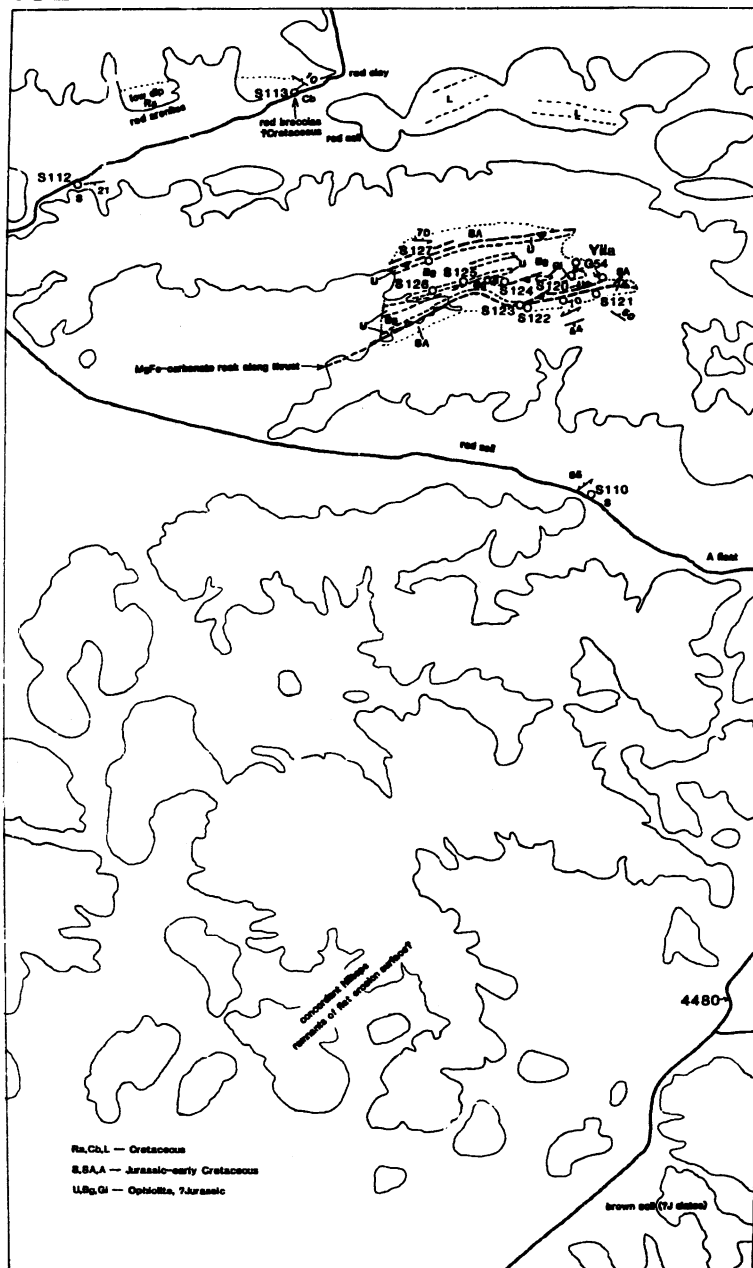




18W

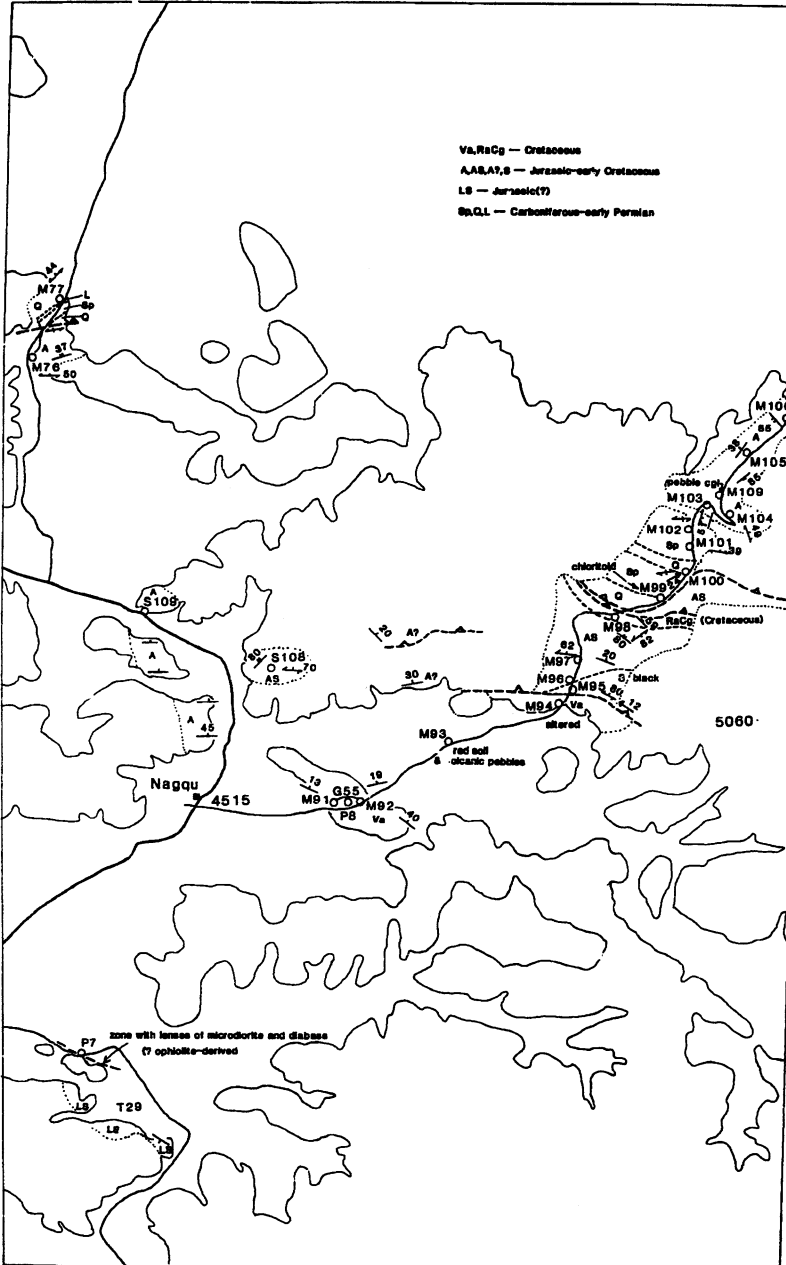


18E

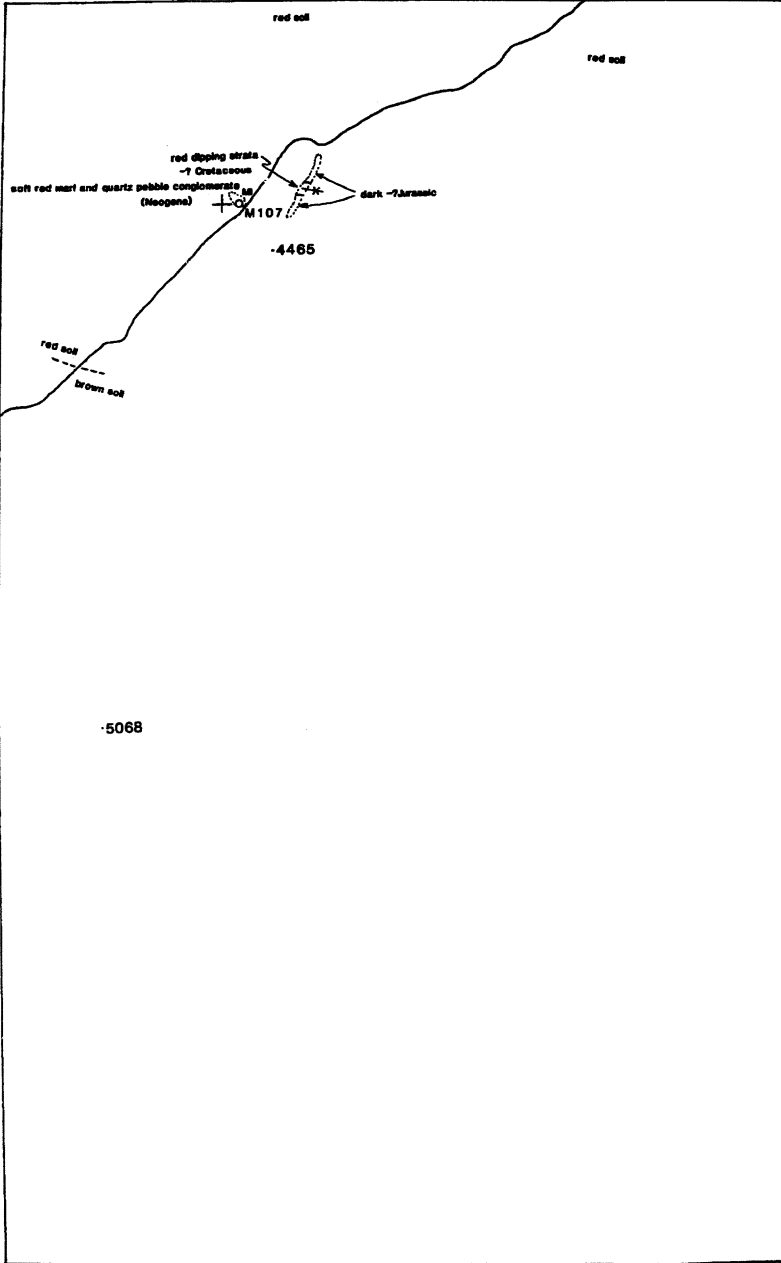


17W

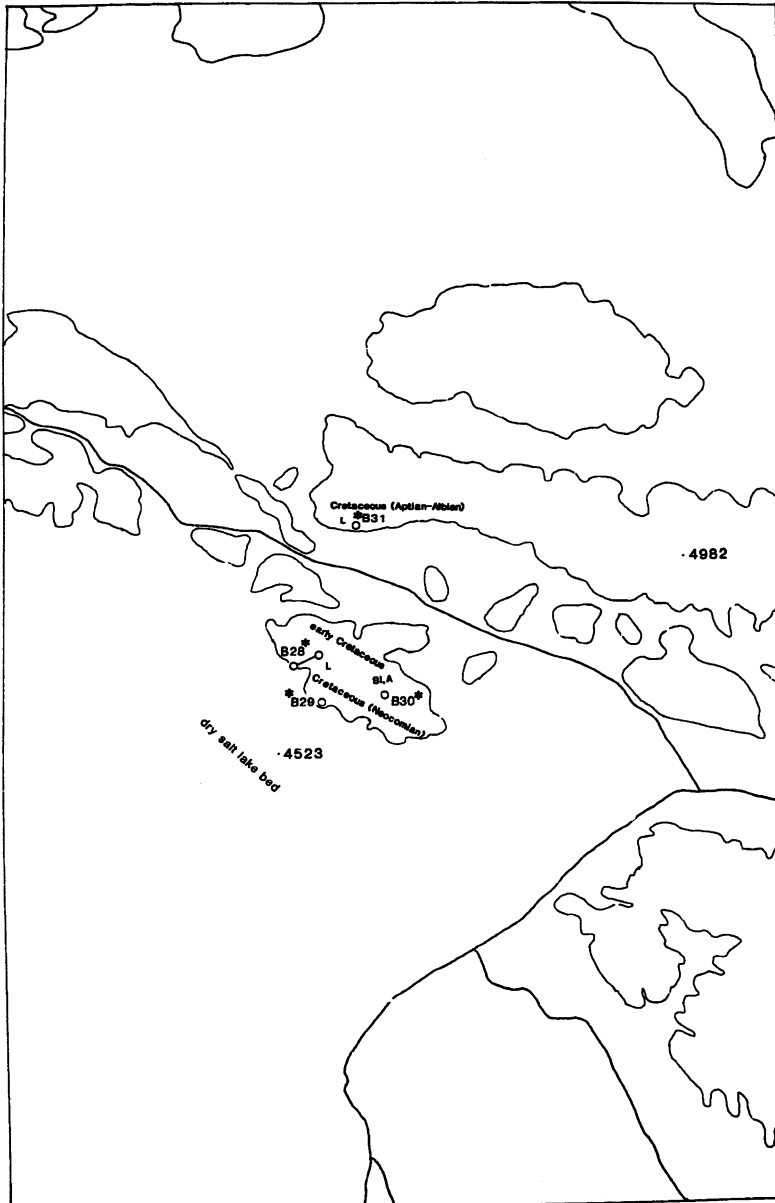
38

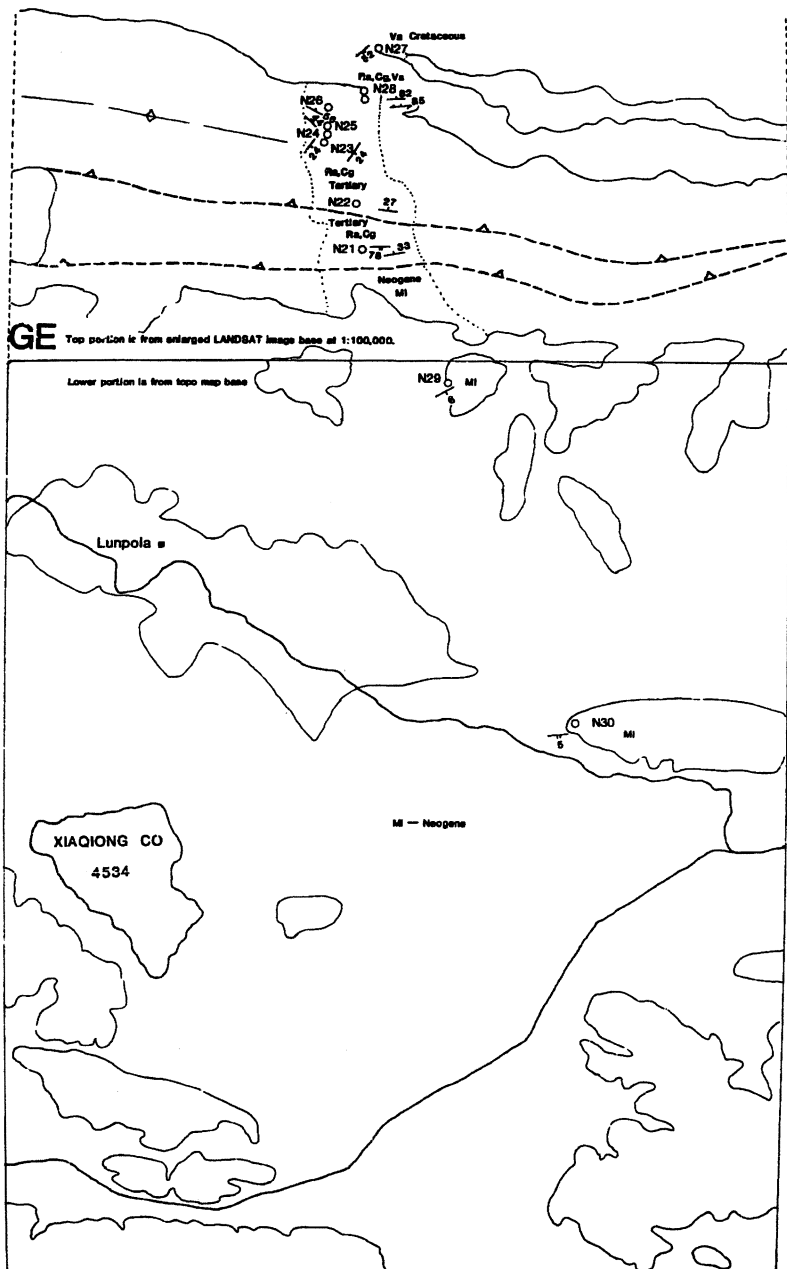


17E



GW

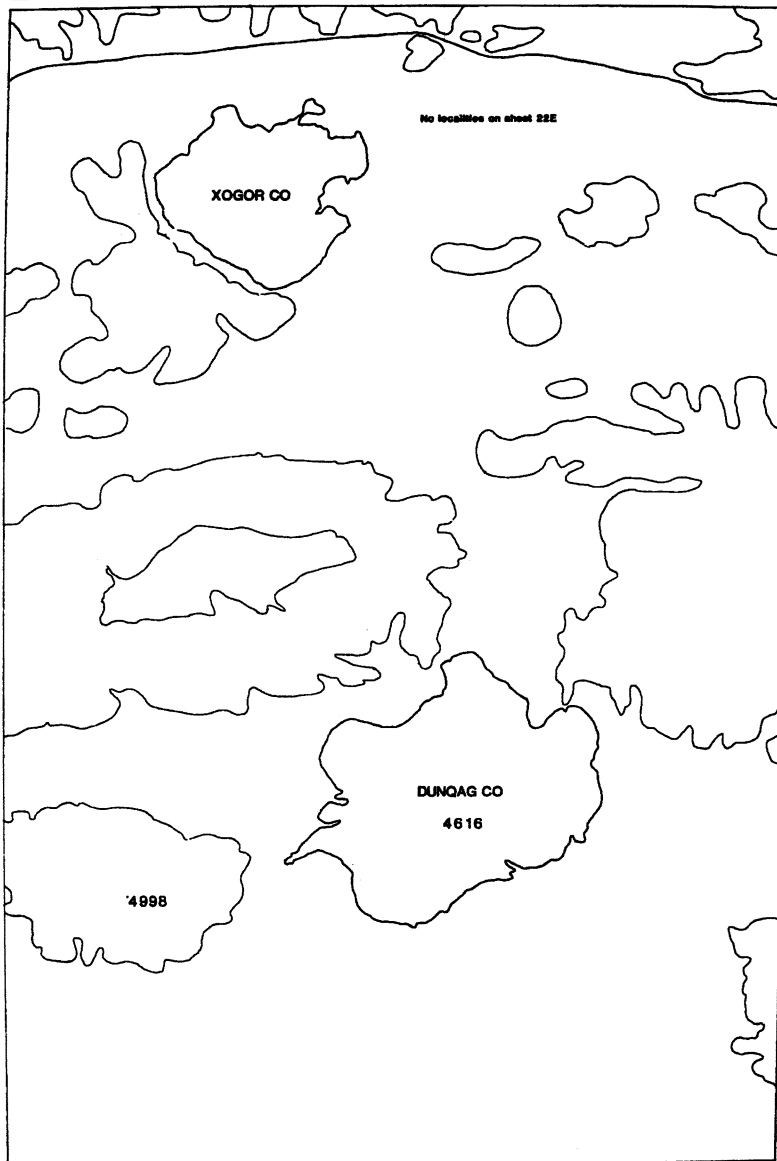




22W



22E

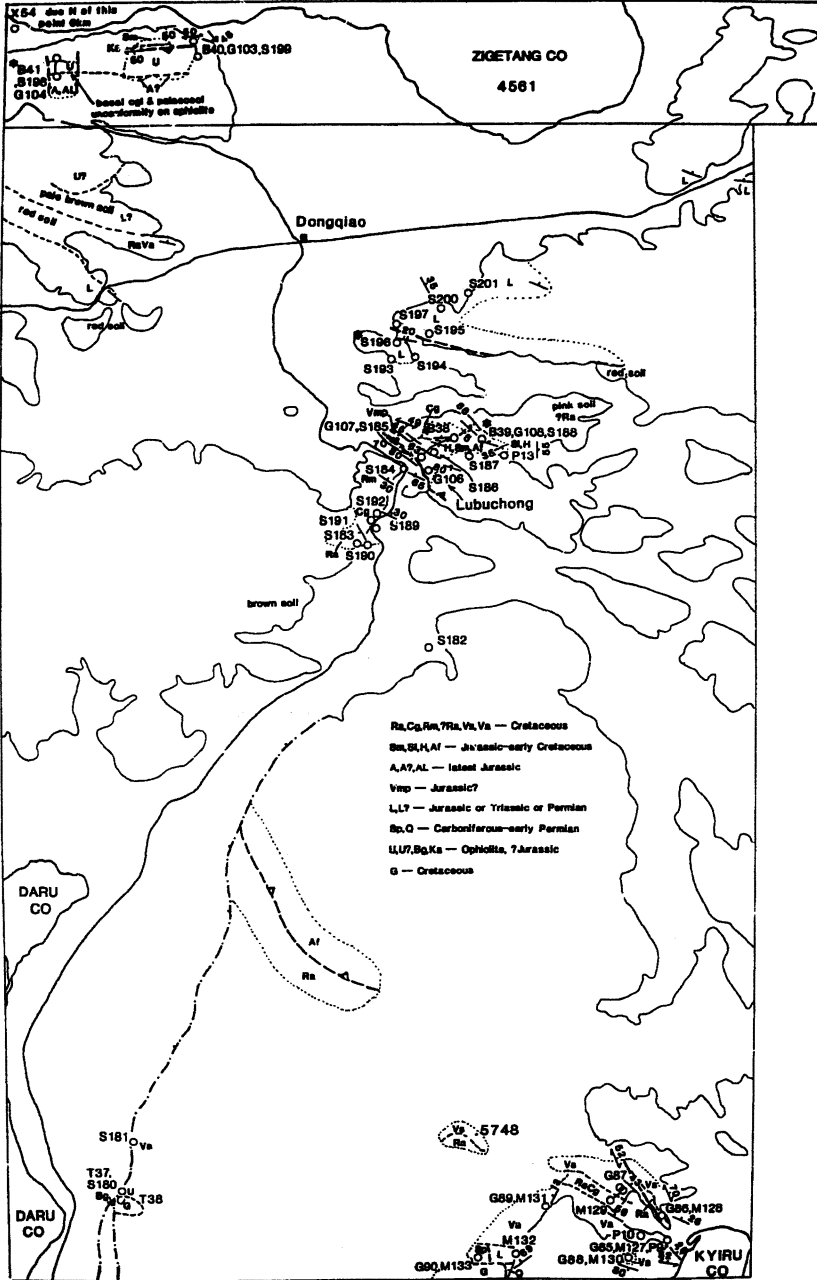




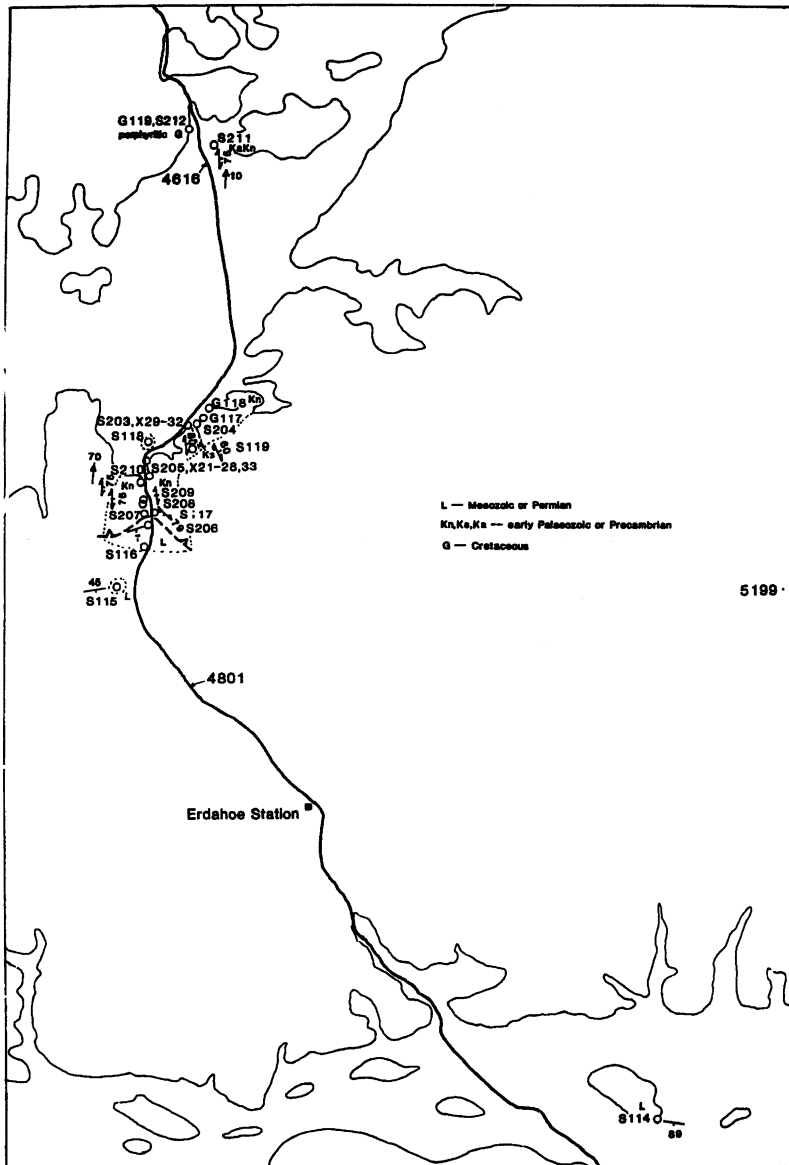
### 23W+30W



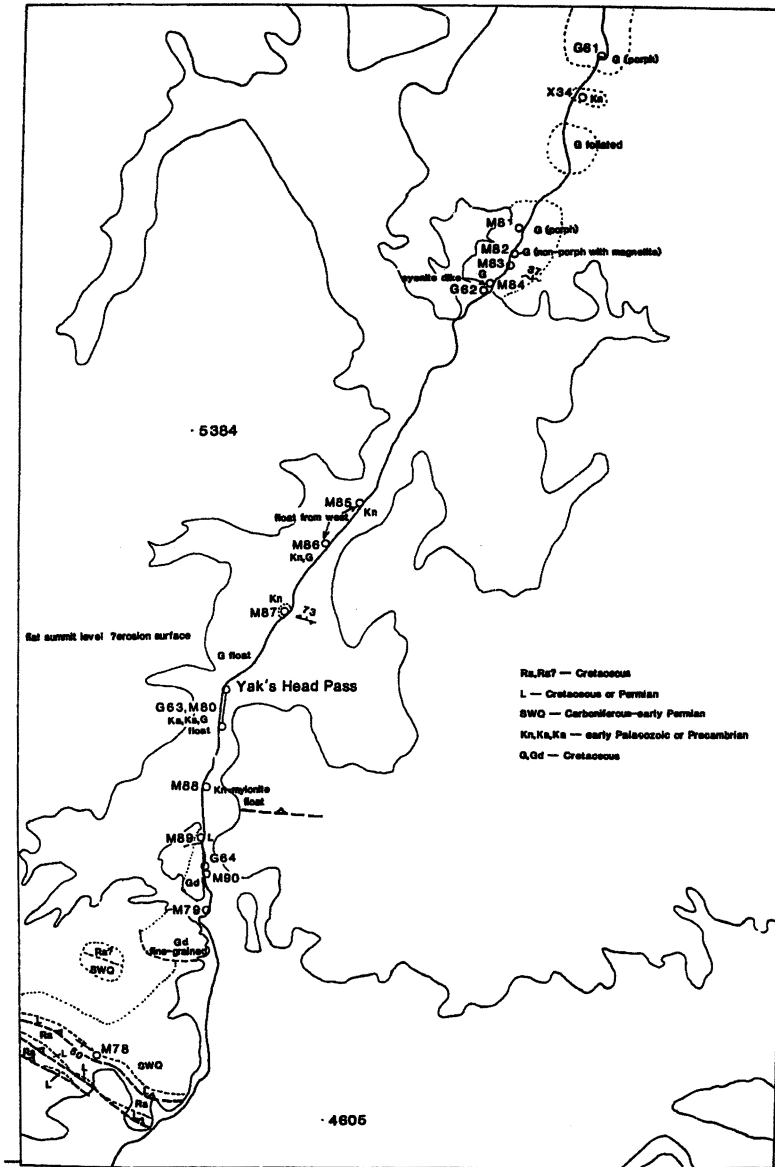
# 23E+30E



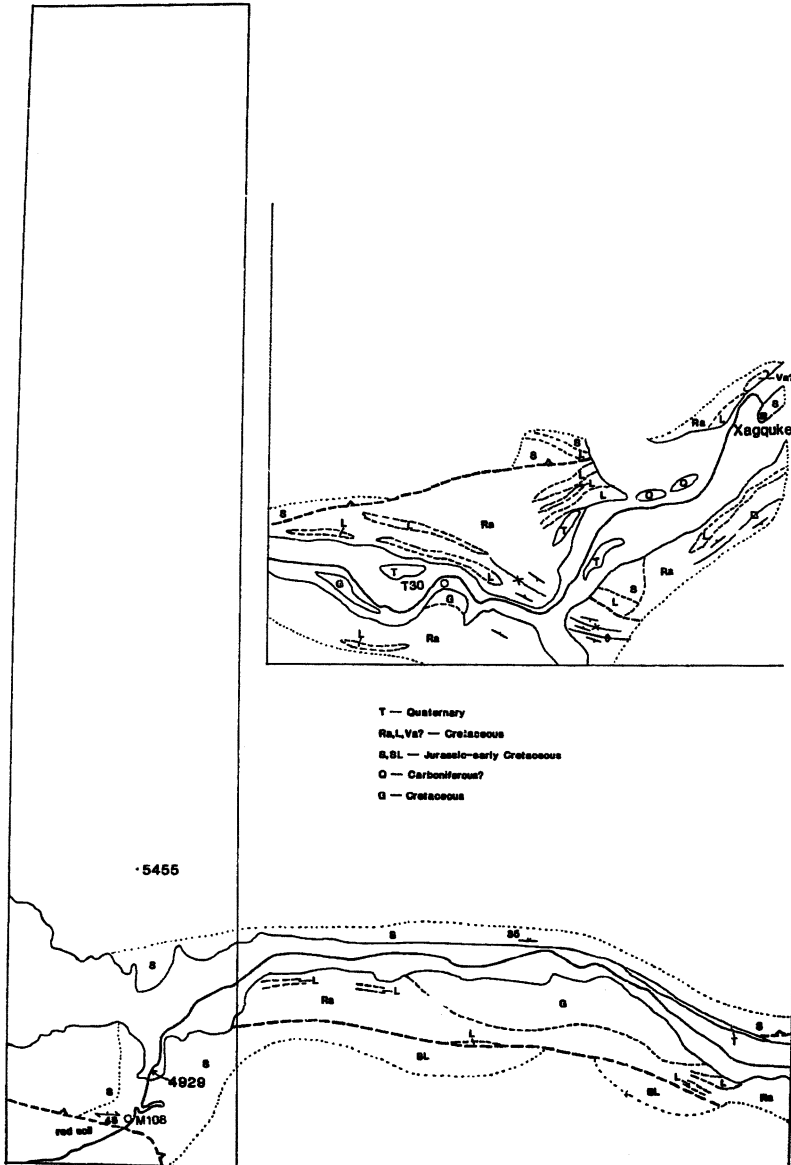
25C



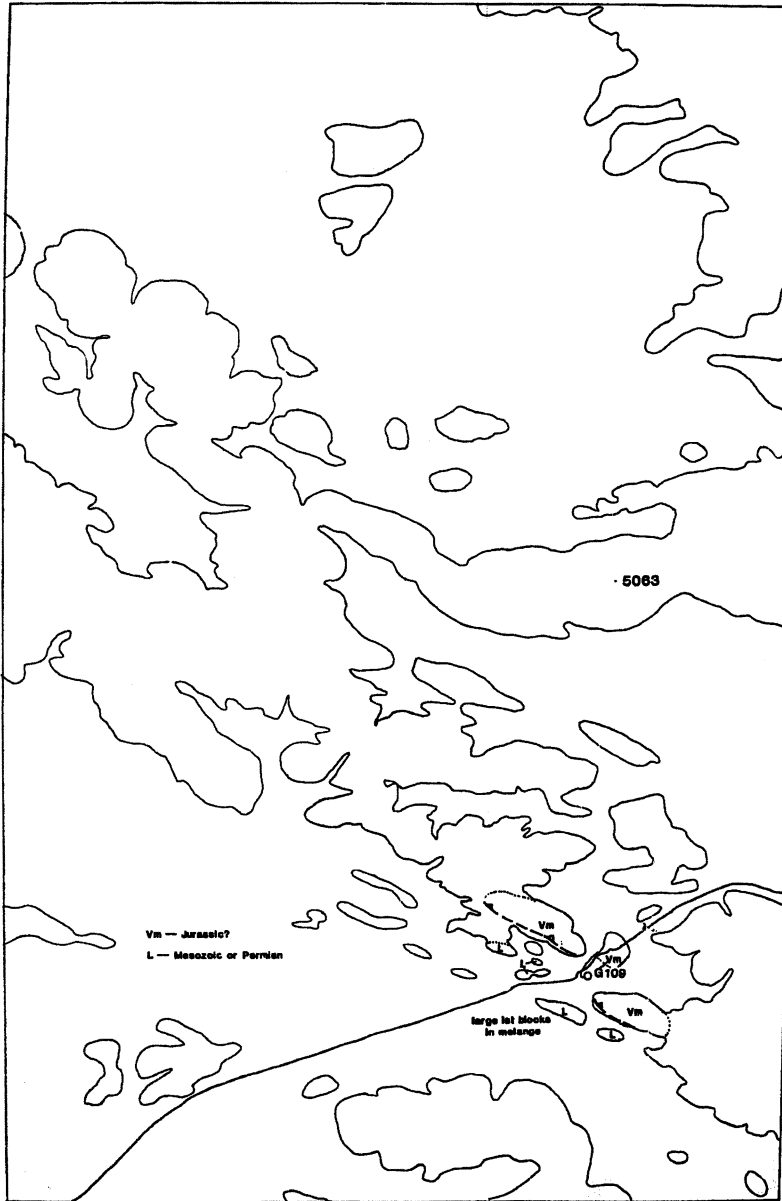
26W



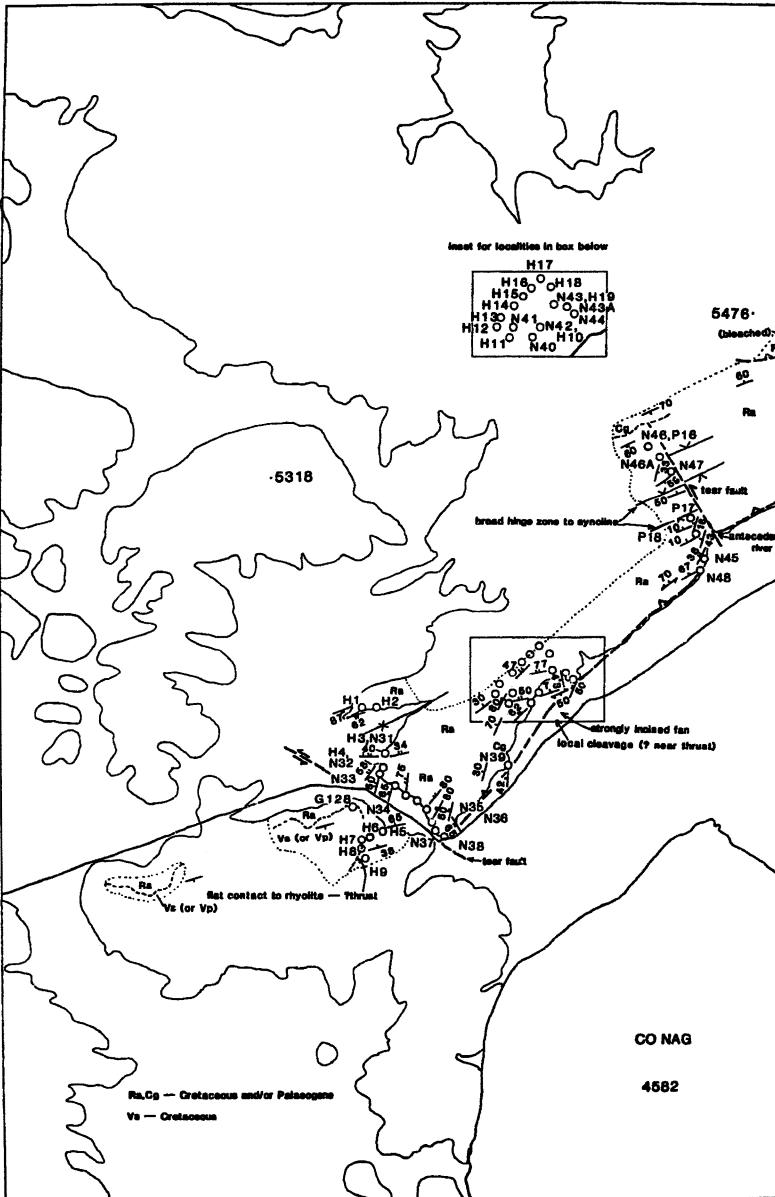
26E+JW+JE



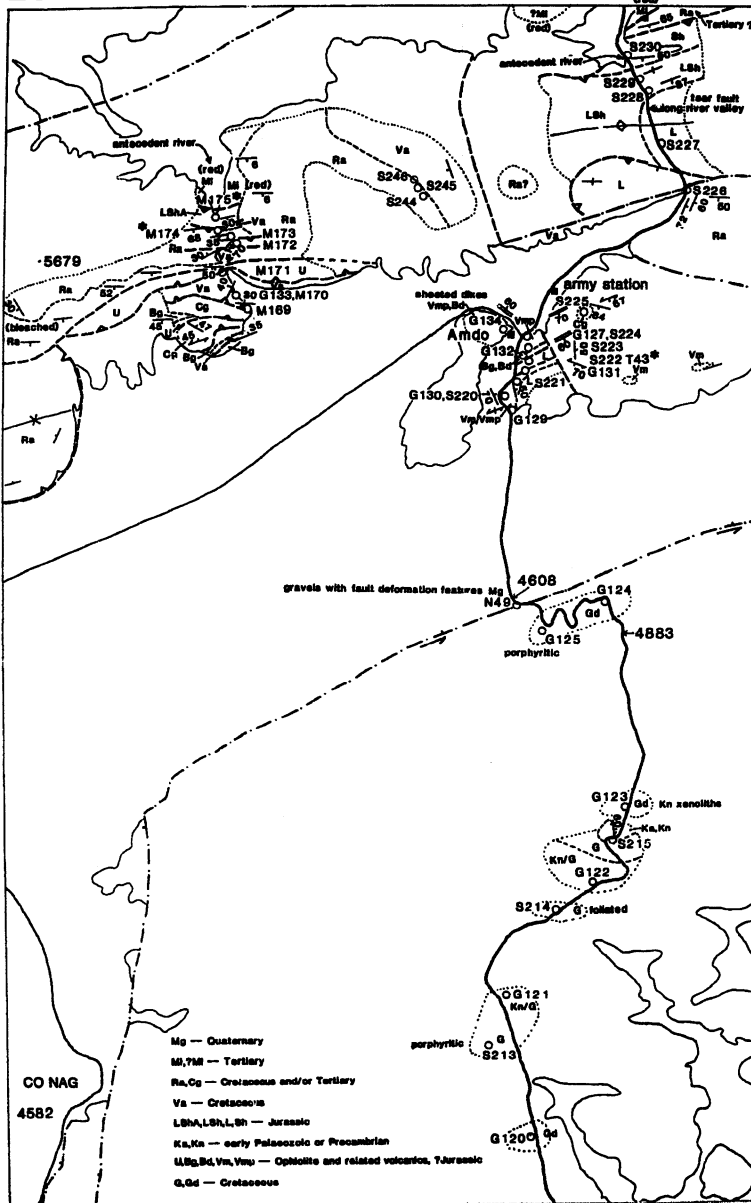
29W



29E

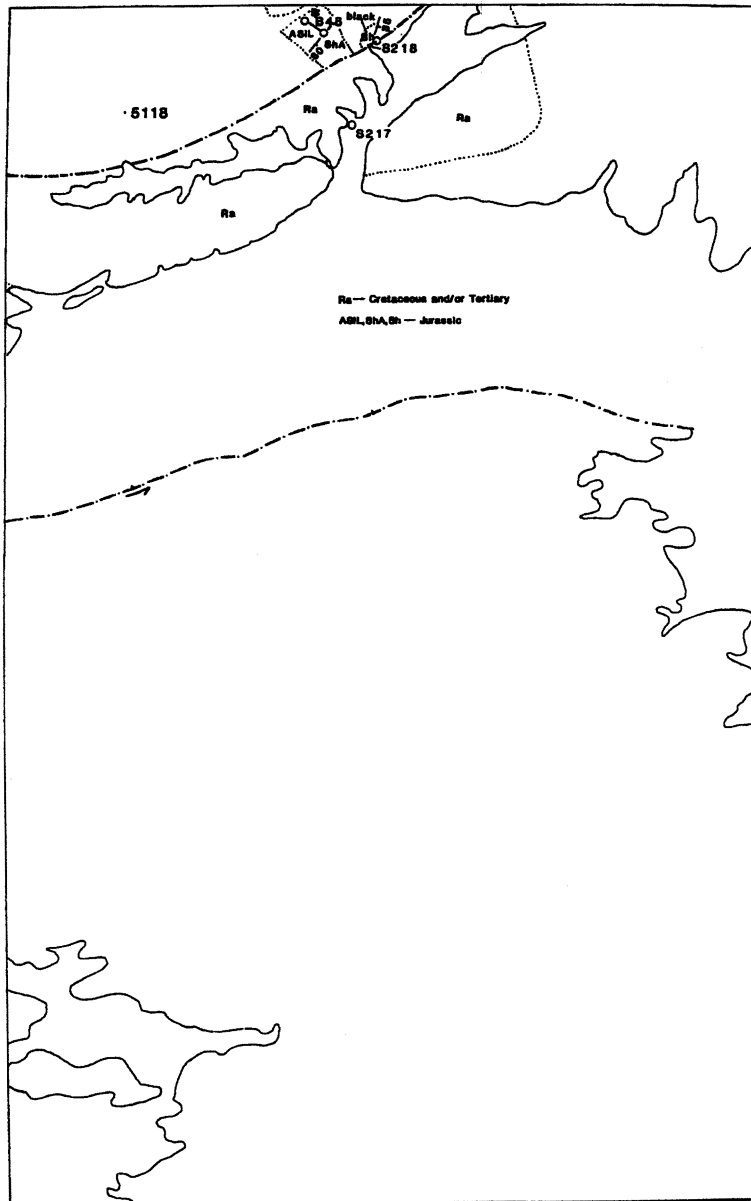


28W

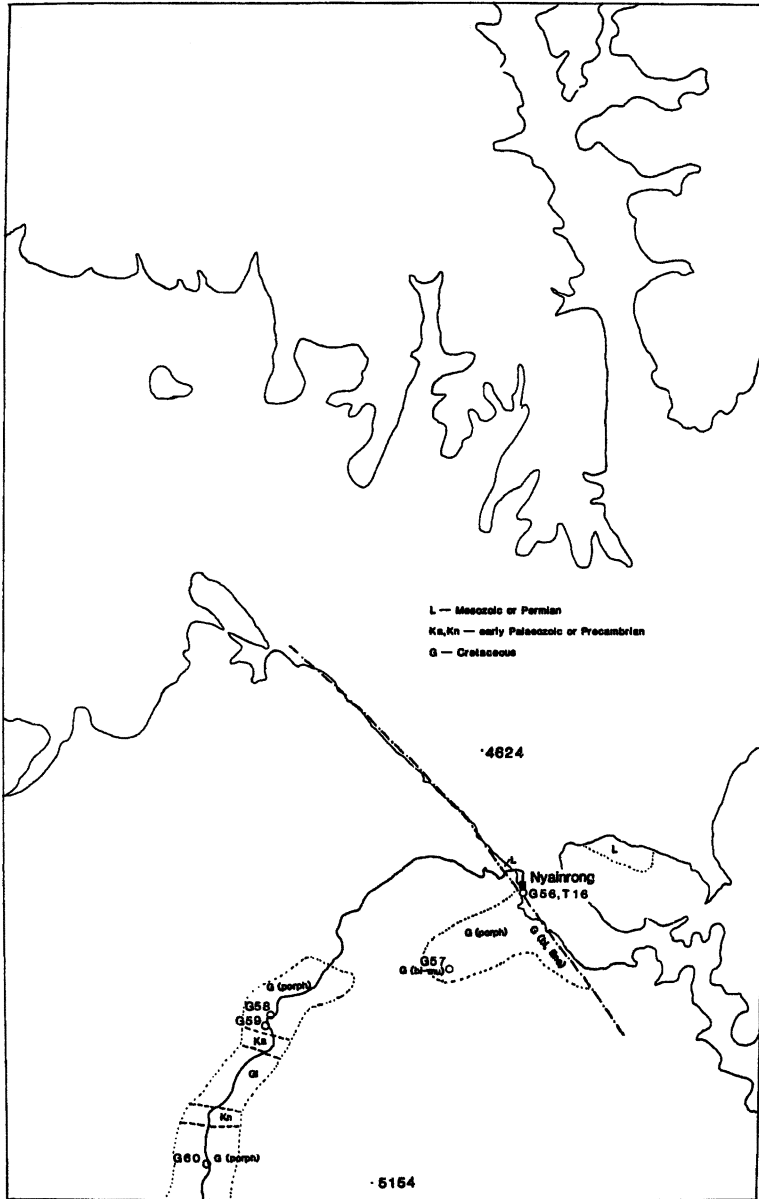




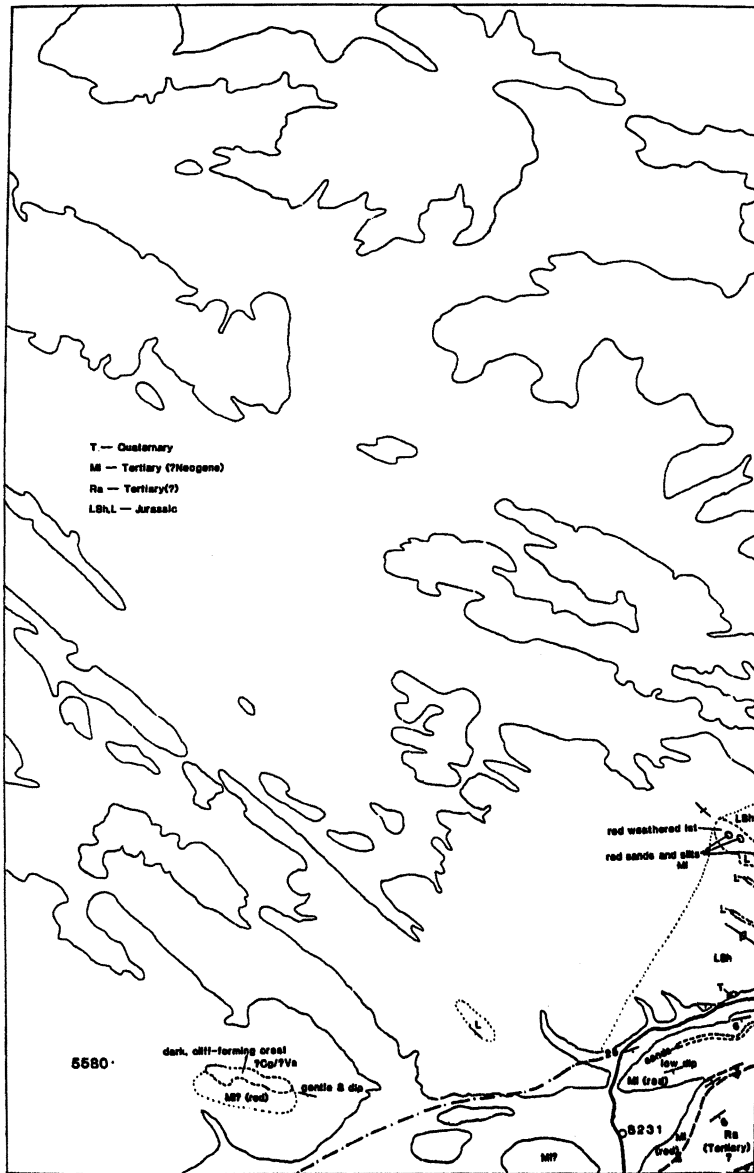
28E



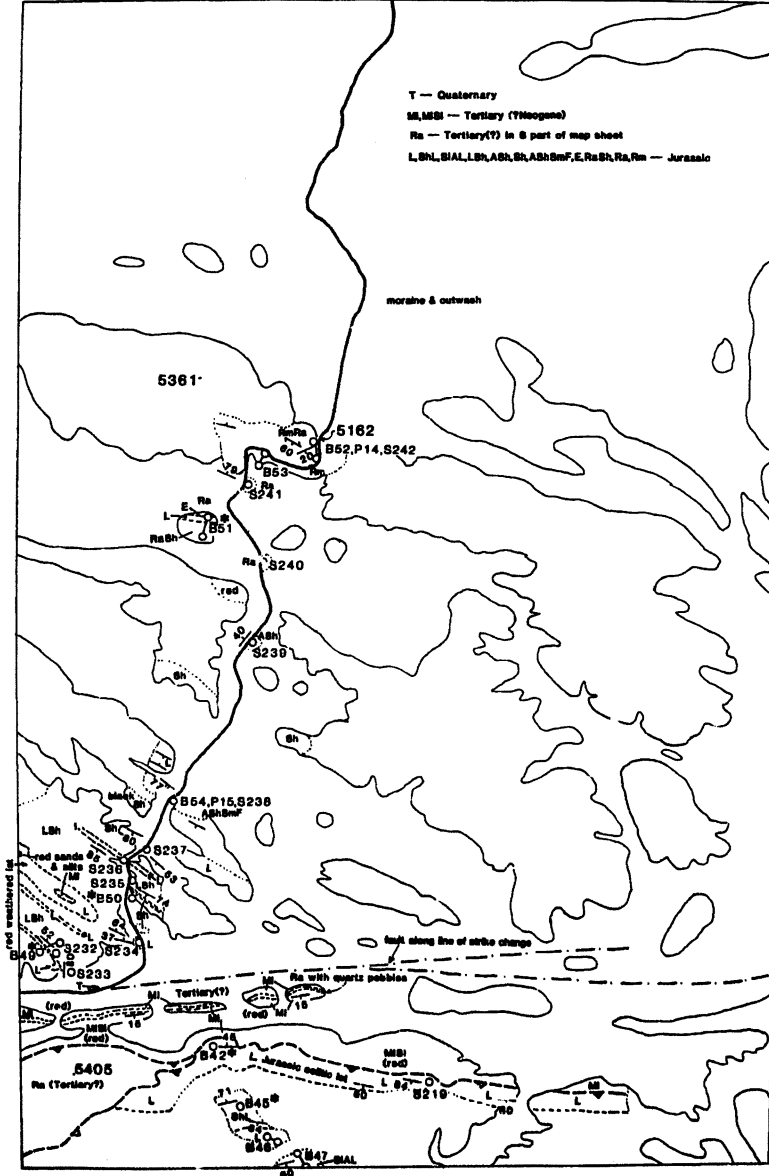
27C



33W

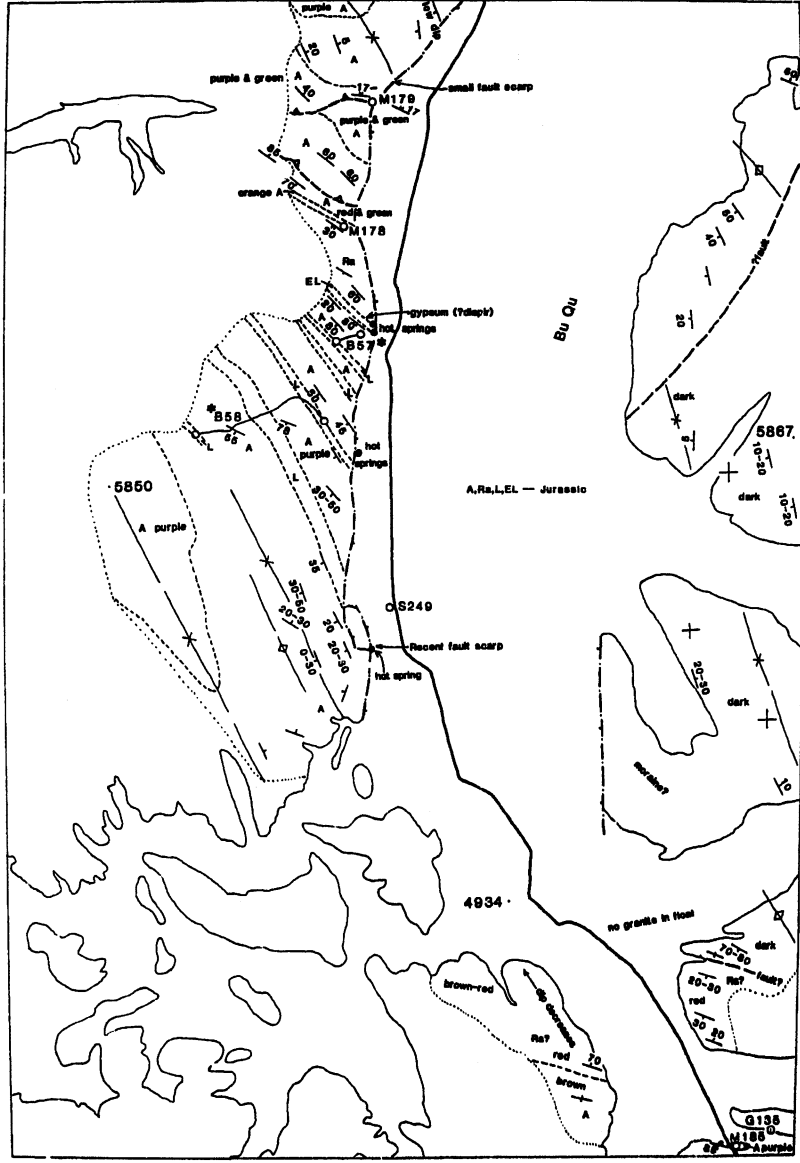


33E

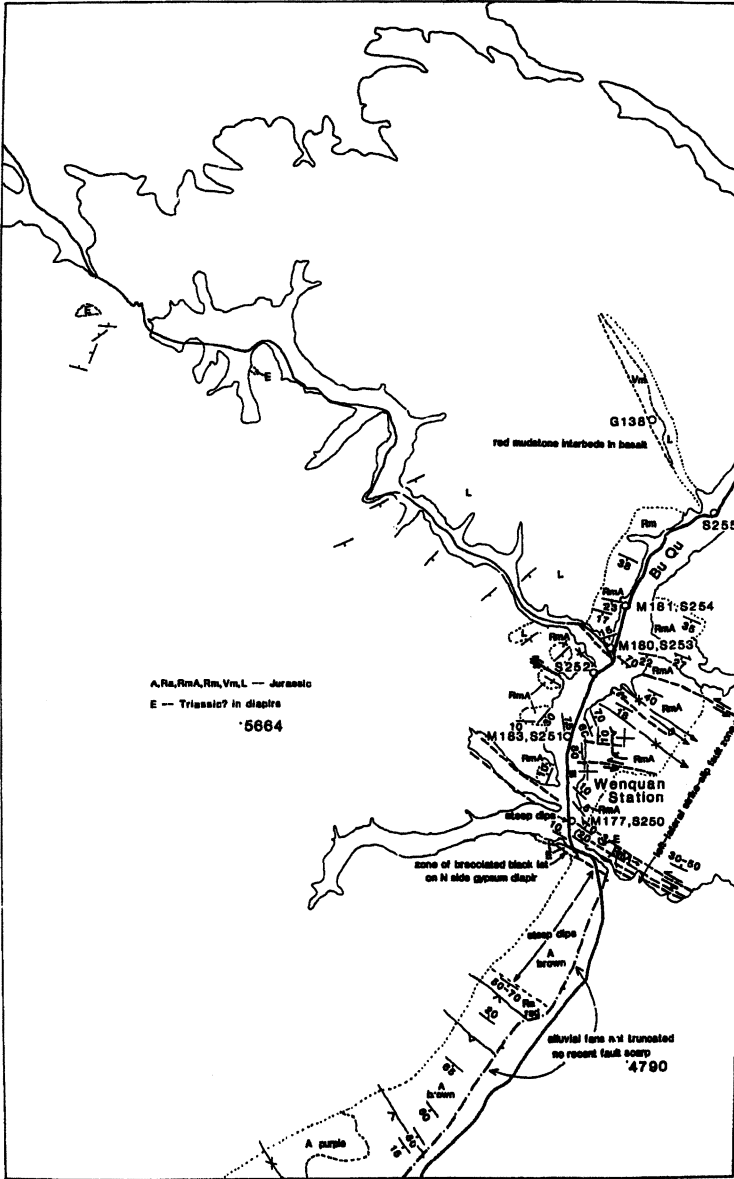




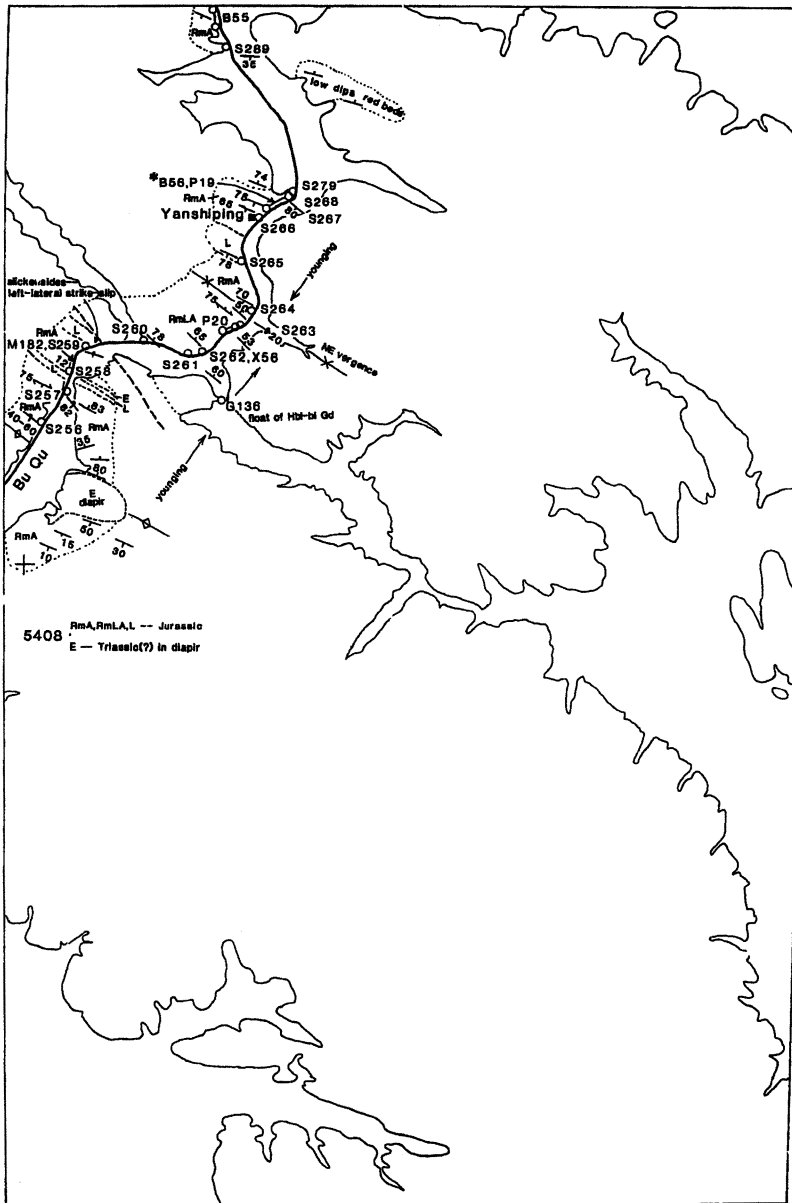
37E



40E

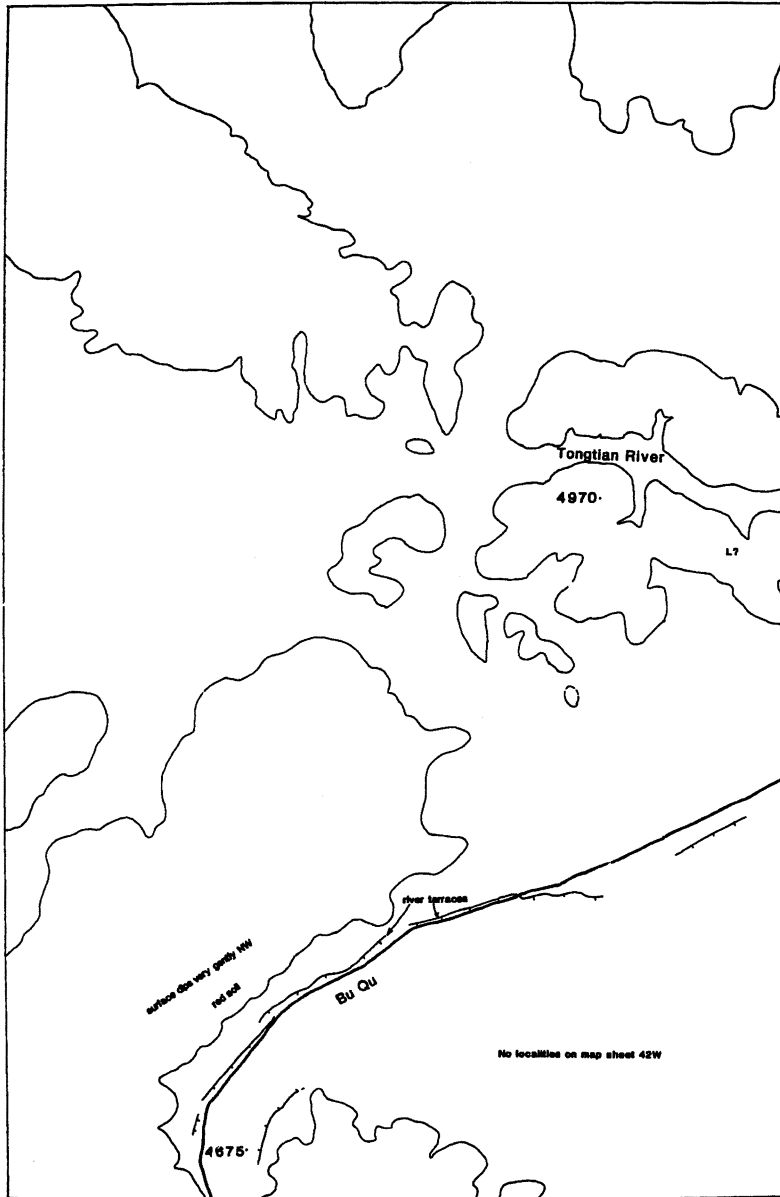


39W

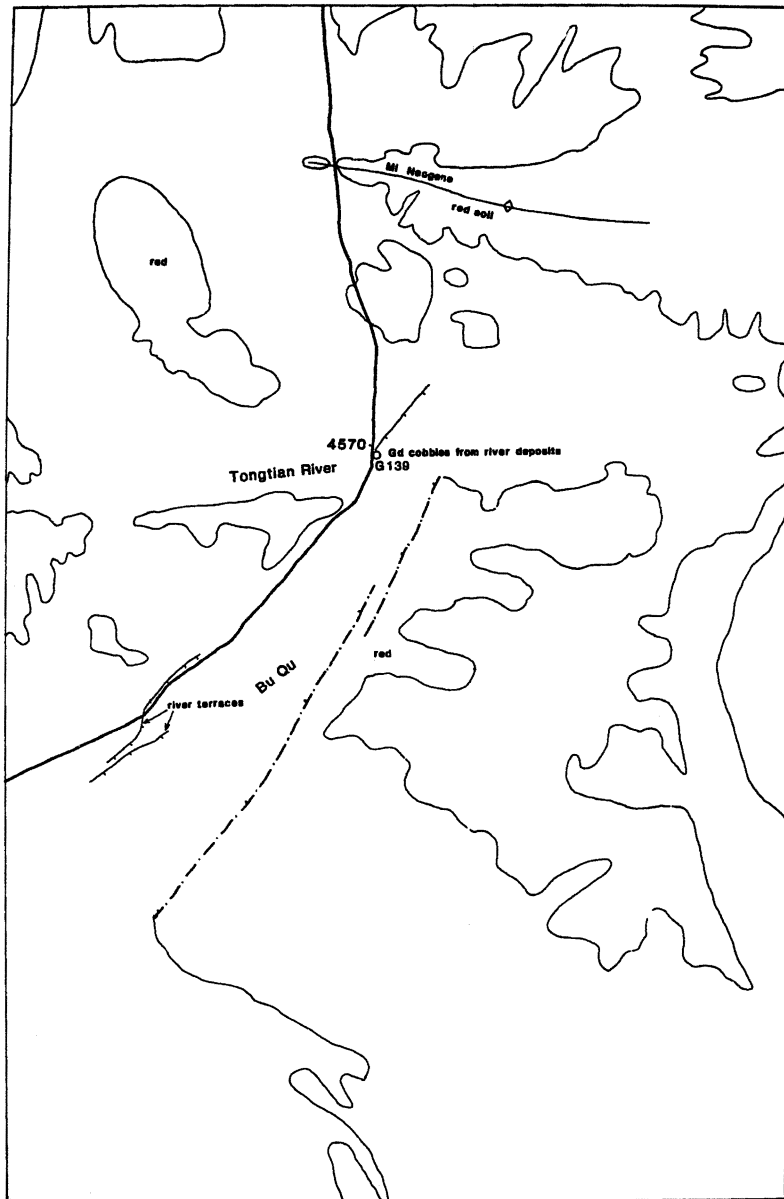




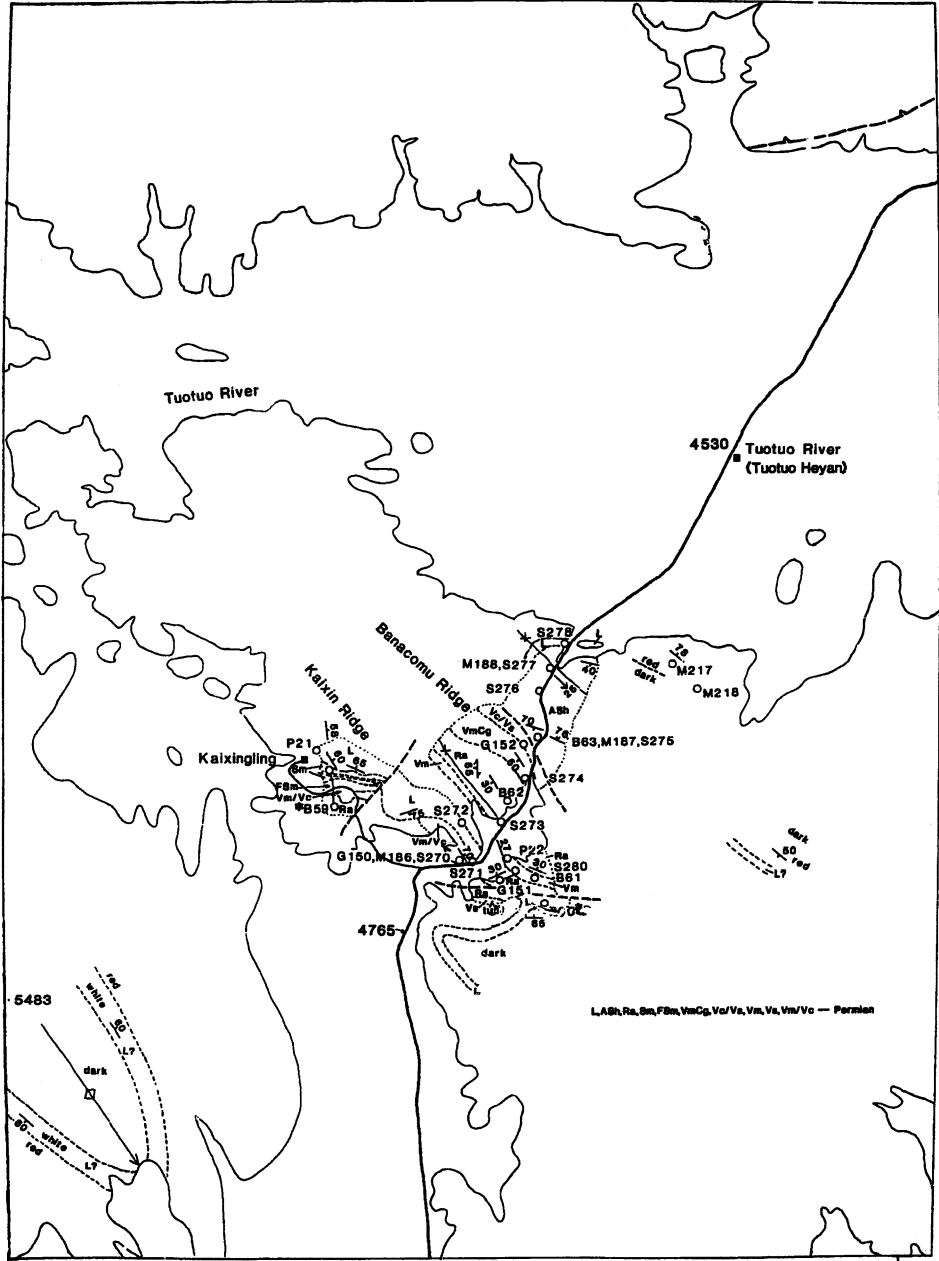
42W



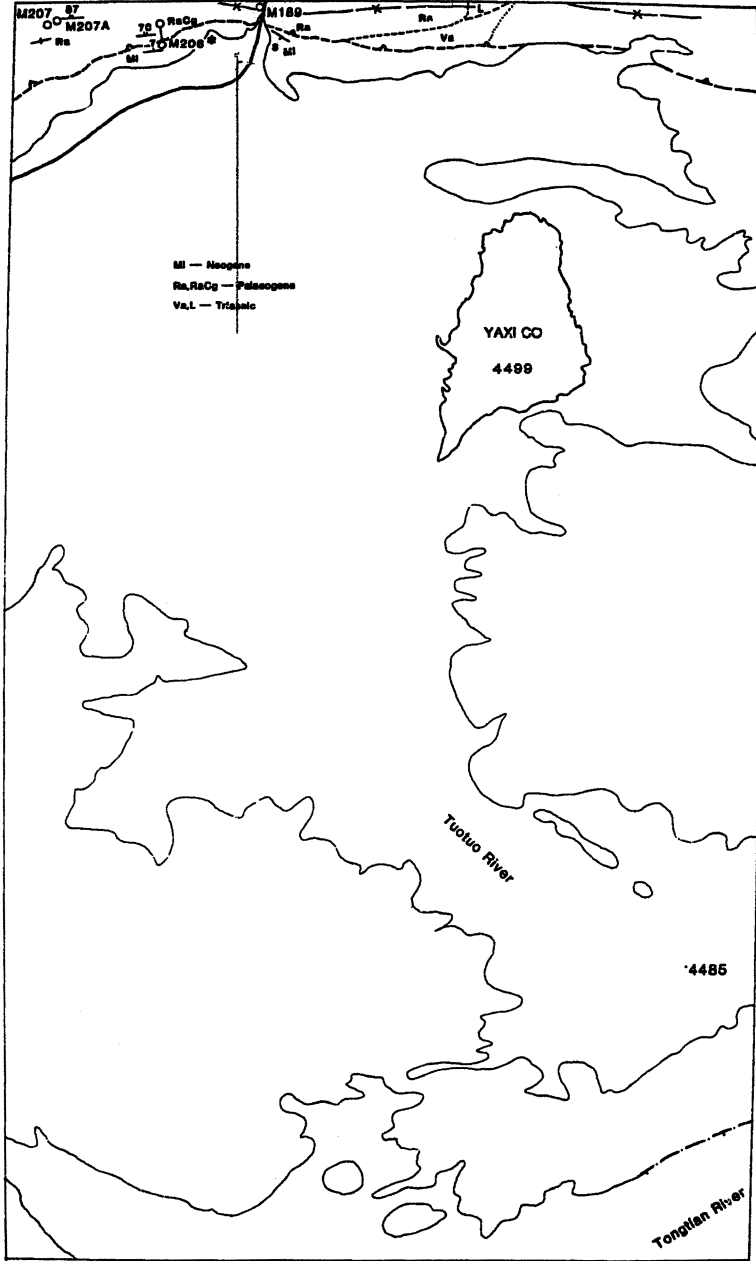
42E



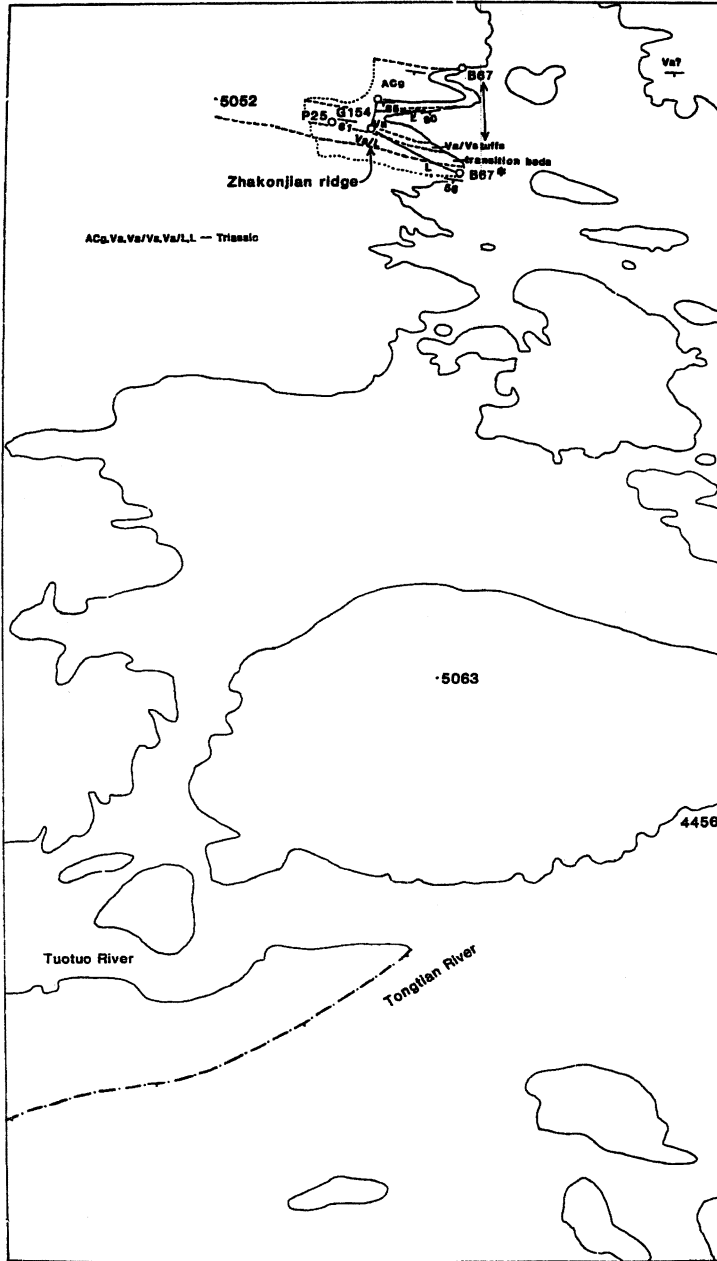
44E



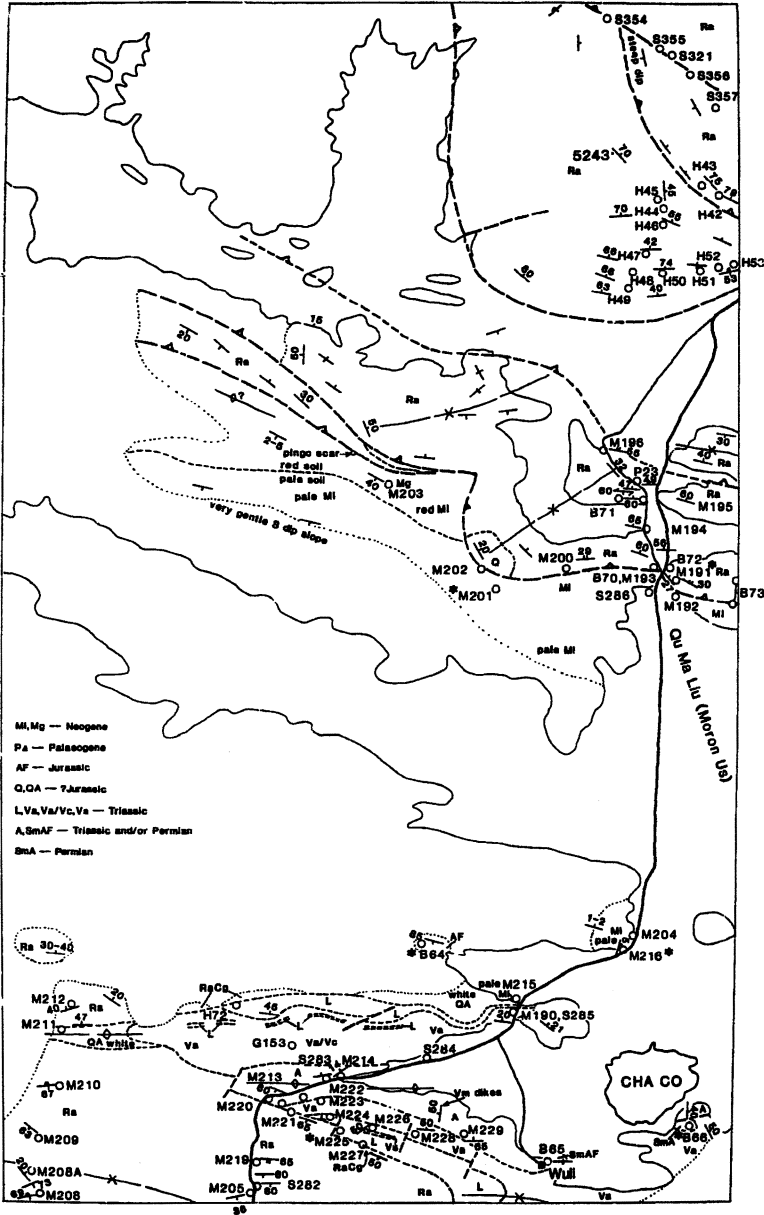
45W



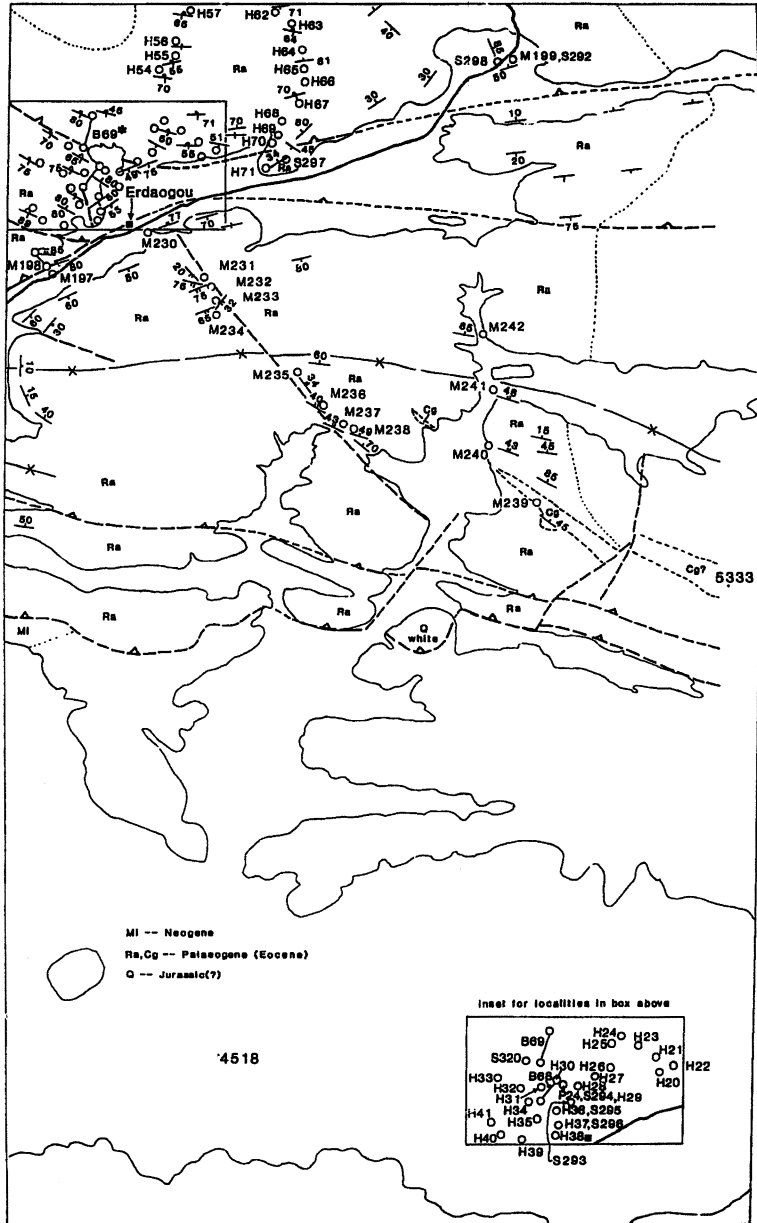
45E



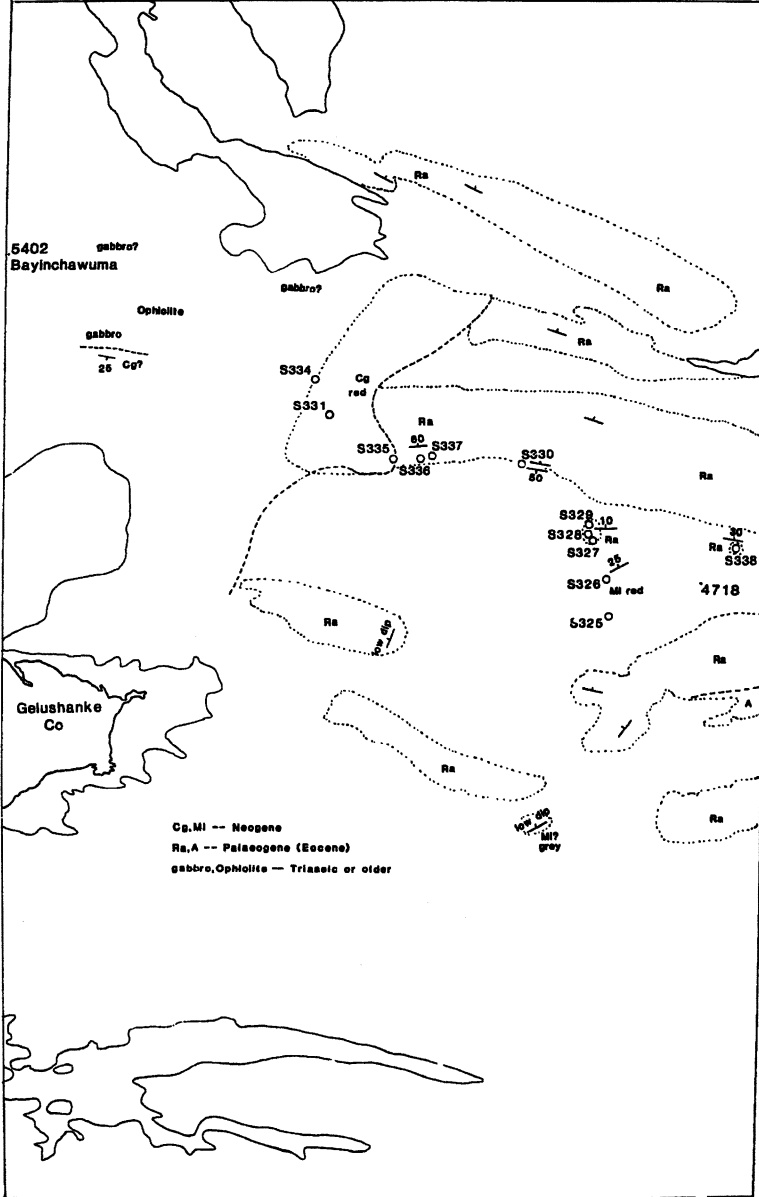
47W



47E

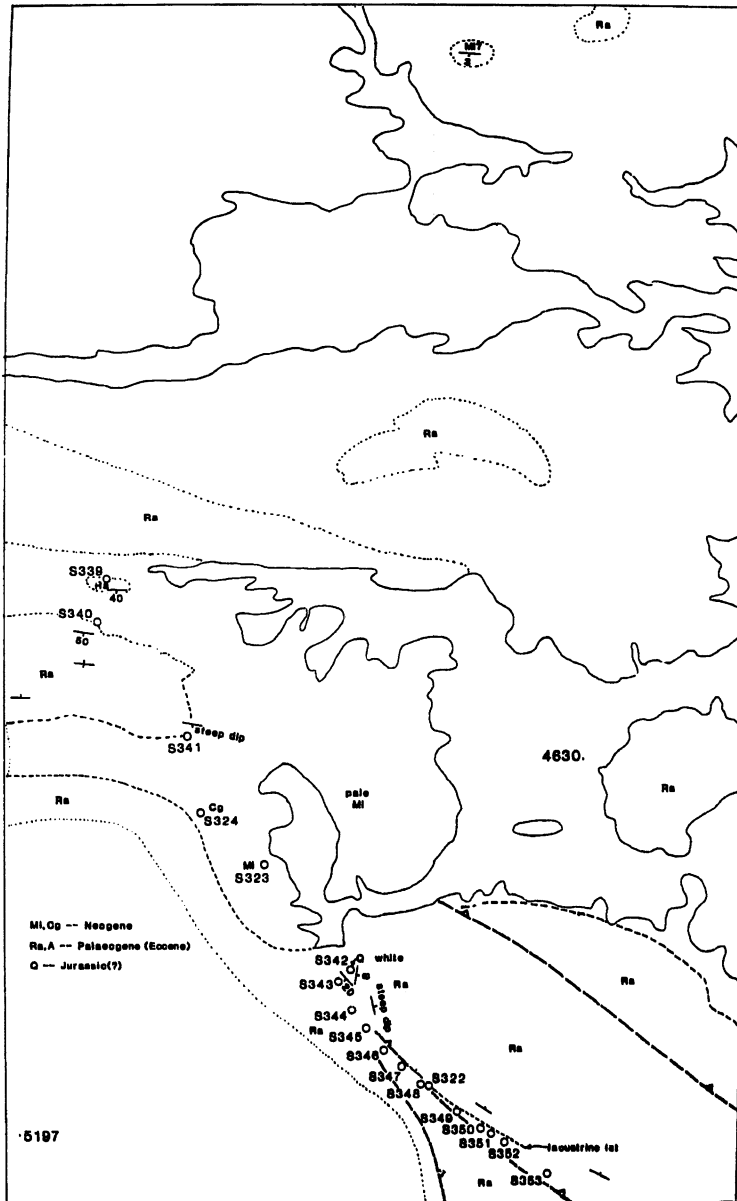


49E



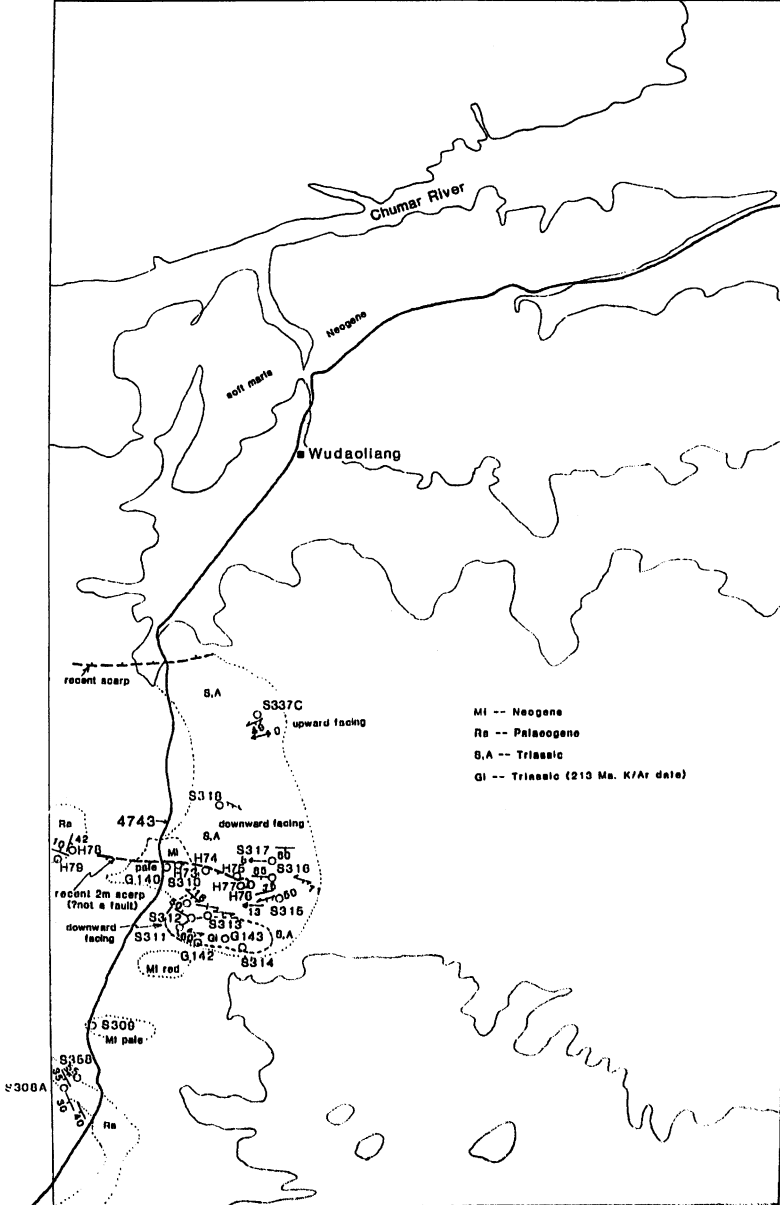


50W

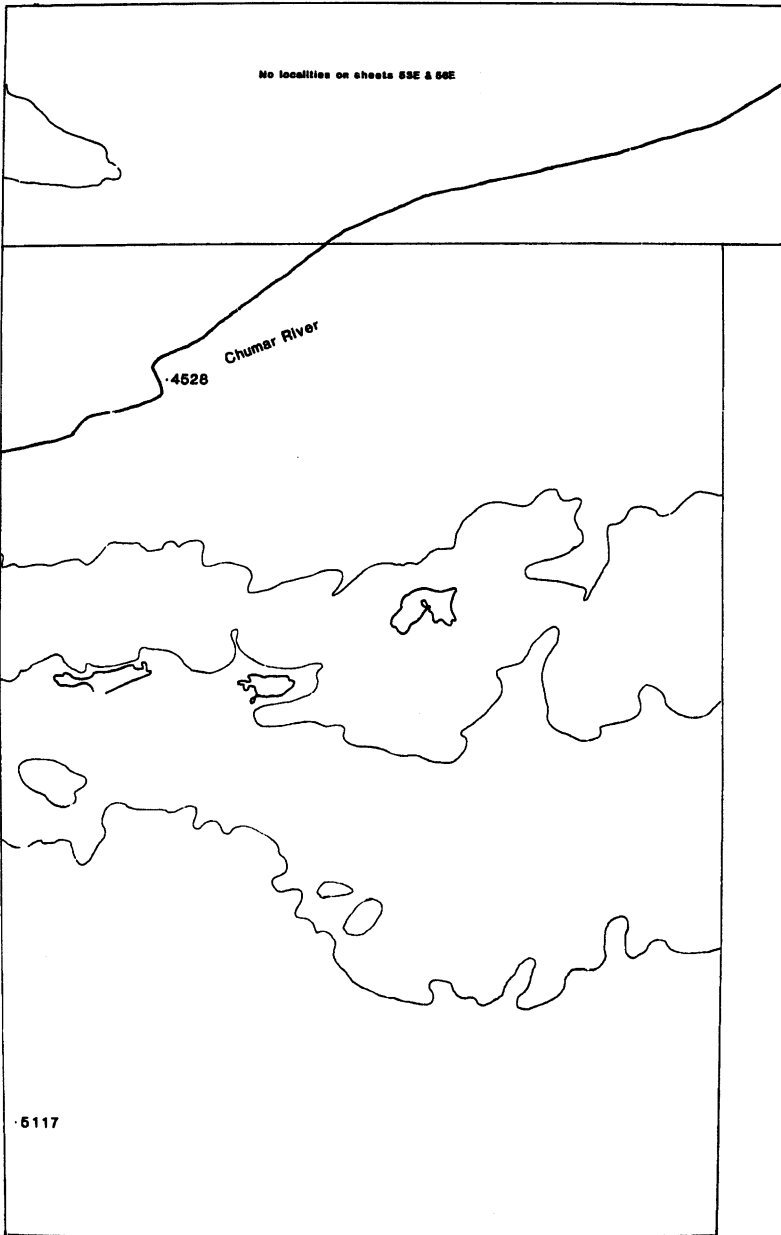




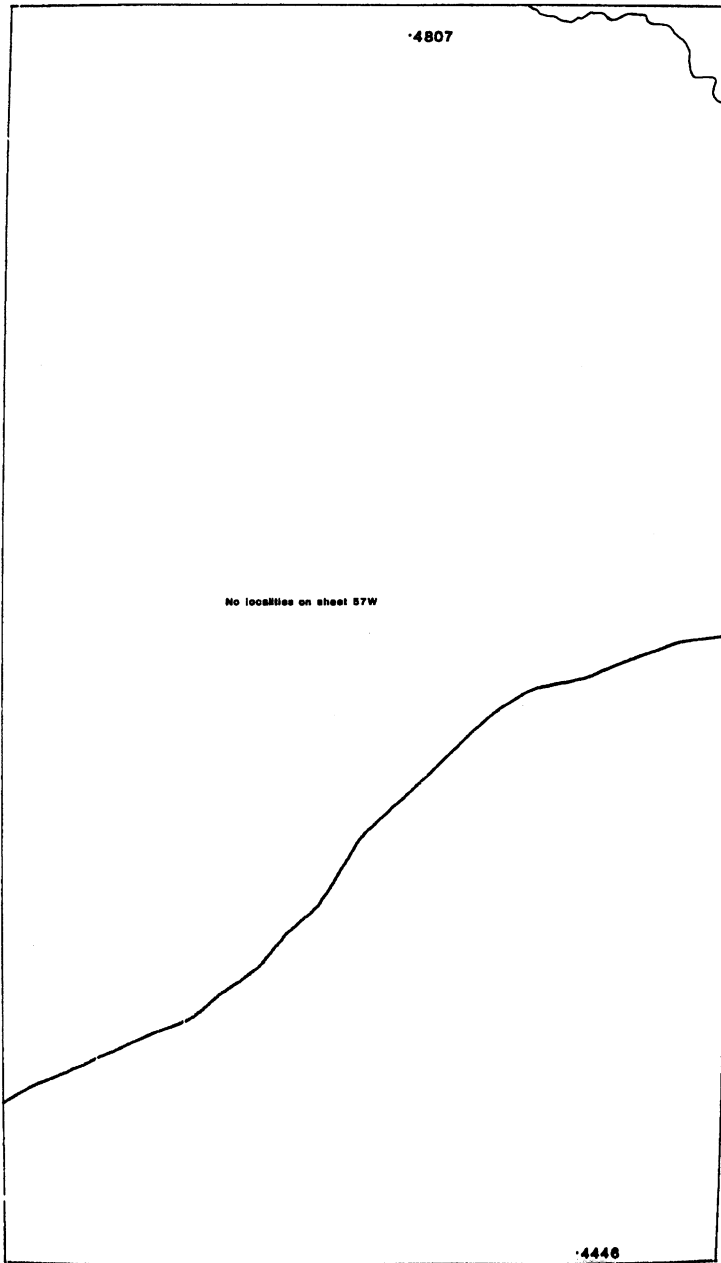
53W



53E+56E



57W

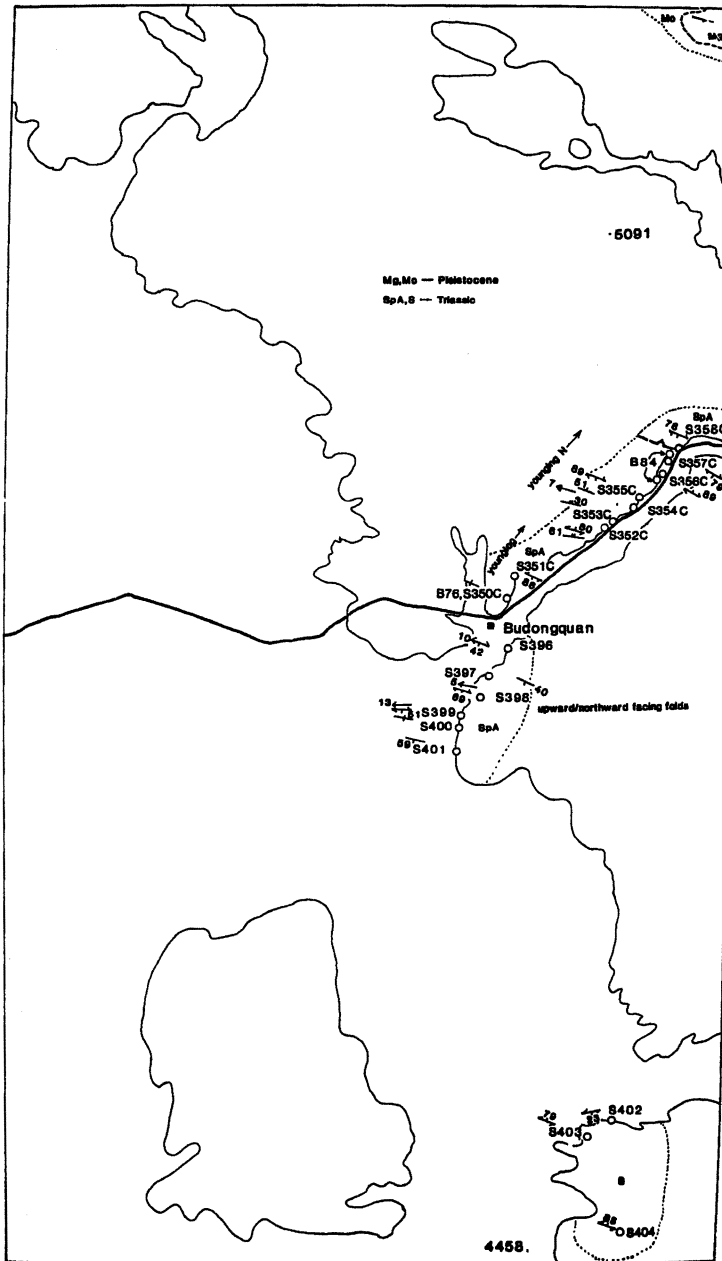


4807

No localities on sheet 57W

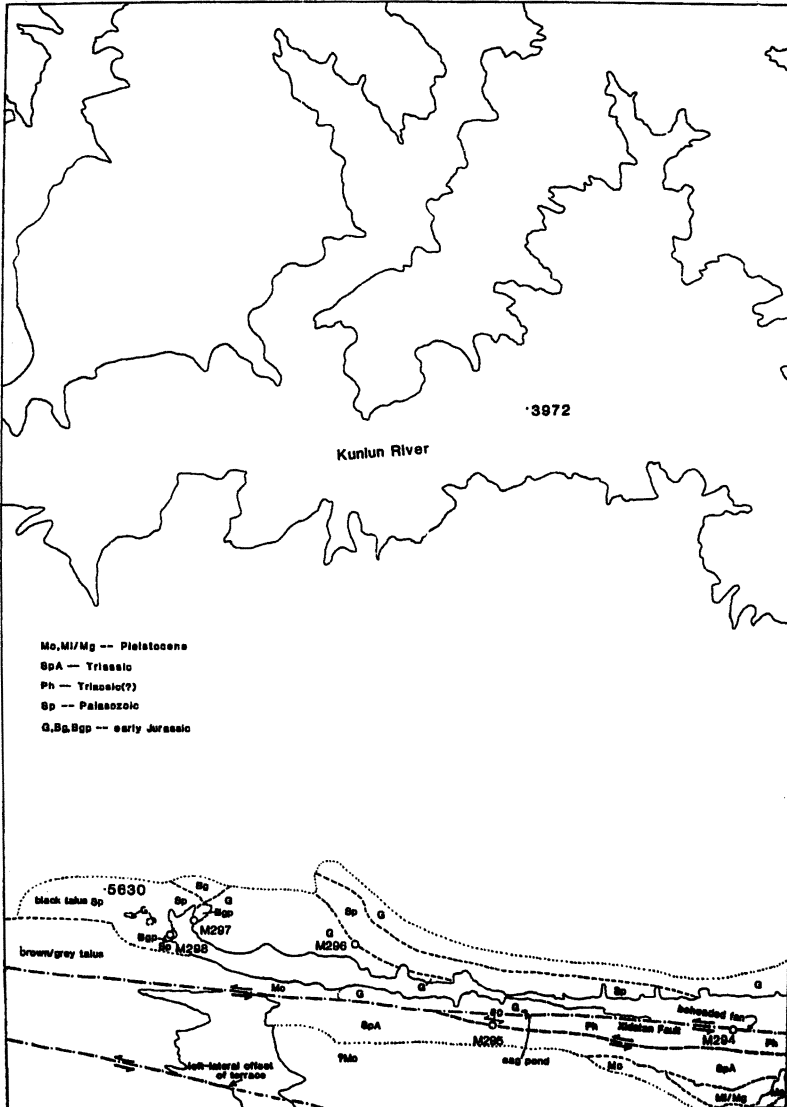
4446

57E



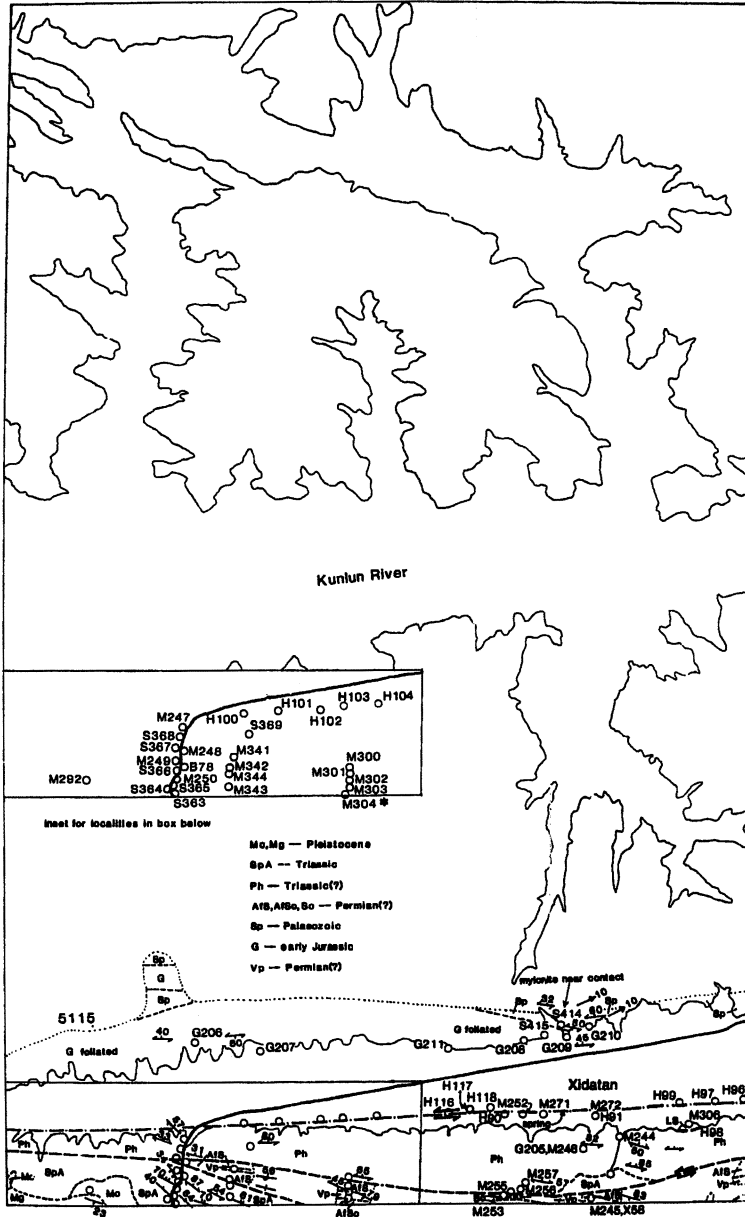


63E

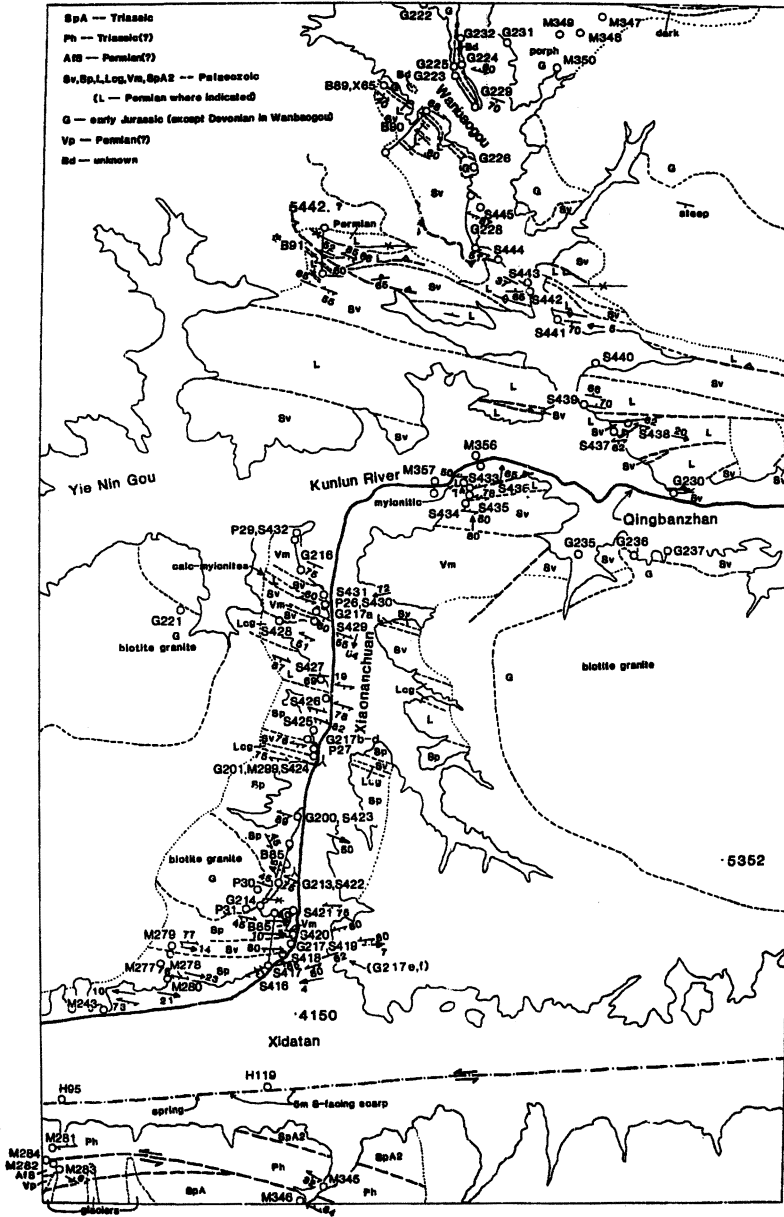




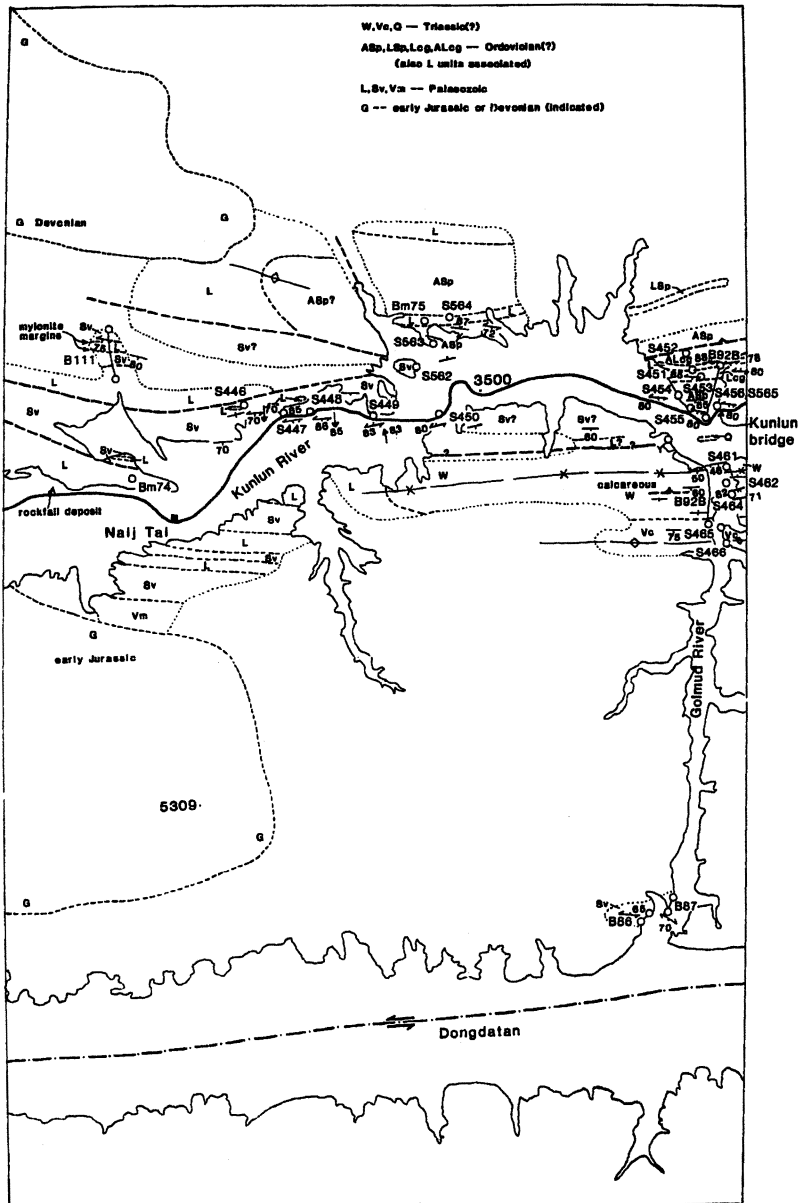
62W



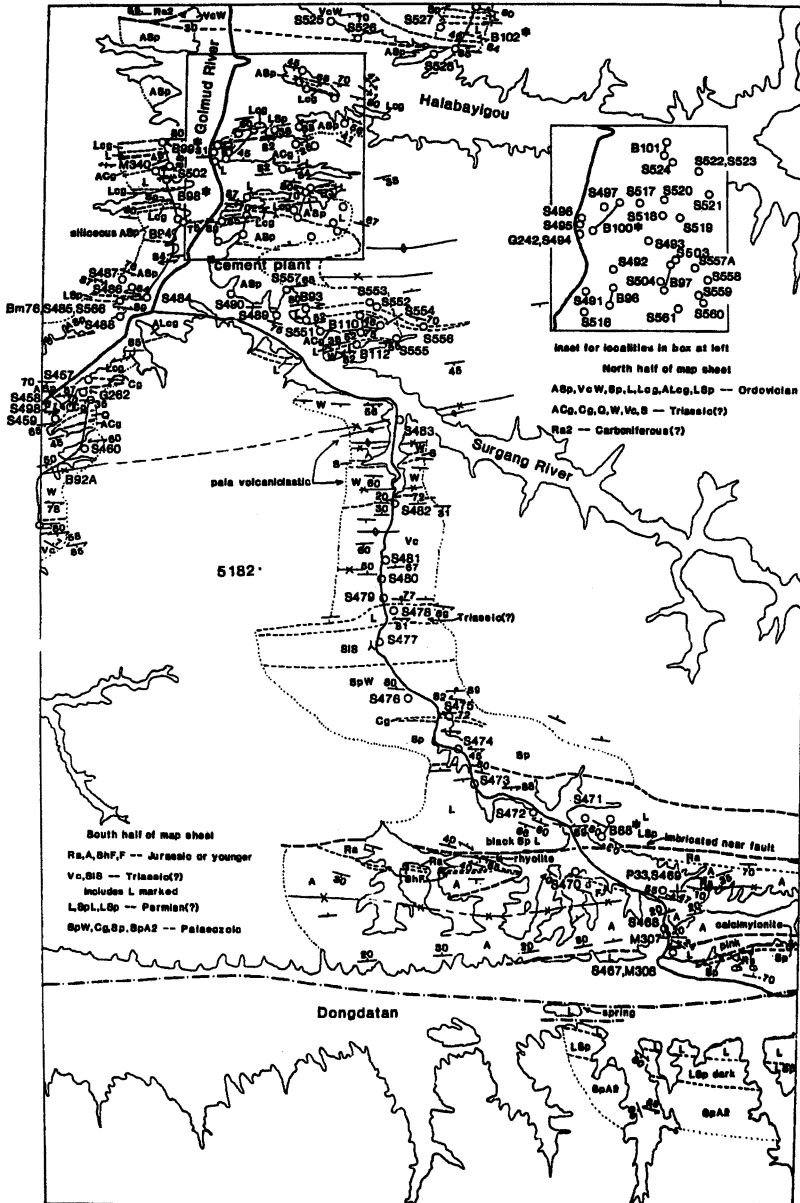
### 62E



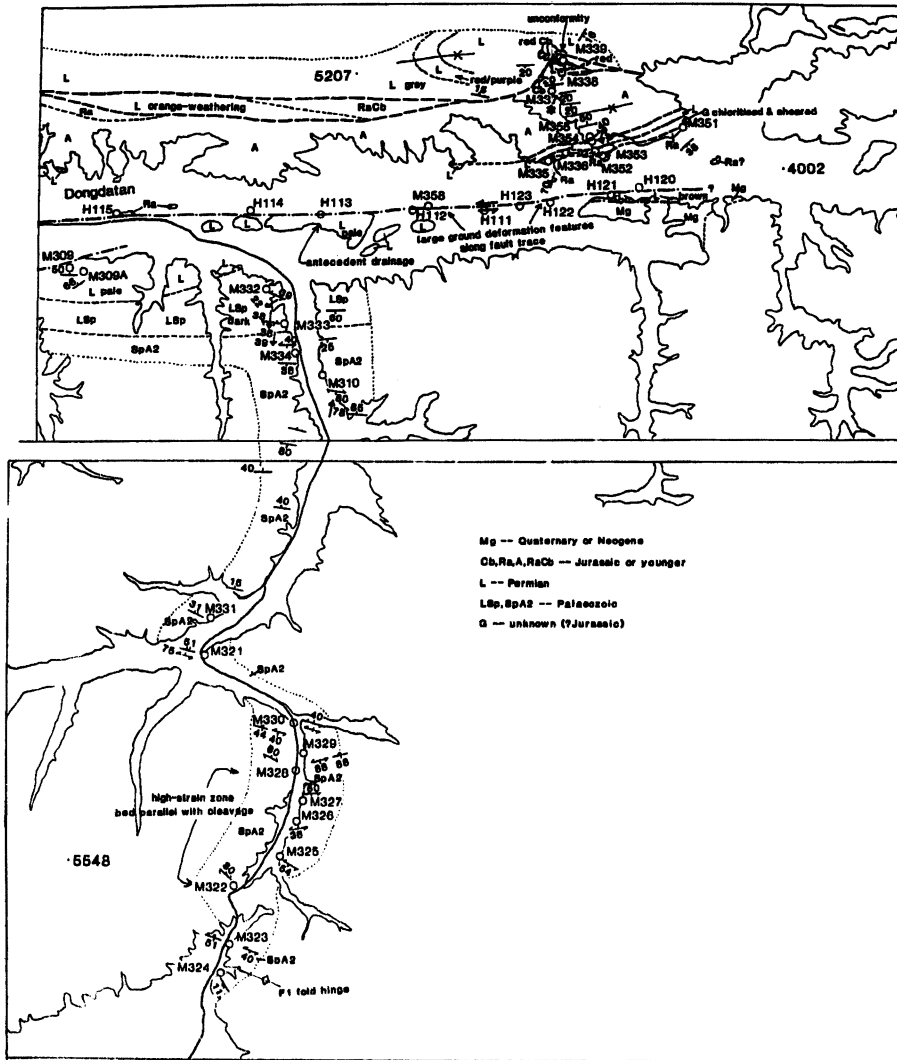
61W



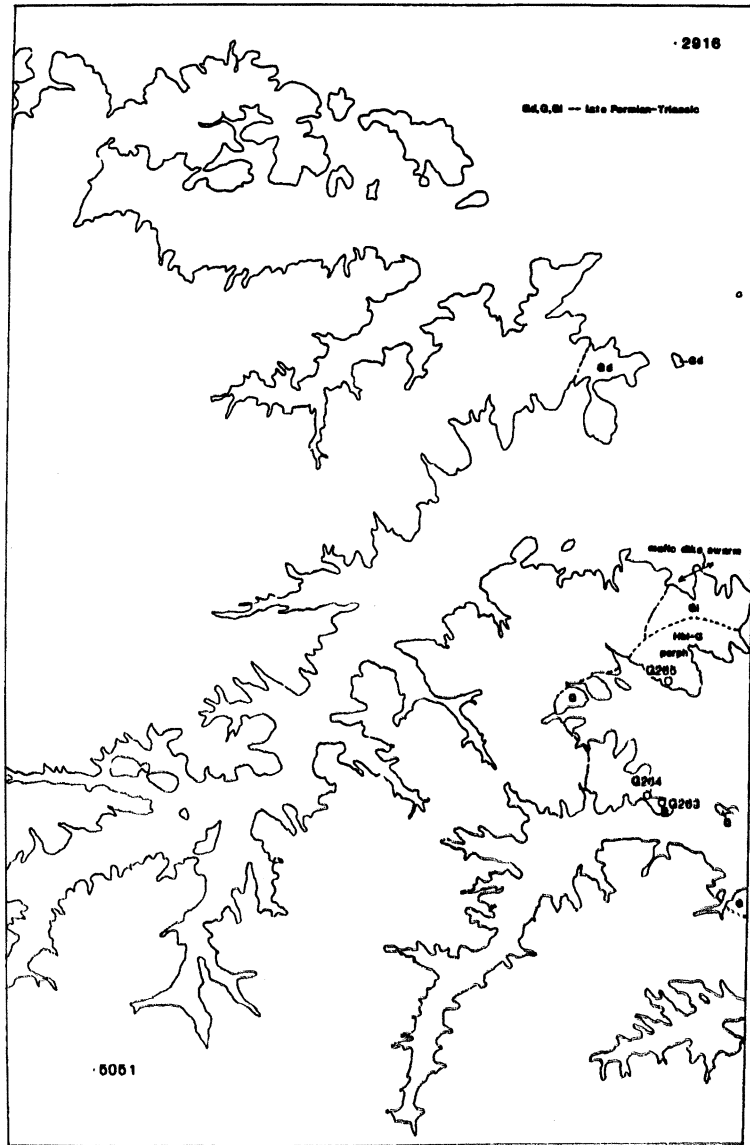
61E



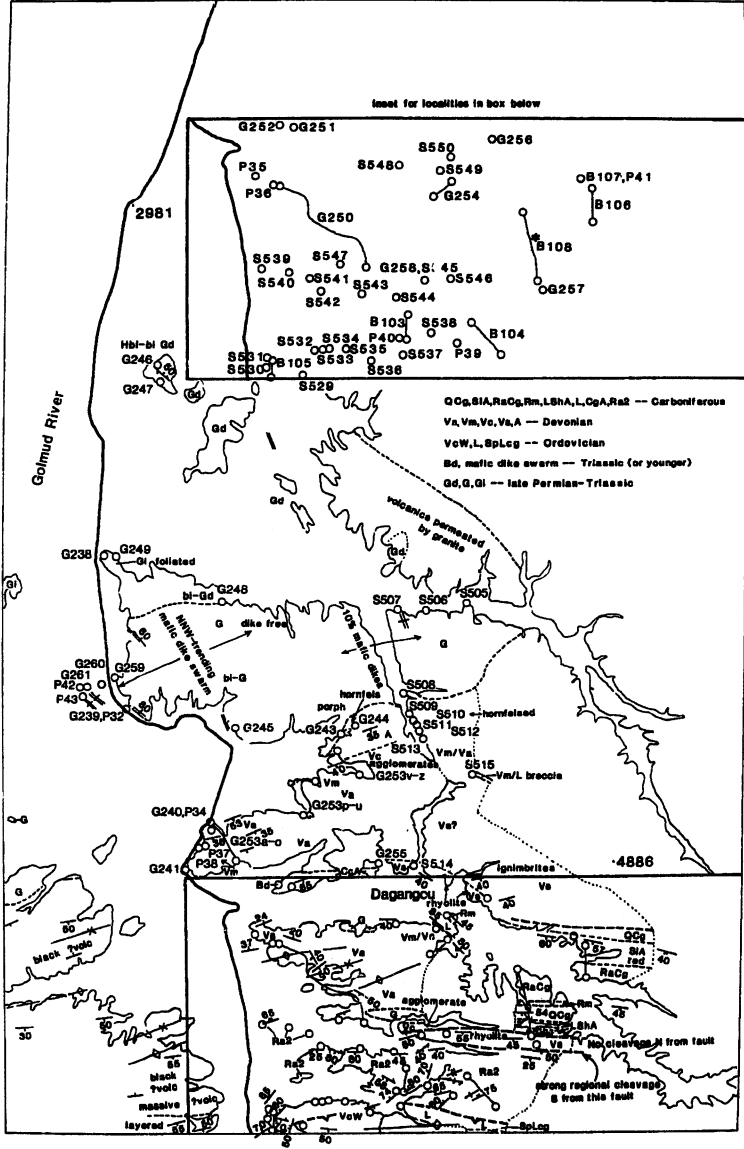
60W+HW



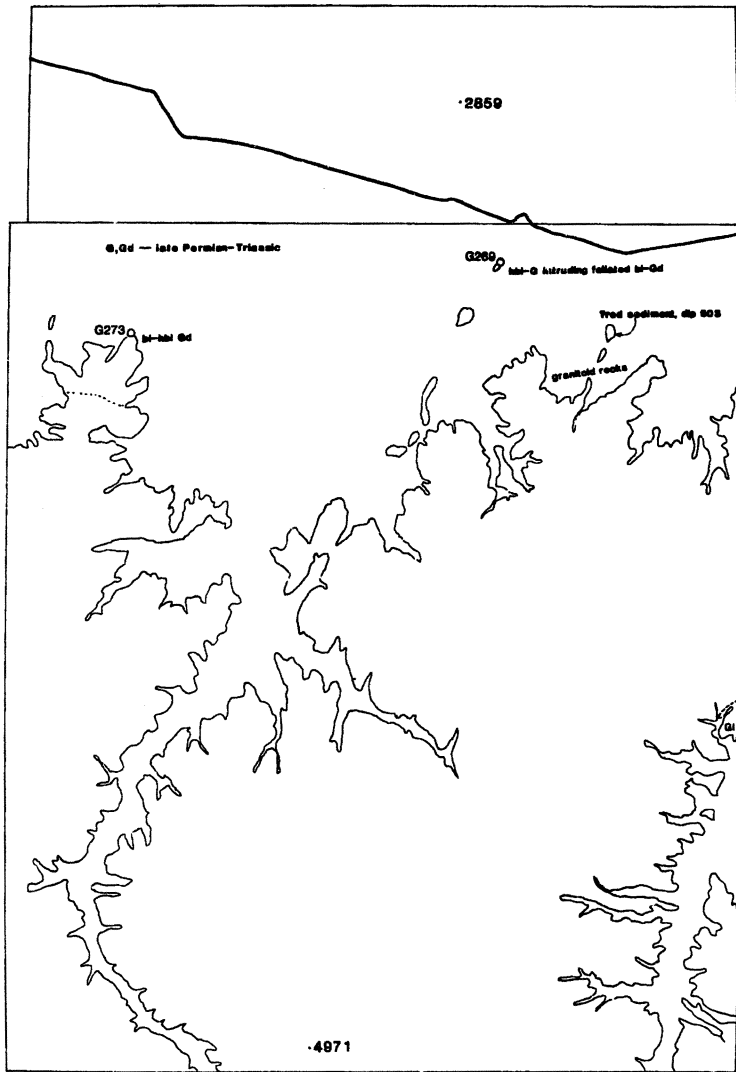
65W



C5E

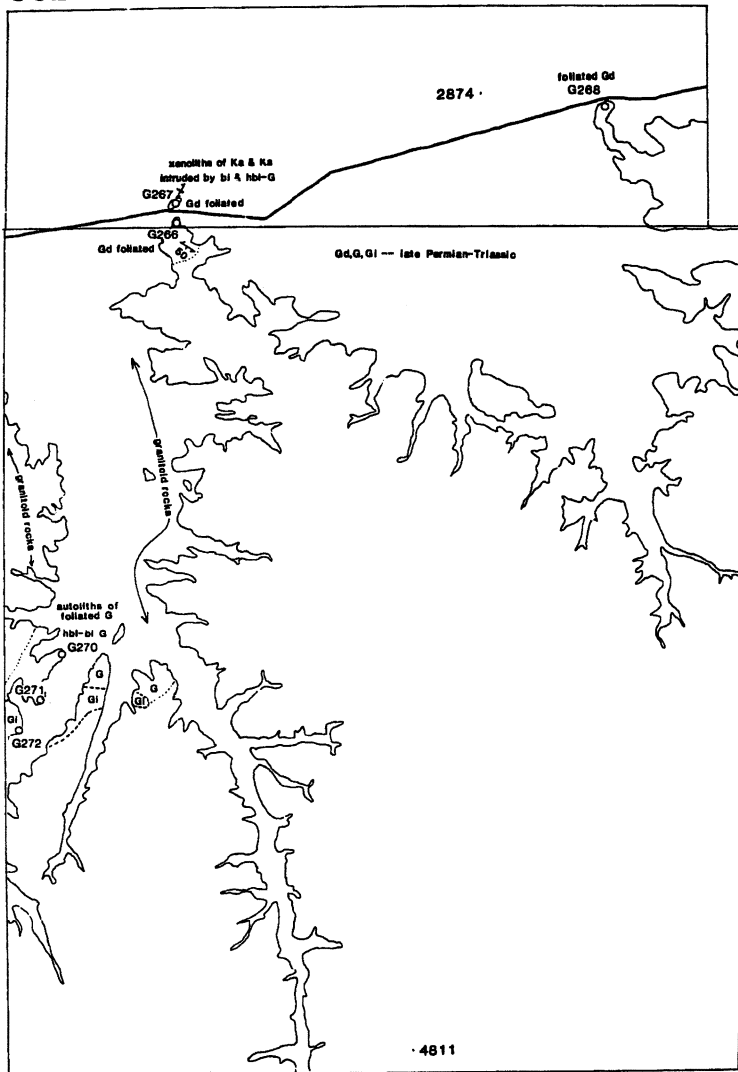


66W+67W

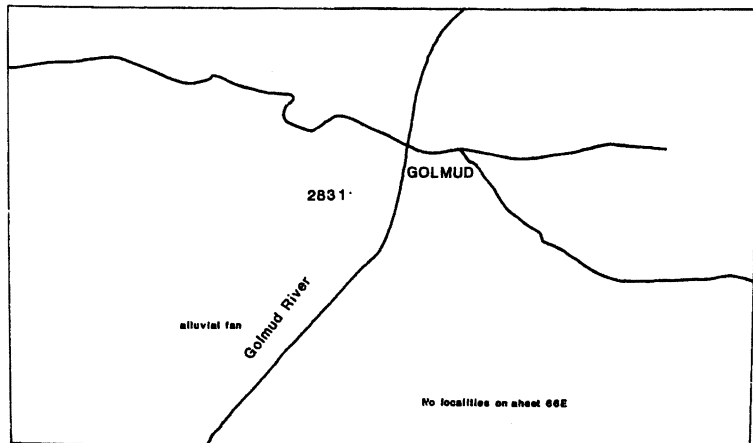




66E+67E



68E



B-localities  
(Smith, Leader)

Locality	Map Sheet	Locality	Map Sheet	Locality	Map Sheet	Locality	Map Sheet
B1	8C	B28	GW	B56	39W	B84	57E
B2	8C	B29	GW	B57	37E	B85	62E
B3	8C	B30	GW	B58	37E	B86	61W
B4	8C	B31	GW	B59	44E	B87	61W
B5	8C	B32	20E	B60	44E	B88	61E
B6	3E	B33	20E	B61	44E	B89	62E
B7	3E	B34	EE	B62	44E	B90	62E
B8	3E	B35	20E	B63	44E	B91	62E
B9	3W	B36	20E	B64	47W	B92	61W
B10	3W	B37	20E	B65	47W	B92A	61E
B10A	3W	B38	23E	B66	47W	B93	61E
B11	4E	B39	23E	B67	45E	B94	61E
B12	4E	B40	30E	B68	47E	B95	dne
B13	4E	B41	30E	B69	47E	B96	61E
B14	4W	B42	33E	B70	47W	B97	61E
B15	4W	B43	dne	B71	47W	B98	61E
B16	4W	B44	dne	B72	47W	B99	61E
B17	10W	B45	33E	B73	47W	B100	61E
B18	10W	B46	33E	B74	50E	B101	67E
B19	10W	B47	33E	B75	50E	B102	61E
B20	10W	B48	28E	B76	57E	B103	65E
B21	10W	B49	33E	B77	58W	B104	65E
B22	10W	B50	33E	B78	62W	B105	65E
B23	10E	B51	33E	B79	58W	B106	65E
B24	FW	B52	33E	B80	58W	B107	65E
B25	FE	B53	33E	B81	58W	B108	65E
B26	FW	B54	33E	B82	58W	B109	dne
B27	FW	B55	39W	B83	58W	B110	61E
BH 74	61W					B111	61W
BH 75	61W					B112	61E
BH 76	61E						

dne = does not exist

T-localities  
(Gansser)

Locality	Map Sheet	Locality	Map Sheet
T1-6	off maps to S & SW of Quxu	T26 (M47)	10W
T7	3E	T27	np
T8	3E	T28	np
T9	3W, 8C	T29	17W
T10	3W	T30	3E
T11	3W	T31	GW
T12	3W	T32	GW
T13	3W	T33	CE
T14	3W	T34	CE
T15	3W	T35	19W
T16	7W	T36	19W
T17	7W	T37	23E
T1E	7W	T38	23E
T1S	7W	T39	np
T20	np	T40	np
T21	np	T41	np
T22	np	T42	np
T23	np	T43 (S222)	28W
T24 (M50)	12W	T44 and beyond	np
T25 (S93)	10W		

np = not provided

G-localities  
(Pearce, Harris)

Locality	Map Sheet	Locality	Map Sheet	Locality	Map Sheet	Locality	Map Sheet
G1	near	G63	26W	G125	28W	G222	62E
G2	Zangbo	G64	26W	G126	36E	G223	62E
G3	bridge	G65	19E	G127	28W	G224	62E
G4	2E	G66	8W	G128	29E	G225	62E
G5	2E	G67	8W	G129	28W	G226	62E
G6	2E	G68	21W	G130	28W	G227	dne
G7	2E	G69	21W	G131	28W	G228	62E
G8	2E	G70	21W	G132	28W	G229	62E
G9	2E	G71	21W	G133	28W	G230	62E
G10	2E	G72	21W	G134	28W	G231	62E
G11	1W	G73	dne	G135	37E	G232	62E
G12	1W	G74	dne	G136	39W	G233	dne
G13	1W	G75	dne	G137	dne	G234	dne
G14	1W	G76	dne	G138	40E	G235	62E
G15	1E	G77	dne	G139	42E	G236	62E
G16	1E	G78	dne	G140	53W	G237	62E
G17	1E	G79	dne	G141	50E	G238	65E
G18	1E	G80	dne	G142	53W	G239	65E
G19	1E	G81	20E	G143	53W	G240	65E
G20	7W	G82	20E	G144	dne	G241	65E
G21	7W	G83	20E	G145	dne	G242	61E
G22	7W	G84	20E	G146	dne	G243	65E
G23	7W	G85	23E	G147	dne	G244	65E
G24	7W	G86	23E	G148	dne	G245	65E
G25	7W	G87	23E	G149	dne	G246	65E
G26	7W	G88	23E	G150	44E	G247	65E
G27	7W	G89	23E	G151	44E	G248	65E
G28	7W	G90	23E	G152	44E	G249	65E
G29	4W	G91	20E	G153	47W	G250	65E
G30	4W	G92	20E	G154	45E	G251	65E
G31	4E	G93	20W	G155	dne	G252	65E
G32	4W	G94	20W	G156	dne	G253	65E
G33	4E	G95	20W	G157	dne	G254	65E
G34	4E	G96	20W	G158	dne	G255	65E
G35	4E	G97	20E	G159	dne	G256	65E
G36	4E	G98	20E	G160	dne	G257	65E
G37	5W	G99	20E	G161	dne	G258	65E
G38	5W	G100	20E	G162	dne	G259	65E
G39	5W	G101	20E	to	dne	G260	65E
G40	6E	G102	20E	G199	dne	G261	65E
G41	7W	G103	30E	G200	62E	G262	61E
G42	7W	G104	30E	G201	62E	G263	65W
G43	11E	G105	30W	G202	58W	G264	65W
G44	11E	G106	23E	G203	58W	G265	65W
G45	7W	G107	23E	G204	58W	G266	66E
G46	7W	G108	23E	G205	62W	G267	67E
G47	dne	G109	29W	G206	62W	G268	67E
G48	dne	G110	dne	G207	62W	G269	66W
G49	dne	G111	30W	G208	62W	G270	66E
G50	11E	G112	30W	G209	62W	G271	66E
G51	11E	G113	30W	G210	62W	G272	66E
G52	11E	G114	30W	G211	62W	G273	66W
G53	13W	G115	30W	G212	dne		
G54	18E	G116	30W	G213	62E		
G55	17W	G117	25W	G214	62E		
G56	27C	G118	25W	G215	58W		
G57	27C	G119	25W	G216	62E		
G58	27C	G120	28W	G217	62E		
G59	27C	G121	28W	G218	58W		
G60	27C	G122	28W	G219	dne		
G61	26W	G123	28W	G220	58W		
G62	26W	G124	28W	G221	62E		

dne = does not exist

N-localities  
(Kidd, Molnar)

Locality	Map Sheet	Locality	Map Sheet	Locality	Map Sheet	Locality	Map Sheet
N1	20W	N14	20W	N27	GE	N40	29E
N2	20W	N15	dne	N28	GE+	N41	29E
N3	20W	N16	dne	N29	GE	N42	29E
N4	20W	N17	dne	N30	GE	N43	29E
N5	20W	N18	dne	N31	29E	N43A	29E
N6	20W	N19	dne	N32	29E	N44	29E
N7	20W	N20	22W	N33	29E	N45	29E
N8	20W	N21	GE+	N34	29E	N46	29E
N9	20W	N22	GE+	N35	29E	N46A	29E
N10	20W	N23	GE+	N36	29E	N47	29E
N11	20W	N24	GE+	N37	29E	N48	29E
N12	20W	N25	GE+	N38	29E	N49	28W
N13	20W	N26	GE+	N39	29E		

dne = does not exist

P-localities  
(Lin, Watts)

Locality	Map Sheet	Locality	Map Sheet	Locality	Map Sheet	Locality	Map Sheet
P1	3W	P12	EE	P23	47W	P34	65E
P2	3W	P13	23E	P24	47E	P35	65E
P3	4W	P14	33E	P25	45E	P36	65E
P4	4E	P15	33E	P26	62E	P37	65E
P5	10W	P16	29E	P27	62E	P38	65E
P6	10W	P17	29E	P28	58W	P39	65E
P7	17W	P18	29E	P29	62E	P40	65E
P8	17W	P19	39W	P30	62E	P41	65E
P9	23E	P20	39W	P31	62E	P42	65E
P10	23E	P21	44E	P32	65E	P43	65E
P11	20E	P22	44E	P33	61E		

H-localities  
(Molnar)

Locality	Map Sheet	Locality	Map Sheet	Locality	Map Sheet	Locality	Map Sheet
H1	29E	H32	47E	H63	47E	H94 (M275)	58W
H2	29E	H33	47E	H64	47E	H95	62E
H3 (N31)	29E	H34	47E	H65	47E	H96	62W
H4 (N32)	29E	H35	47E	H66	47E	H97	62W
H5	29E	H36	47E	H67	47E	H98 (N306)	62W
H6	29E	H37	47E	H68	47E	H99	62W
H7	29E	H38	47E	H69	47E	H100	62W
H8	29E	H39	47E	H70	47E	H101	62W
H9	29E	H40	47E	H71	47E	H102	62W
H10 (N42)	29E	H41	47E	H72	47W	H103	62W
H11	29E	H42	47W	H73	53W	H104	62W
H12	29E	H43	47W	H74	53W	H105	58W
H13	29E	H44	47W	H75	53W	H106	58W
H14	29E	H45	47W	H76	53W	H107 (M261)	58W
H15	29E	H46	47W	H77	53W	H108	58W
H16	29E	H47	47W	H78	53W	H109	58W
H17	29E	H48	47W	H79	53W	H110	58W
H18	29E	H49	47W	H80 (S405)	58W	H111	60W
H19 (N43)	29E	H50	47W	H81	58W	H112	60W
H20	47E	H51	47W	H82	58W	H113	60W
H21	47E	H52	47W	H83	58W	H114	60W
H22	47E	H53	47W	H84	58W	H115	60W
H23	47E	H54	47E	H85 (S411)	58W	H116	52W
H24	47E	H55	47E	H86 (S412)	58W	H117	62W
H25	47E	H56	47E	H87	58W	H118	62W
H26	47E	H57	47E	H88	58W	H119	62E
H27	47E	H58	50E	H89 (M263)	58W	H120	60W
H28	47E	H59	50E	H90	62W	H121	60W
H29	47E	H60	50E	H91 (M272)	62W	H122	60W
H30	47E	H61	50E	H92	58W	H123	60W
H31	47E	H62	47E	H93	58W		
H201	CW						
H202	CW						
H203	CE						
H204	CE						
H205	CE						

M-localities  
(Kidd, Dewey)

Locality	Map Sheet	Locality	Map Sheet	Locality	Map Sheet	Locality	Map Sheet
M1	1W	M96	17W	M191	47W	M284	62E
M2	1W	M97	17W	M192	47W	M285	58W
M3	S of Zangbo	M98	17W	M193	47W	M286	58W
M4	to Kamba-la	M99	17W	M194	47W	M287	58W
M5	"	M100	17W	M195	47W	M288	58W
M6	"	M101	17W	M196	47W	M289	58W
M7	"	M102	17W	M197	47E	M290	58W
M8	1W	M103	17W	M198	47E	M291	58E
M9	1W	M104	17W	M199	47E	M292	42W
M10	1W	M105	17W	M200	47W	M293	58W
M11	1E	M106	17W	M201	47W	M294	63E
M12	1W	M107	17E	M202	47W	M295	63E
M13	1E	M108	26E	M203	47W	M296	63E
M14	1E	M109	17W	M204	47W	M297	63E
M15	1E	M110	19E	M205	47W	M298	63E
M16	1E	M111	20E	M206	45W	M299	62E
M17	AW	M112	20E	M207	45W	M300	62W
M18	AW	M113	20E	M207A	45W	M301	62W
M19	AW	M114	20E	M208	47W	M302	62W
M20	AW	M115	20E	M208A	47W	M303	62W
M21	AW	M116	20E	M209	47W	M304	62W & 58W
M22	AW	M117	20E	M210	47W	M305	62W
M23	AW	M118	20E	M211	47W	M306	62W
M24	AW	M119	30E	M212	47W	M307	61E
M25	AW	M120	20E	M213	47W	M308	61E
M26	AW	M121	20E	M214	47W	M309	60W
M27	3E	M122	20E	M215	47W	M309A	60W
M28	3E	M123	20E	M216	47W	M310	60W
M29	3E	M124	20E	M217	44E	M311	58W
M30	3E	M125	20E	M218	44E	M312	58W
M31	3E	M126	20E	M219	47W	M313	58W
M32	1E	M127	23E	M220	47W	M314	58W
M33	1E	M128	23E	M221	47W	M315	58W
M34	3E	M129	23E	M222	47W	M316	58W
M35	3E	M130	23E	M223	47W	M317	58W
M36	3E	M131	23E	M224	47W	M318	58W
M37	3E	M132	23E	M225	47W	M319	58W
M38	3E	M133	23E	M226	47W	M320	58W
M39	3E	M134	20E	M227	47W	M321	60W
M40	3E	M135	20E	M228	47W	M322	60W
M41	3E	M136	20E	M229	47W	M323	60W
M42	3E	M137	20E	M230	47E	M324	60W
M43	5W	M138	20E	M231	47E	M325	60W
M44	10W	M139	20E	M232	47E	M326	60W
M45	10W	M140	20E	M233	47E	M327	60W
M46	10W	M141	20E	M234	47E	M328	60W
M47	10W	M142	20E	M235	47E	M329	60W
M48	12W	M143	20E	M236	47E	M330	60W
M49	12W	M144	20E	M237	47E	M331	60W
M50	12W	M145	20E	M238	47E	M332	60W
M51	12W	M146	20E	M239	47E	M333	60W
M52	12W	M147	20E	M240	47E	M334	60W
M53	12W	M148	20E	M241	47E	M335	60W
M54	12W	M149	20E	M242	47E	M336	60W
M55	12W	M150	20E	M243	62E	M337	60W
M56	10W	M151	20E	M244	62W	M338	60W
M57	10W	M152	20E	M245	62W	M339	60W
M58	10W	M153	20E	M246	62W	M340	61E
M59	10W	M154	20E	M247	62W	M341	62W
M60	10W	M155	20E	M248	62W	M34C	62W
M61	10W	M156	20E	M249	62W	M343	62W
M62	10W	M157	20E	M250	62W	M344	62W
M63	10W	M158	20E	M251	58W	M345	62E
M64	11E	M159	20E	M252	62W	M346	62E
M65	11E	M160	20E	M253	62W	M347	62E
M66	11E	M161	20E	M254	58W	M348	62E
M67	11E	M162	20E	M255	62W	M349	62E
M68	10W	M163	20E	M256	62W	M350	62E
M69	10E	M164	20E	M257	62W	M351	60W
M70	10E	M165	20E	M258	58W	M352	60W
M71	13W	M166	20E	M259	58W	M353	60W
M72	15C	M167	20E	M260	58W	M354	60W
M73	15C	M168	20E	M261	58W	M355	60W
M74	15C	M169	28W	M262	58W	M356	62E
M75	15C	M170	28W	M263	58W	M357	62E
M76	17W	M171	28W	M264	58W	M358	60W
M77	17W	M172	28W	M265	58W	M359	dne
M78	26W	M173	28W	M266	58W	M360	3E
M79	26W	M174	28W	M267	58W	M361	3E
M80	26W	M175	28W	M268	58W	M362	1E
M81	26W	M176	36E	M269	58W	M363	3W
M82	26W	M177	40E	M270	58W	M364	3W
M83	26W	M178	37E	M271	62W	M365	3W
M84	26W	M179	37E	M272	62W	M366	3W
M85	26W	M180	40E	M273	58W	M367	3W
M86	26W	M181	40E	M274	58W	M368	3W
M87	26W	M182	39W	M275	58W	M369	1W
M88	26W	M183	40E	M276	58W	M370	1W
M89	26W	M184	36E	M277	62E	M371	1W
M90	26W	M185	37E	M278	62E	M372	1W
M91	17W	M186	44E	M279	62E	M373	1W
M92	17W	M167	44E	M280	62E		
M93	17W	M188	44E	M281	62E		
M94	17W	M189	45W	M282	62E		
M95	17W	M190	47W	M283	62E		

dne = does not exist

S-localities  
(Shackleton, Coward)

Locality	Map Sheet	Locality	Map Sheet	Locality	Map Sheet	Locality	Map Sheet
S1	1W	S87	12W	S173	20E	S258	39W
S2	1W	S88	12W	S174	20E	S259	39W
S3	off maps	S89	12W	S175	20E	S260	39W
S4	Kamba-la	S90	10W	S176	20E	S261	39W
S5	to Zangbo	S91	10W	S177	20E	S262	39W
S6	"	S92	10W	S178	20E	S263	39W
S7	"	S93	10W	S179	20E	S264	39W
S8	"	S94	10W	S180	23E	S265	39W
S9	"	S95	10W	S181	23E	S266	39W
S10	"	S96	10W	S182	23E	S267	39W
S11	"	S97	10W	S183	23E	S268	39W
S12	"	S98	10W	S184	23E	S269	39W
S13	"	S99	10W	S185	23E	S270	44E
S14	"	S100	10W	S186	23E	S271	44E
S15	2E	S101	10W	S187	23E	S272	44E
S16	2E	S102	10E	S188	23E	S273	44E
S17	2E	S103	13W	S189	23E	S274	44E
S18	2E	S104	13W	S190	23E	S275	44E
S19	2E	S105	15C	S191	23E	S276	44E
S20	2E	S106	15C	S192	23E	S277	44E
S21	2E	S107	15C	S193	23E	S278	44E
S22	2E	S108	17W	S194	23E	S279	39W
S23	2E	S109	17W	S195	23E	S280	44E
S24	2E	S110	18E	S196	23E	S281	50E
S25	2E	S111	18W	S197	23E	S282	47W
S26	2E	S112	18E	S198	30E	S283	47W
S27	2E	S113	18E	S199	30E	S284	47W
S28	2E	S114	25C	S200	30E	S285	47W
S29	2E	S115	25C	S201	23E	S286	47W
S30	3E	S116	25C	S202	dne	S287	50E
S31	3E	S117	25C	S203	25C	S288	50E
S32	3E	S118	25C	S204	25C	S289	50E
S33	3W	S119	25C	S205	25C	S290	50E
S34	3W	S120	18E	S206	25C	S291	50E
S35	3E	S121	18E	S207	25C	S292	47E
S36	3E	S122	18E	S208	25C	S293	47E
S37	8C	S123	18E	S209	25C	S294	47E
S38	3E	S124	18E	S210	25C	S295	47E
S39	3E	S125	18E	S211	25C	S296	47E
S40	3E	S126	18E	S212	25C	S297	47E
S41	3E	S127	18E	S213	28W	S298	47E
S42	3E	S128	19E	S214	28W	S299	50E
S43	3E	S129	19W	S215	28W	S300	50E
S44	3W	S130	20E	S216	dne	S301	50E
S45	dne	S131	20E	S217	28E	S302	50E
S46	3W	S132	EE	S218	28E	S303	50E
S47	4W	S133	EE	S219	33E	S304	50E
S48	4W	S134	EE	S220	28W	S305	50E
S49	4W	S135	EE	S221	28W	S306	50E
S50	4W	S136	EE	S222	28W	S307	50E
S51	4W	S137	EE	S223	28W	S308	50E
S52	4W	S138	EE	S224	28W	S308A	53W
S53	4W	S139	EE	S225	28W	S309	53W
S54	4W	S140	CE	S226	28W	S310	53W
S55	4W	S141	CE	S227	28W	S311	53W
S56	4W	S142	CW	S228	28W	S312	53W
S57	4W	S143	CW	S229	28W	S313	53W
S58	4W	S144	CW	S230	28W	S314	53W
S59	4W	S145	BW	S231	33W	S315	53W
S60	4W	S146	BW	S232	33E	S316	53W
S61	4W	S147	B-	S233	33E	S317	53W
S62	4W	S148	CW	S234	33E	S318	53W
S63	4W	S149	CW	S235	33E	S319	50E
S64	4W	S150	CW	S236	33E	S320	47E
S65	5W	S151	CW	S237	33E	S321	47W
S66	5W	S152	CW	S238	33E	S322	50W
S67	5W	S153	CW	S239	33E	S323	50W
S68	5W	S154	CE	S240	33E	S324	50W
S69	6E	S155	CE	S241	33E	S325	49E
S70	6E	S156	DW	S242	33E	S326	49E
S71	6E	S157	BW	S243	33E	S327	49E
S72	7W	S158	BW	S243A	33E	S328	49E
S73	10W	S159	BW	S244	28W	S329	49E
S74	10W	S160	BW	S245	28W	S330	49E
S75	10W	S161	20E	S246	28W	S331	49E
S76	10W	S162	20E	S247	33E	S332	dne
S77	10E	S163	19W	S248	33E	S333	dne
S78	10E	S164	19W	S249	37E	S334	49E
S79	10E	S165	19W	S250	40E	S335	49E
S80	10E	S166	19W	S251	40E	S336	49E
S81	10E	S167	19W	S252	40E	S337	49E
S82	10E	S168	19W	S253	40E	S337C	53W
S83	10W	S169	19W	S254	40E	S338	49E
S84	12W	S170	20E	S255	40E	S339	50W
S85	12W	S171	20E	S256	39W	S340	50W
S86	12W	S172	20E	S257	39W	S341	50W

S342	50W	S410	58W	S470	61E	S530	65E
S343	50W	S411	58W	S471	61E	S531	65E
S344	50W	S412	58W	S472	62E	S532	65E
S345	50W	S413	58W	S473	61E	S533	65E
S346	50W	S414	62W	S474	61E	S534	65E
S347	50W	S415	62W	S475	61E	S535	65E
S348	50W	S416	62E	S476	61E	S536	65E
S349	50W	S417	62E	S477	61E	S537	65E
S350	50W	S418	62E	S478	61E	S538	65E
S350C	57E	S419	62E	S479	61E	S539	65E
S351	50W	S420	62E	S480	61E	S540	65E
S351C	57E	S421	62E	S481	61E	S541	65E
S352	50W	S422	62E	S482	61E	S542	65E
S352C	57E	S423	62E	S483	61E	S543	65E
S353	50W	S424	62E	S484	61E	S544	65E
S353C	57E	S425	62E	S485	61E	S545	65E
S354	47W	S426	62E	S486	61E	S546	65E
S354C	57E	S427	62E	S487	61E	S547	65E
S355	47W	S428	62E	S488	61E	S548	65E
S355C	57E	S429	62E	S489	61E	S549	65E
S356	47W	S430	62E	S490	61E	S550	65E
S356C	57E	S431	62E	S491	61E	S551	61E
S357	47W	S432	62E	S492	61E	S552	61E
S357C	57E	S433	62E	S493	61E	S553	61E
S358	53W	S434	62E	S494	61E	S554	61E
S358C	57E	S435	62E	S495	61E	S555	61E
S359	58W	S436	62E	S496	61E	S556	61E
S360	58W	S437	62E	S497	61E	S557	61E
S361	58W	S438	62E	S498	61E	S558	61E
S362	58W	S439	62E	S499	dne	S559	61E
S363	62W	S440	62E	S500	dne	S560	61E
S364	62W	S441	62E	S501	dne	S561	61E
S365	62W	S442	62E	S502	61E	S562	61W
S366	62W	S443	62E	S503	61E	S563	61W
S367	62W	S444	62E	S504	61E	S564	61W
S368	62W	S445	62E	S505	65E	S565	61W
S369	62W	S446	61W	S506	65E	S566	61E
S370	58W	S447	61W	S507	65E	S567	dne
S371	58W	S448	61W	S508	65E	to	dne
S372	58W	S449	61W	S509	65E	to	dne
S373	58W	S450	61W	S510	65E	S601	3W
S374	58W	S451	61W	S511	65E	S602	3W
S375	58W	S452	61W	S512	65E	S603	3W
S376	dne	S453	61W	S513	65E	S604	3W
to	dne	S454	61W	S514	65E	S605	3W
S395	dne	S455	61W	S515	65E	S606	3W
S396	57E	S456	61W	S516	61E	S607	3W
S397	57E	S457	61E	S517	61E	S608	dne
S398	57E	S458	61E	S518	61E	S609	dne
S399	57E	S459	61E	S519	61E	S610	dne
S400	57E	S460	61E	S520	61E	S611	3W
S401	57E	S461	61W	S521	61E	S612	3W
S402	57E	S462	61W	S522	62E	S613	3W
S403	57E	S463	61W	S523	61E	S614	3W
S404	57E	S464	61W	S524	61E	S615	3W
S405	58W	S465	61W	S525	61E	S616	3W
S406	58W	S466	61W	S526	61E	S617	3W
S407	58W	S467	61E	S527	61E		
S408	58W	S468	61E	S528	61E		
S409	58W	S469	61E	S529	65E		

dne = does not exist  
(S 337C; 350C-358C are Coward only)



X-localities

(Samples from S,M,B and T localities renumbered by G - Pearce, Harris)  
A few do not correspond with an S,M,B,M, or T number, and are shown separately on the microfiche maps. Most of the rest are not shown separately on the maps.

Sample	Equivalent locality	Map Sheet	Sample	Equivalent locality	Map Sheet	Sample	Equivalent locality	Map Sheet
X1	T11	3W	X25	S205	25C	X49	X167	19W
X2	M8	1W	X26	S205	25C	X50	143	CM
X3	S70	6E	X27	S205	25C	X51	8146	BW
X4	S70	6E	X28	S205	25C	X52	S145	BW
X5	M47	10W	X29	S203	25C	X53	B24	FW
X6	M47	10W	X30	S203	25C	X54	--	30E
X7	M47	10W	X31	S203	25C	X55	S245	28W
X8	M47	10W	X32	S203	25C	X56	S262	39W
X9	M64	11E	X33	S205	25C	X57	B67	45E
X10	M64	11E	X34	--	26W	X58	M245	62W
X11	M64	11E	X35	M81	26W	X59	M253	62W
X12	M64	11E	X36	M82	26W	X60	M254	58W
X13	M64	11E	X37	M86	26W	X61	B77	58W
X14	S94	10W	X38	M80	26W	X62	M262	58W
X15	S94	10W	X39	M90	26W	X63	B85	62E
X16	S94	10W	X40	M98	17W	X64	M279	62E
X17	M71	13W	X41	M98	17W	X65	B89	62E
X18	M71	13W	X42	M146	20E	X66	S475	61E
X19	M71	13W	X43	M142	20E	X67	M296	63E
X20	M71	13W	X44	M139	20E	X68	M297	63E
X21	S205	25C	X45	S160	EW	X69	S458	61E
X22	S205	25C	X46	S159	EW	X70	S550	65E
X23	S205	25C	X47	S167	19W	X71	S546	65E
X24	S205	25C	X48	S166	19W			

Equivalents of section numbers used by Pearce and Mei (Volcanics - Chapter 6)

Sequence	Maps	Locality number(s)
L71	Dagze	1W, 1E, 3E
L72	Quesang	4W, 4E
LP1	Naqu	4W, 4E
LP2	Yangbajian	7W
LJ1	Lubuchong	23E
LJ2	S. Amdo	28W
LC1	Naggu	17W
LC2	Norbuzhong	20E
LC3	Pamu Co/Kyiru Co.	23E
LGA	Amdo	28W
QJ1	N. Wonquan	40E
QP1	Kaixin Ridge	44E
QP2	Banacomu Ridge	44E
QT1	Zhakonjian	45E
KP1	Wantaogou	62E
KD1	N. Kunlun (N)	65E
KD2	N. Kunlun (S)	65E
KT1	N. Kunlun dikas	65E
QH1	Zhengmaxikong	50E
		G14, 16, 17, 18, 19
		G32
		G29, 31, 33, 36
		G41, 45, 46
		G106, 107
		G129, 130, 131
		G55
		G98, 99
		G85-89
		G133
		G138
		G150, 151
		G152
		G154
		G216, 228, 230
		G240, 241, 243, 244, 251, 253, 255, 256
		G250, 254, 257, 258
		G239, 240, 241, 245, 252, 259-261
		G141

Localities in sections discussed in Pearce and Deng (Ophiolites - Chapter 8)

Sections	Maps	Localities
BG1	Baila	G94-97; N5-11
BG2	Halong	G91-92; S161, 164-167
BG3	Lubuchong	G106, 107
BG4	Dongqiao	G103, 104, 105
BG5	Amdo	G127, 132, 134
BG6	Amdo (S)	G129-131
--	Ado	G81
--	Yila	G54; S120-12,